Enhancing Radiotherapy Efficacy in Glioblastoma by Inhibiting BRD9

by

Serdar Aksel Çelikkol

Dissertation Submitted to the

Graduate School of Health Sciences

in Partial Fulfillment of the Requirements for

the Degree of

Master of Science

in

Cellular and Molecular Medicine

KOÇ
ÜNİVERSİTESİ

August, 2025

Enhancing Radiotherapy Efficacy in Glioblastoma by Inhibiting BRD9

Koç University

Graduate School of Health Sciences

This is to certify that I have examined this copy of a master's thesis by

Serdar Aksel Çelikkol

and have found that it is complete and satisfactory in all respects,

and that any and all revisions required by the final

examining committee have been made.

Prof. Tuğba Bağcı Önder (Advisor)

Asst. Prof. Gözde Korkmaz

Prof. Dilek Telci

Date: 04.08.2025

To my family, my friends, and my beloved dog Pia,

with love and gratitude.

ABSTRACT

Enhancing Radiotherapy Efficacy in Glioblastoma by Inhibiting BRD9

Serdar Aksel Çelikkol

Master of Science in Cellular and Molecular Medicine

4 August, 2025

Glioblastoma (GBM) remains one of the most aggressive and treatment-resistant forms of brain cancer, marked by high heterogeneity, invasive growth, and limited therapeutic options. Despite current standard therapies such as surgical resection, radiotherapy, and temozolomide chemotherapy (Stupp protocol), recurrence and resistance are still frequently seen. In this study, we aimed to enhance the radiotherapeutic response in GBM by targeting the epigenetic regulator BRD9, a bromodomain-containing protein implicated in chromatin remodeling and transcriptional control. Using U373 and U87MG cells, we combined a selective inhibitor (I-BRD9) and CRISPR-mediated BRD9 knockout with ionizing radiation (IR). BRD9 loss impaired viability and further reduced clonogenic survival in combination with IR. To capture early chromatin effects, we performed a histone Western-blot panel that included BRD9-linked acetylation marks, revealing a global reduction in active-chromatin signatures upon BRD9 inhibition/knockout. These data indicated that BRD9 remodeling the epigenetic landscape may underlie the observed radiosensitization.

To uncover the pathways altered by BRD9 loss, we next carried out transcriptomic profiling in two glioblastoma models (U373 and U87MG) exposed either to BRD9 inhibition or genetic knockout. Due to the downregulatory effect of BRD9, our studies focused more on genes with decreased expression that are intersecting in four different RNA sequencings. 31 downregulated genes were common in different conditions, which were linked to MYC signaling and translation machinery as a result of pathway analysis. BRD9 perturbation consistently rewired translation, MYC signaling, and ribosome biogenesis programs, with 31 genes reproducibly downregulated; many encode components of the translational machinery and tRNA aminoacylation. We focused on a MYC-associated axis involving aminoacyl-tRNA synthetases (AARS1, CARS1, GARS1, WARS1, YARS1) and EIF2S2. qPCR validated the coordinated suppression of these targets. Mechanistically, our data support a functional BRD9–MYC axis that coordinates aaRS/EIF2S2 expression and

ribosome biogenesis. MYC overexpression restored translation-related transcripts and ribosome-biogenesis markers, reversing the effects of BRD9 inhibition and reinforcing this dependency. In parallel, transcripts for rRNA species essential to ribosome production (47S, 28S, 18S, 5.8S, 5S) decreased upon BRD9 inhibition/knockout, aligning with the epigenetic shift and supporting a model in which BRD9 sustains translational capacity. Together, these findings nominate BRD9 as an epigenetic regulator that regulates chromatin accessibility for protein synthesis in GBM and suggest that targeting BRD9 can disrupt the translational machinery and enhance radiotherapeutic response. Further studies will elucidate the direct genomic occupancy for BRD9 and MYC while also revealing the interacting partners of BRD9. Moreover, test in vivo whether disrupting the BRD9–MYC–aaRS/EIF2S2 circuit durably sensitizes GBM to radiation.

ÖZETÇE

Glioblastoma'da Radyoterapi Etkinliğini BRD9 İnhibisyonu ile Artırmak
Serdar Aksel Çelikkol

Hücresel ve Moleküler Tıp

4 Ağustos, 2025

Glioblastoma (GBM), yüksek heterojenite, invaziv büyüme ve sınırlı tedavi seçenekleri ile karakterize edilen, en agresif ve tedaviye dirençli beyin tümörlerinden biri olmaya devam etmektedir. Cerrahi rezeksiyon, radyoterapi ve temozolomid kemoterapisini (Stupp protokolü) içeren güncel standart tedavilere rağmen, nüks ve direnç hâlâ sıkça görülmektedir. Bu çalışmada, kromatin yeniden şekillenmesi ve transkripsiyonel kontrolle ilişkili bromodomain içeren bir protein olan epigenetik düzenleyici BRD9'u hedefleyerek GBM'de radyoterapiye yanıtı artırmayı amaçladık. U373 ve U87MG hücrelerinde seçici bir inhibitör (I-BRD9) ve CRISPR aracılı BRD9 silinmesini iyonizan radyasyon (IR) ile birleştirdik. BRD9 kaybı hücre canlılığını azalttı ve IR ile kombinasyonda klonojenik sağkalımı daha da düşürdü. Erken kromatin etkilerini değerlendirmek için BRD9 ile ilişkili asetilasyon işaretlerini içeren bir histon Western blot paneli uyguladık ve BRD9 inhibisyonu/knock-out sonrası aktif kromatin imzalarında küresel bir azalma tespit ettik. Bu bulgular, BRD9'un epigenetik manzarayı yeniden şekillendirerek gözlenen radyosensitizasyona katkıda bulunabileceğini gösterdi.

BRD9 kaybıyla değişen yolakları ortaya koymak için, U373 ve U87MG GBM hücre hattında BRD9 inhibisyonu veya genetik silinmeye maruz bırakarak transkriptomik profilleme gerçekleştirdik. BRD9'un aşağı düzenleyici etkisi nedeniyle, çalışmalarımız dört farklı RNA-seq analizinde kesişen ve ekspresyonu azalan genlere odaklandı. Farklı koşullarda ortak olarak 31 genin aşağı regüle edildiği bulundu ve yolak analizi bu genlerin MYC sinyalleşmesi ve translasyon makinesi ile ilişkili olduğunu gösterdi. BRD9 bozulması, translasyon, MYC sinyalleşmesi ve ribozom biyogenezi programlarını sürekli olarak yeniden şekillendirdi; 31 genin çoğu translasyon makinesi ve tRNA aminoaçilasyonu bileşenlerini kodluyordu. Çalışmamızda özellikle aminoaçil-tRNA sentetazları (AARS1, CARS1, GARS1, WARS1, YARS1) ve EIF2S2'ye odaklandık. qPCR, bu hedeflerin koordineli baskılanmasını doğruladı.Mekanistik olarak verilerimiz, aaRS/EIF2S2 ekspresyonunu ve

ribozom biyogenezini koordine eden işlevsel bir BRD9–MYC eksenini desteklemektedir. MYC aşırı ekspresyonu, translasyonla ilişkili transkriptleri ve ribozom biyogenezi belirteçlerini geri kazandırarak BRD9 inhibisyonunun etkilerini tersine çevirdi ve bu bağımlılığı pekiştirdi. Buna paralel olarak, ribozom üretimi için gerekli rRNA türlerinin (47S, 28S, 18S, 5.8S, 5S) transkriptleri BRD9 inhibisyonu/knock-out sonrasında azaldı; bu durum epigenetik kaymayla uyumlu olup BRD9'un translasyon kapasitesini sürdürdüğünü destekledi. Tüm bu bulgular, BRD9'un GBM'de kromatin erişilebilirliğini protein sentezi lehine düzenleyen bir epigenetik düzenleyici olduğunu ve hedeflenmesinin translasyon makinesini bozarak radyoterapiye duyarlılığı artırabileceğini göstermektedir. İleriye dönük çalışmalar BRD9 ve MYC'nin genomik bağlanma bölgelerini ve etkileşim ortaklarını ortaya çıkaracak, ayrıca BRD9–MYC–aaRS/EIF2S2 devresinin bozulmasının GBM'yi in vivo koşullarda radyasyona kalıcı olarak duyarlılaştırıp duyarlılaştırmadığını test edecektir.

ACKNOWLEDGEMENTS

First and foremost, I would like to express my sincere gratitude to my advisor, Prof. Tuğba Bağcı-Önder, for her continuous guidance, encouragement, and patience throughout my graduate studies. Her mentorship has greatly shaped my scientific thinking and supported my development as a researcher.

I would also like to thank the members of my thesis committee, Assist. Prof. Gözde Korkmaz and Prof. Dilek Telci Temeltaş, for their valuable feedback and thought-provoking questions during the development and defense of this work. I am sincerely thankful to Koç University, Koç University Research Center for Translational Medicine (KUTTAM), and Health Institutes of Turkey (TÜSEB) for the research environment and financial support that enabled the completion of this project.

Special thanks go to all current and former members of the TBO, who provided not only technical advice and assistance but also made the lab a supportive and enjoyable environment. I am especially grateful to Assoc. Prof. Gözde Korkmaz for her warm presence and enriching discussions that helped deepen my understanding of the literature. I would like to thank Dr. Nareg Değirmenci, who has been both a long-time friend and an academic mentor to me throughout my journey; his guidance in and outside the lab has been truly formative. As fellow members of the IR team, Beyza Nur Köseoğlu and I shared not only experiments but also a shared path of growth—her support, warmth, and technical wisdom were a source of constant encouragement. I also thank İpek Kök, Sedef Saraç, and Ayşegül Durgun, with whom I began my MSc adventure. From the very first days, they became not only lab mates but also companions in both science and life. Together, we navigated the highs and lows of graduate life— sharing and supporting each step forward, traveling abroad to present our work and collecting unforgettable memories along the way. From conference posters to late-night walks, our shared experiences created a bond filled with warmth, laughter, and quiet strength that carried us through it all. These years would not have been the same without their presence. Canan Bayraktar deserves special thanks for her generosity in sharing her bench, thoughtful guidance, and genuine support. I am also grateful to Erdem Ercan and Altar Özbıyık for their friendship, humor, and the many scientific and philosophical discussions that made even the longest experiments enjoyable. My sincere

thanks to Dr. Özlem Yedier-Bayram for always offering help with steady guidance and insightful support, and to Ebru Yılmaz and Elisa Simone for their support during this journey. I am thankful to Gözde Vidin for her coordination efforts in the lab, and to our former members Dr. Yağmur Kala, Dr. Göktuğ Karabıyık, Dr. Ahmet Cingöz, Beril Esin, and Mina Küçüktaş for their openness, generosity, and the welcoming spirit they brought into the lab, making it a space filled with energy, laughter, and shared curiosity. I also want to acknowledge Gamze Turan for her unwavering friendship, shared scientific curiosity, and the collaborative spirit we shared across different research spaces. From countless bus rides that turned into inspiring conversations to her steady support during challenging moments, her presence made a meaningful impact on both my personal and academic life. Her thoughtful perspective and collaborative spirit were a constant source of motivation throughout this journey.

I would also like to thank the new lab members İbrahim Özyıldız, Yiğit Emre Altın, and Elif Ayça Güvener for bringing joy and positive energy to the lab. My thanks also go to Hande Özkan, Barış Sergi, İpek Bulut, Büşra Yıldırım, Batuhan Altay, Ezgi Karyemez, Mert Gayretli, and Arda Odabaş for their support and friendly collaboration within and beyond the lab.

I would also like to thank my dear friends Melis, Şahin, Alen, Sarven, Aykun, Bedros, Oğuz, Göktuğ, Kemal, Kevin, Arden, and Meryem for their presence and support throughout this journey. Their encouragement and company played a meaningful role in making this period more enjoyable and well-balanced.

Finally, I would like to thank my family—especially my mother, to whom I owe a special debt of gratitude for her endless love and strength. Their support has been instrumental in reaching this point, and I appreciate the rest of my family for standing by me at every step and sharing in this journey.

TABLE OF CONTENTS

LIST OF TABLES

LIST OF FIGURES

ABBRIVIATIONS

Acute myeloid leukemia	AML
Alanyl–tRNA synthetase 1	AARS1
Aminoacyl- tRNA synthetase-interacting multifunctional proteins 1, 2, and 3	AIMP1-2-3
Aminoacyl- tRNA synthetases	aaRSs
Apoptosis signal-regulating kinase 1	ASK1
Associated scaffolding factor	XRCC4
AT-rich interactive domains	ARIDs
Ataxia-telangiectasia mutated and Rad3-related protein	ATR
Ataxia-telangiectasia mutated kinase	ATM
Base excision repair	BER
Blood-brain barrier	BBB
Blood-brain tumor barrier	BBTB
BRG1/BRM-associated factor	BAF
Bromodomain containing protein 9	BRD9
Bromodomains	BRDs
Canonical BAF	cBAF
Central Brain Tumour Registry of the United States	CBTRUS
Central nervous system	CNS
Chromodomain Helicase DNA-binding	CHD
Chromodomains	CDs
Compared to supramaximal resection	STR
Cysteinyl–tRNA synthetase 1	CARS1
Deubiquitinating enzymes	DUBs
Differentially expressed genes	DEG
DNA damage repair	DDR
DNA methyltransferases	DNMTs
DNA-dependent protein kinase	DNA-PK
Dopamine receptor d2	DRD2

Double strand breaks	DSBs
Eukaryotic translation initiation factor 2 subunit 2 (beta)	EIF2S2
Enhancer of zeste homolog 2	EZH2
Epidermal growth factor receptor	EGFR
F-box/WD repeat-containing protein 7	FBW7
Glioblastoma	GBM
Glioma initiating cells	GICs
Glutaminyl– tRNA Synthetase	QARS1
Glycyl–tRNA synthetase 1	GARS1
Gray	Gy
High mobility group box domains	HMGs
Histone acetyltransferase	HATs
Histone deacetylases	HDACs
Histone methyltransferases	HMTs
Homologous recombination	HR
Host cell factor	HCF-1
Hypoxia-inducible factor 1	HIF-1
Imitation switch	ISWI
Inositol requiring 80	INO80
Ionizing radiation	IR
Knockout	KO
Leucyl– tRNA Synthetase	LARS1
Methionyl– tRNA Synthetase	MARS1
Micromolar	mM
Microgram	mg
Millimolar	mM
Mismatch repair	MMR
Mre11-rad50-nbs1	MRN
Multi-aminoacyl- tRNA synthetase complex	MCS
Multiple myeloma	MM
Multiplicity of Infection	MOI

Nanometer	nM
National cancer institute's	NCI
Non-canonical BAF	ncBAF
Non-homologous end joining	NHEJ
O6-Methylguanine DNA methyltransferase	MGMT
Plant homeodomains	PHDs
Poly (ADP-ribose) polymerase	PARP
Polybromo-associated BAF	PBAF
Polycomb repressive complex	PRC2
Population doubling level	Pdl
Principal component analysis	PCA
Proliferating cell nuclear antigen	PCNA
Radiotherapy	RT
Reactive oxygen species	ROS
Rhabdoid tumor	RT
Ribosomal proteins	RPs
Ribosomal RNAs	rRNAs
Signal transducer and activator of transcription 5	STAT5
Single strand breaks	SSBs
Small nuclear RNAs	snRNAs
Small nucleolar RNAs	snoRNAs
Sterol regulatory element-binding protein 2	SREBP2
Sumo proteases	SENPs
Surveillance Epidemiology and End Results Program	SEER
SWI/SNF-related matrix-associated actin-dependent regulator of chromatin subfamily B	SMARCB1
Switch/sucrose non-fermentable	SWI/SNF
Temozolomide	TMZ
Total gross resection	TGR
Transfer RNAs	TRNAs
Translation initiation factors	eIFs

tRNA nucleotidyltransferase	TRNT1
Tryptophanyl–tRNA synthetase 1	WARS1
Tumor protein	p53
Tyrosyl–tRNA synthetase 1	YARS1
Vascular endothelial growth factor	VEGF
World Health Organization	WHO
XRCC4-like factor	XLF
Zinc-finger domains	ZFDs

Chapter 1:
INTRODUCTION

1.1. Glioblastoma

Central nervous system (CNS) tumors account for approximately 2% of all cancer types, and 95% of them end up with malignant tumor occurrence. According to the statistical data of the National Cancer Institute's (NCI) Surveillance Epidemiology and End Results Program (SEER), among all cancers, brain and other central nervous system cancers account for 1.3% in the US between 2018 to 2022. The global annual incidence rate is 4 cases per 100,000 individuals, predominantly observed in the elderly. In the US, the median age of diagnosis is 60, while the age of death is 67(Cruz & Wishart, 2019). 75% of these aggressive tumors originate from a brain cell type called glial cells, which are called gliomas. According to the classification of the World Health Organization (WHO) of all adult type diffuse gliomas, there are 2 branches through their IDH statuses (S. Han et al., 2020). IDH wild-type gliomas are glioblastoma (Grade IV) and astrocytoma (Grade II-III), while IDH gliomas are astrocytoma (Grade II-IV) and oligodendroglioma (Grade II-III). These tumors are graded based on their molecular abnormalities. Glioblastoma (GBM) is considered a grade IV glioma, which is the most common and aggressive type of primary brain tumor. In terms of the epidemiological aspect, it accounts for 45.2% of all CNS tumors. Based on the 2013 Central Brain Tumour Registry of the United States (CBTRUS) reports, the age-adjusted incidence rate is higher in males at 3.9 per 100,000 population, while in females it is 3.1 per 100,000 population(*CBTRUS Fact Sheet*, n.d.). According to the general statistics of CNS tumors, the male female ratio of incidence is still show that GBM is more prevalence among man which is 1.2 to 2.6(Yalamarty et al., 2023) while the median age at diagnosis is 64 years, while the survival rate of 2 years is 14.8(Weller et al., 2015). While 85% of the GBM cases arise from the supratentorial part of the brain (frontal lobe), rarely can also originate from the brainstem, spinal cord, and cerebellum.

In the sense of molecular properties of GBM, there can be several genetic and epigenetic alterations. While common molecular lesions include EGFR amplification, TERT promoter

mutation, PTEN mutation, chromosome 7p gains, and loss of chromosome 10q, there are many other mutations due to the subtypes of GBM.

Although GBM shares some properties with other cancer types, it exhibits unique properties that can be considered hallmarks of GBM, which make it more aggressive and lethal. Hallmarks specific to GBM are high heterogeneity, hypoxia-induced necrosis, microvascular proliferation, high mitotic activity, adaptation of the brain microenvironment, and therapy resistance(Torrisi et al., 2022).

1.2. Treatment of GBM

The therapy process of GBM includes a multidisciplinary strategy that requires different professions. The golden standard for the therapy of GBM contains 3 stages, which are surgical resection, radiotherapy, and chemotherapy. Although advancements in surgical imaging have enabled more extensive tumor resections, achieving a balance between aggressive tumor removal and preserving brain function remains crucial, with a focus on maintaining patients' quality of life and overall well-being. Due to the invasiveness and rapid growth of GBM, the tumor margins, location in the brain, and molecular aspects can vary over time. Compared to supramaximal resection (STR), total gross resection (TGR) improves 1-year survival by nearly 60% and 2-year survival by around 20%(Tejaswi Kanderi et al., 2024). Unfortunately, TGR can only be possible when the disease is diagnosed early because of its aggressive nature. Post-surgical treatment for high-grade GBM followed by an established protocol defined as “Stupp Protocol”. This therapy procedure consists of two steps, which are simultaneous radiotherapy and the use of a chemotherapeutic agent called Temozolomide (TMZ), an oral agent. A dose of 75mg/m^2/day for six weeks and 30 fractions of a total 60 Grays (Gy) radiotherapy is administered during concurrent treatment, followed by 150–200 mg/m^2 daily for 5 days within a 28-day cycle. The reason behind this two-phase treatment is first increasing the sensitization of the tumor for a better outcome of radiotherapy by generating DNA damage and genomic instability, and then direct killing of remaining tumor cells with a higher dose of TMZ(Stupp et al., 2005). Eventually, however, most of the GBM patients experience recurrence.

1.2.1. Chemotherapy

Chemotherapy is the primary strategy for GBM treatment. While radiotherapy serves as an additional treatment option, chemotherapy is used routinely. The main reasons for using chemotherapeutic agents are to induce DNA damage and inhibit repair, interfere with cell cycle progression, induce oxidative stress, inhibit angiogenesis, and modify the activity of epigenetic regulators (Wu et al., 2021). Unfortunately, due to treatment challenges, the list of drugs that can be used is limited.

The agent used during GBM treatment depends on the molecular structure since the efficacy of the drug relies on the mutations present in the tumor. Firstly, the most widely used chemotherapeutic for GBM treatment is TMZ, which is an alkylating agent capable of penetrating through blood-brain barrier. It is directly converted to its active form, which methylates guanine at the O6 and N7 positions, causing mismatches during DNA replication and DNA double-strand breaks. While healthy cells can repair this damage easily, GBM cells methylated at the O6-Methylguanine DNA methyltransferase (MGMT) promoter site are unable to repair the damage, leading to apoptosis (Jezierzański et al., 2024). The double-strand break property of TMZ is also used to enhance the effects of radiotherapy during concurrent treatment. Another important chemotherapeutic agents are Cisplatin and Lomustine (CCNU), which work similarly to TMZ through their DNA-alkylating capabilities. Lomustine is generally used as an alternative drug after first-line treatment fails. Besides DNA-alkylating agents, other strategies such as mitotic inhibition and angiogenesis inhibition are employed to fight GBM. Vincristine is a chemotherapeutic agent with an antimitotic effect by disrupting microtubule structure. However, due to its hydrophilic nature and high molecular weight, its effectiveness is limited compared to TMZ (Rusak et al., 2025). Despite these drawbacks, it can be combined with TMZ to achieve better treatment outcomes. Ultimately, Bevacizumab, a humanized monoclonal antibody, is used to reduce tumor blood vessel formation by blocking vascular endothelial growth factor (VEGF) (Rahman & Ali, 2024). However, due to its limited efficacy, proangiogenic properties after treatment, and resistance development, this drug is not yet the main component of treatment (Z. L. Liu et al., 2023).

1.2.2. Radiotherapy (RT)

Another essential component of GBM, radiotherapy plays a pivotal role during treatment, as almost 60% of all cancer patients receive RT. The main reason behind the use of RT is to eliminate the remaining microscopic tumor mass after resection and to prevent the recurrence of GBM. Even though this application must take place in most cases, it is important to cause minimal damage to healthy tissue and obtain the maximum removal of remaining GBM cells with high precision. Moreover, in some cases, due to the location of the tumor, the only option can be RT itself.

Developments in the biomedical field have led to the emergence of new radiotherapy methods, including three-dimensional conformal radiotherapy, intensity-modulated radiotherapy, image-guided radiotherapy, and stereotactic radiotherapy. At the same time, it is also used during surgery to obtain much higher efficacy from surgery. All these technologies use X-rays, which are accelerated electron beams that can ionize molecules on their path and disrupt biomolecules. The mechanism of action is divided into two, which are indirect or direct effects. While ionizing radiation is exposed, it contacts with water molecules and causes the production of ionized water that can further dissociate into free radicals. These free radicals can interact with other water molecules, creating reactive oxygen species ·OH, $O_2^{\cdot -}$, and H_2O_2, which are toxic for the cells and can interact with other

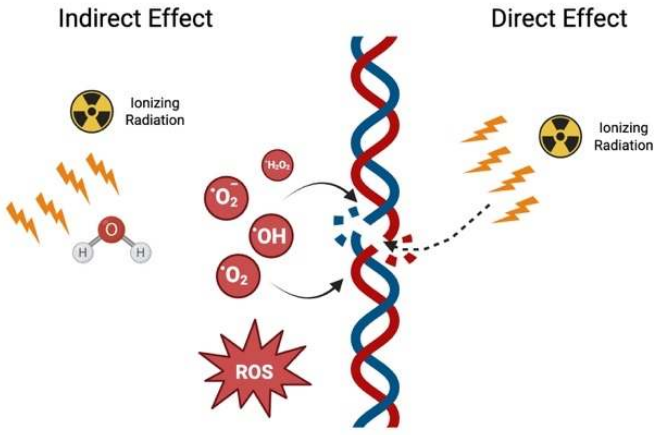

Figure 1.1 Schematic representation of the direct and indirect effects of ionizing radiation on DNA (Generated in Biorender).

biomolecules such as DNA, proteins, and lipids. This leads to high toxicity, thus, cell death. The direct effect is the interaction of ionizing radiation directly.

with DNA. This interaction led to double-strand breaks (DSBs), single-strand breaks (SSBs), or base mismatches in DNA. Since the cancer cells divide more frequently, if the damage accumulation is enough, IR will give much more harm to the tumor compared to healthy tissue.

Tumors are composed of thousands of cells; therefore, the damage caused by IR cannot have an equal impact on each cancer cell. Thus, radiation treatment is conducted by fractionation to be able to distribute the damage.

1.2.3. Chemoradiotherapy and Radiosensitization

As mentioned before, across multiple cancer types, including GBM, combining ionizing radiation (IR) with targeted or cytotoxic agents is a widely adopted strategy to potentiate therapeutic outcomes and improve treatment efficiency. Use of TMZ with IR in the Stupp Protocol is the most established way of GBM treatment, which aims to trigger apoptosis and autophagy; some other strategies are emerging according to the needs. The main drawback of this strategy is the rise of hematological toxicity(Gerber et al., 2007).

Another novel resveratrol, which is a herbal compound that displays antitumoral, antiaging, antioxidant properties by involving different cellular processes such as cell cycle and proliferation, apoptosis, hypoxia, etc. In order to overcome the high radioresistant capacity of GBM, enhancement of radiosensitivity is one of the key aims for drug development. Recent studies showed that resveratrol suppresses phosphorylated STAT3, a stemness, angiogenesis, and cell survival-associated gene, which results in increased apoptosis, less stemness, thus radiosensitization (Arabzadeh et al., 2021; Yang et al., 2012). Moreover, this drug can inhibit one of the main resistance factors, HIF-1α, which elevates DNA repair and radioresistance. This causes enhanced DNA damage and malfunction in the DNA damage repair (DDR) mechanism, thus radiosensitivity increases even in hypoxic conditions(Khoei et al., 2016). Another study conducted on the neurotransmitter pathway, a Dopamine Receptor D2 (DRD2), which is related to cholesterol metabolism, PI3K/AKT/mTOR pathways(Bhat et al., 2021). DRD2 activation sustains the activity of sterol regulatory

element-binding protein 2 (SREBP2), a regulator of cholesterol biogenesis. Cholesterol biosynthesis has a role in DDR, oxidative stress management, and therefore, radioresistance(Yu et al., 2023). When DRD2 is inhibited with Trifluoperazine, SREBP2 is suppressed, which results in deterioration of cell membrane repair, decrease in DDR complex stabilization, and proliferation. Therefore, decreased metabolic support, DDR, and increased DNA damage and apoptotic signal lead to radiosensitization(Bhat et al., 2021).

Although radiotherapy and chemotherapy, or in combination, remain fundamental components of glioblastoma treatment, they frequently fail to generate clinically significant long-term efficacy. This is largely linked to the GBM's intrinsic features, including its invasive growth, genomic instability, and capacity for rapid adaptation. As treatment resistance continues to emerge through various biological mechanisms, the overall response to standard therapies remains limited.

1.2.4. Treatment Challenges

Surgery is the first order of therapy for GBM. While the tumor should be resected at least 85%, some GBM patients cannot have an operation due to the progression of the disease. Apart from subsequent results of incomplete resection, there are several biological and physiological challenges that are encountered during the treatment of GBM. Barriers such as the blood-brain barrier (BBB) and the blood-brain tumor barrier (BBTB) are specialized boundaries that segregate the brain and the circulatory system, which control the nutrient entry into the brain, thus drug delivery to the tumor site is precluded(Wu et al., 2021). Moreover, expression of resistance proteins like P-glycoprotein and multidrug resistance proteins in BBB reduces the accumulation of drug therefore providing a natural shield to the tumor (Yalamarty et al., 2023) When GBM progress enough, it disrupts the BBB and BBBT for inflating into other parts of brain. Yet, the BBB structure is only disrupted at the primary tumor site but not at the metastatic site. Along with the high infiltration capacity, GBM uses brain physiology for its own good, which is still one of the main issues for researchers to solve with newly emerged technologies called nanoparticles to increase the permeability and diffusion capacity of drugs.

The other main challenges in the treatment of GBM are the intratumoral and intertumoral heterogeneity. While intratumoral heterogeneity means genetic, epigenetic, and phenotypic

variations among the other cells in the same tumor, intertumoral heterogeneity refers to the difference between molecular and genetic profiles in different patients. Intratumoral heterogeneity causes the occurrence of subpopulations that can have different mutations, deletions, or epigenetic architecture. When some have high infiltration capacity, some can have radioresistance due to a microenvironment that provides a low oxygen environment(Wu et al., 2021). Even though GBM patients can be gathered under the same branch, each patient has their own molecular and genetic profile, which necessitates personalized medicine since the standard therapy cannot succeed because of intertumoral heterogeneity. Additionally, this heterogeneity can be driven by extracellular vesicles synthesized by GBM cells that can transfer biomolecules or genetic mutations to convert healthy cells into tumor cells(Yalamarty et al., 2023).

The core part of GBM tumor contains glioma initiating cells (GICs) which can self-renewal and differentiate. These cells alter the DNA damage repair systems to increase the repair capacity of radiotherapy-induced damage. Such as induction of the Chk1 and Chk2 translation, by expressing proteins such as Chk1 and Chk2 to increase the efficiency of DSB. Moreover, overexpression of proliferating cell nuclear antigen (PCNA) associated factor (PAF) (Ong et al., 2017), GICs can bypass the DNA damage with error-free repair, which provides radioresistance and increases proliferation capacity (M. Y. Ali et al., 2020).

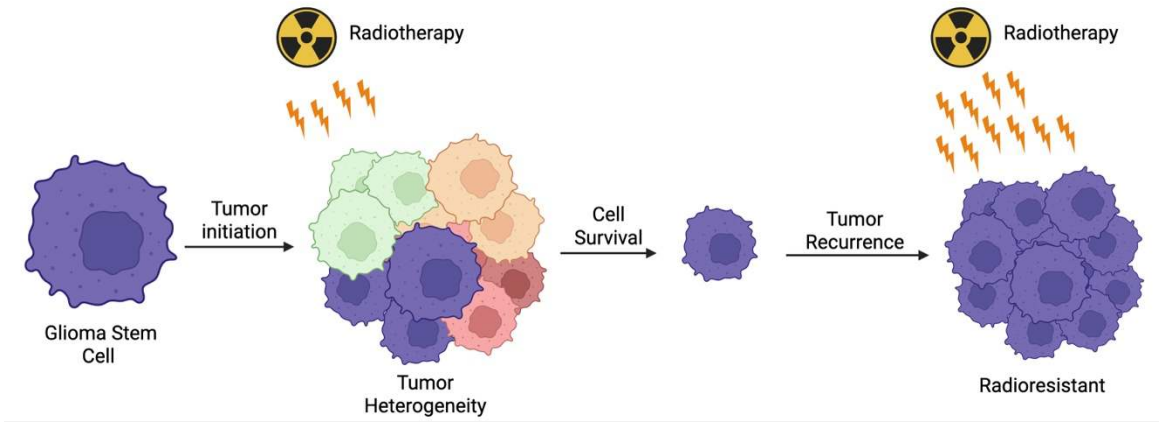

Figure 1.2 Schematic illustration of glioma stem cell-mediated tumor recurrence and radioresistance **(**Generated in Biorender).

1.3. Chemo/Radioresistance of GICs

GBM remains one of the most challenging cancers to treat; therefore, physicians use multiple drugs and treatment strategies simultaneously due to rapid changes at the biomolecular level and physiological reasons. Hereinbefore, GBM tumor contains a cell subpopulation called GICs that can exhibit high self-renewal capacity, differentiation, and propagation of the tumor. This dynamic adaptability mechanism provides resistance to cytotoxic therapies. GICs rely on their altered features, such as enhanced cell cycle and DNA repair capacity, epigenetic modification, transporter overexpression, and hypoxia, while using the environmental factors as the BBB, to circumvent the therapeutic effects, infiltrate, and expand throughout the brain. (Lathia et al., 2015)

1.4. Enhanced DNA Repair Capacity

While the successful outcome of TMZ chemotherapy is dependent on the MGMT status of the cell, which is a part of MMR machinery, the other therapy strategy, radiotherapy, directly damages the DNA by generating single strand breaks (SSBs) and double strand breaks (DSBs) or indirectly damages by generation of reactive oxygen species. When a cell encounters a DNA lesion, it initiates a molecular cascade that is called the DNA damage response (DDR). DDR pathway activity is central to the efficacy of the treatment because cell fate is associated with the outcome of DDR. According to the type of DNA damage, the recruited DDR pathway varies. SSBs are repaired through the base excision repair (BER) system, and primarily poly (ADP-ribose) polymerase (PARP) initiates the repairing activity. DSBs are repaired by two independent pathways, which are homologous recombination (HR) and non-homologous end joining (NHEJ). (Lord & Ashworth, 2012).

NHEJ is the most preferred DSB repair pathway due to its convenience, which is represented in **Figure 1.3**. The pathways start with recognition of DSB by DNA-dependent protein kinase (DNA-PK) and its binding domains Ku70-Ku80, which afterwards result in the recruitment of other NHEJ factors such as DNA-dependent protein kinase catalytic subunits (DNA-PKcs), DNA ligase IV, associated scaffolding factor (XRCC4), XRCC4-like factor (XLF), paralogue of XRCC4 and XLF, PAXX(Scully et al., 2019). DNA ends are closely aligned and protected by the nuclease activity through XRCC4, XLF, and DNA-PKcs. Lastly, DNA ligase IV and XLF/XRCC4 complex the strand in the overhang(Mohiuddin & Kang, 2019).

Although NHEJ can occur throughout the cell cycle steps, HR is restricted to only the late-S/G2 phase of the cell cycle. HR is a repair mechanism that uses sister chromatids as a template to repair the DNA. DSB is later recognized by a complex composed of RAD50, Mre11, and NBS1(MRN). In the next step, Ataxia-telangiectasia mutated kinase (ATM) and Ataxia-telangiectasia mutated and Rad3-related protein (ATR) are recruited to the site of damage for the initiation of DDR. HR is first operated by two proteins, ATM and ATR. ATM is a kinase that phosphorylates a histone variant, γ-H2AX, the main marker of DSB (Hockings & Miller, 2023).

Both ATM and ATR lead the repair machinery by phosphorylating of other key proteins such as p53, Chk1, and Chk2. The phosphorylation of proteins involved in HR determines the fate of the cell by influencing whether it will be arrested at the G1/S or G2/M checkpoints(Majd et al., 2021). Consequently, the excessive activity of the enzymes related to these DSB repair pathways provides better coping ability with the cytotoxic effect of DSB, which results in decreased sensitivity upon radiation treatment, thus the generation of radioresistance by the GICs.

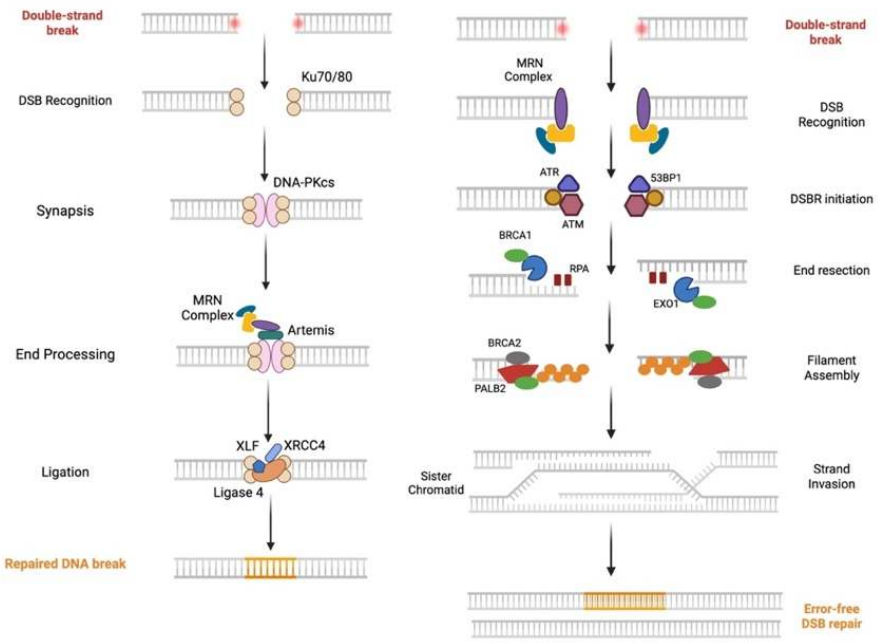

Figure 1.3 Schematic representation of the mechanisms of DNA double-strand break (DSB) repair (Generated in Biorender).

1.5. Hypoxia

Tumor hypoxia is another major reason that reduces the effectiveness of radiotherapy, which is also the cause of poor prognosis for most cancer types. Due to the rapid proliferation and abnormal vasculature of the tumors, oxygen cannot diffuse homogenously throughout the tumor. This hypoxic environment leads to the development of new GICs with a radioresistant profile due to the lack of adequate ROS formation. Thus, while the oxygen concentration in a cell is directly proportional to IR response, it is inversely proportional to total tumor volume and GIC development. The main indicator of hypoxia is the expression of hypoxia-inducible factor 1(HIF-1), which is also involved in the stimulation of oncogenic pathways and ultimately high survival, proliferation, infiltration capacity, and therapy resistance (Yalamarty et al., 2023). Moreover, HIF-1 expression causes hypoxia-induced autophagy. Autophagy is a process that promotes the cell to recycle biomolecules and damaged organelles(Jawhari et al., 2016). As a result, GICs can sequester or degrade the chemotherapeutic agent, whereas they mitigate the irradiated ROS and damaged DNA, which promotes therapy resistance.

1.6. Altered Signaling Pathways

Key signaling pathways play an essential role in reinforcing glioblastoma's resistance to therapy, contributing to its aggressive phenotype and ability to evade treatment. These pathways regulate critical processes such as cell survival, proliferation, and interaction with the tumor microenvironment, making them significant contributors to both tumor progression and therapeutic resistance. The PI3K/AKT/mTOR signaling pathway is one of the most frequently activated pathways in GBM(Behrooz et al., 2022). Mutations that alter the activity or expression of PI3K lead to the activation of downstream effectors AKT and mTOR. Tumor cells upregulate anti-apoptotic proteins like Bcl-2 and Survivin, upregulate VEGF, and promotes glycolysis (Liu et al., 2020). Also, research shows that overactivation of these pathways directly alters the cell cycle regulation, DNA repair, and survival mechanisms. AKT, for instance, enhances the DSB repair machinery by promoting the formation of γ-H2AX foci. Epidermal growth factor receptor (EGFR) signaling pathway is the other crucial pathway that is involved in resistance. Excessive activation of EGFR leads to continuous autocrine and paracrine signaling. The activity of this pathway directly orchestrates other

important pathways such as NF-κB, Ras, MAPK, and PI3K/AKT/mTOR pathways(Lurje & Lenz, 2010).

1.7. Epigenetic alterations in GBM

The term "Epigenetics" indicates the static regulation of chemical changes in transcriptional activity and chromatin structure, distinct from altering the DNA sequence. This regulatory mechanism is directly in interaction with the transcriptome, DNA repair, and chromosome architecture.

Eukaryotic DNA is compacted through a hierarchical structure. This process starts by using the core component of this event, nucleosomes, to wrap DNA, which is composed of 8 histone proteins. Nucleosome is composed of two copies of 4 types of histones, H2A, H2B, H3, and H4, forming an octameric structure (Luger et al., 1997). Each histone is wrapped by a DNA piece. DNA can have either a loose structure called "euchromatin" or a tight structure called "heterochromatin" (Kouzarides, 2007). Being euchromatin or heterochromatin is related with the transcriptional accessibility of the genomic regions. Histone proteins have an N-terminal domain rich in arginine and lysine residues, which are modified by constant addition and removal of chemical groups such as acetylation, methylation, butyrylation, ubiquitinoylation, and SUMOylation(Bannister & Kouzarides, 2011; Sabari et al., 2017). The single or multiple addition of these groups constitutes the "Epigenetic Code" (Q. W. Chen et al., 2014). This leads to fluctuation of DNA accessibility, subsequently altering the activity of downstream pathways, which can directly affect the cell states and cause diseases, such as cancer. These posttranslational modifications (PTMs) are conducted by three types of epigenetic actors, which are writer, eraser, and reader proteins **(Figure 1.4)**. Writer enzymes, for instance, histone acetyltransferase (HATs), histone methyltransferases (HMTs), Poly (ADP-ribose) Polymerases (PARPs), SUMO Ligases, Ubiquitin Ligases, and Kinases modify nucleotide bases or amino acids located on the histone tail by adding chemical groups. Erasers are a diverse range of proteins that remove the histone mark and act conversely to writer proteins. Histone deacetylases (HDACs), histone demethylases, phosphatases, Deubiquitinating Enzymes (DUBs) and SUMO Proteases (SENPs) are among eraser proteins. Lastly, PTMs can act as docking sites for reader proteins that have their specific domains recognizing a histone mark. For instance, acetylated lysine is recognized by

bromodomains (BRDs), while chromodomains (CDs) bind to methylated lysine, influencing subsequent processes through either attraction or repulsion of associated proteins.

Epigenetic regulation can also involve DNA methylation of CpG islands, post-transcriptional modifications, chromatin remodeling, and RNA-mediated gene silencing (**Figure 1.5)**(Q. W. Chen et al., 2014).

DNA methylation is a biochemical process that involves the covalent transfer of a methyl group to the C-5 position of the cytosine ring of DNA, which primarily occurs where cytosine is followed by guanine. This reaction is catalyzed by DNA methyltransferases (DNMTs), which mainly occurs in the cytosine-guanine dinucleotide-rich CpG islands, which are regions rich in cytosine-guanine dinucleotides (B. Jin et al., 2011). This event is considered a stable gene silencing mechanism. In a healthy individual, CpG-containing gene bodies such as promoters or enhancers are mostly unmethylated. On the other hand, hypermethylation of CpG islands is a common characteristic of cancers (Q. W. Chen et al., 2014).

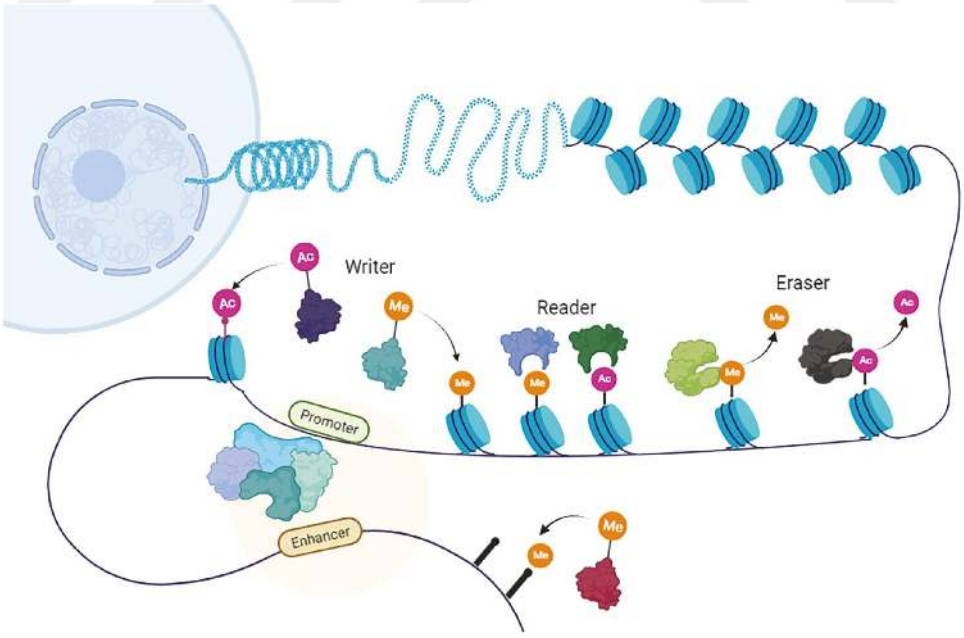

Figure 1.4 Histone modifications are regulated by writer, reader, and eraser proteins that control gene expression epigenetically. Adapted from Zhang et al., 2023, (Generated in Biorender).

1.7.1. Chromatin Remodeling

Chromatin remodeling is a pivotal process for gene regulation, which involves the ejection, repositioning, or restructuring of nucleosomes by recruiting ATP-dependent remodeling complexes. This highly regulated machinery controls the transcription system, replication factors, and DNA damage repair (Clapier et al., 2017). Chromatin remodeling process is conducted by 4 evolutionary conserved classes of ATP-dependent multi-subunit complexes in mammals, which are Imitation Switch (ISWI), Chromodomain Helicase DNA-binding (CHD), Inositol Requiring 80 (INO80), and Switch/Sucrose Non-Fermentable (SWI/SNF) (Clapier et al., 2017).

1.7.2. SWI/SNF Complex

SWI/SNF is a multi-subunit chromatin remodeling complex composed of up to 15 subunits, almost 30 encoded genes, and 1400 potential assembly combinations, which have broad roles in biological processes such as cell proliferation, differentiation, cell cycle control, and DNA repair. SWI/SNF is associated with high occupancy around promoters and enhancers. A study shows that SWI/SNF interaction has been discovered with p300, a histone acetyltransferase, in mouse embryonic fibroblast and many cancer cell line models to modulate H3K27ac the enhance the influence on many biological processes **(Figure 1.5)** (Alver et al., 2017). Moreover, after conducting a proteomic and bioinformatic analysis on the involvement of SWI/SNF complexes in human diseases, researchers discovered that almost 20% of all human tumors carry SWI/SNF mutations, which highlights the potential targetability of SWI/SNF and its subunits as a potent therapeutic(Kadoch et al., 2013). SWI/SNF complexes contain subunits that have nucleosome binding properties such as AT-rich interactive domains (ARIDs), zinc-finger domains or high mobility group box domains (HMGs), and histone-binding domains, such as bromodomains (BRDs), plant homeodomains (PHDs), and chromodomains(Kadoch & Crabtree, 2015). 3 mammalian SWI/SNF complexes were identified, which differ in terms of some structural features: BRG1/BRM-associated factor (BAF), polybromo-associated BAF (pBAF), and non-canonical BAF (ncBAF). Although each contains mutually exclusive ATPase subunit SMARCA2/4 and all include 5 subunits BCL7A-C, ACTB, ACTL6A, SMARCC1, and MARCD1, there are some lineage-specific subunits. While canonical BAF is specialized with DPF1-3, SS18, and ARID1A/B, pBAF is

specialized by BRD7, PHF10, and PBRM1 domains. The novel complex ncBAF has its signature subunits such as GLTSCR1/GLTSCR1L and Bromodomain Containing Protein 9 (BRD9)(Wanior et al., 2021).

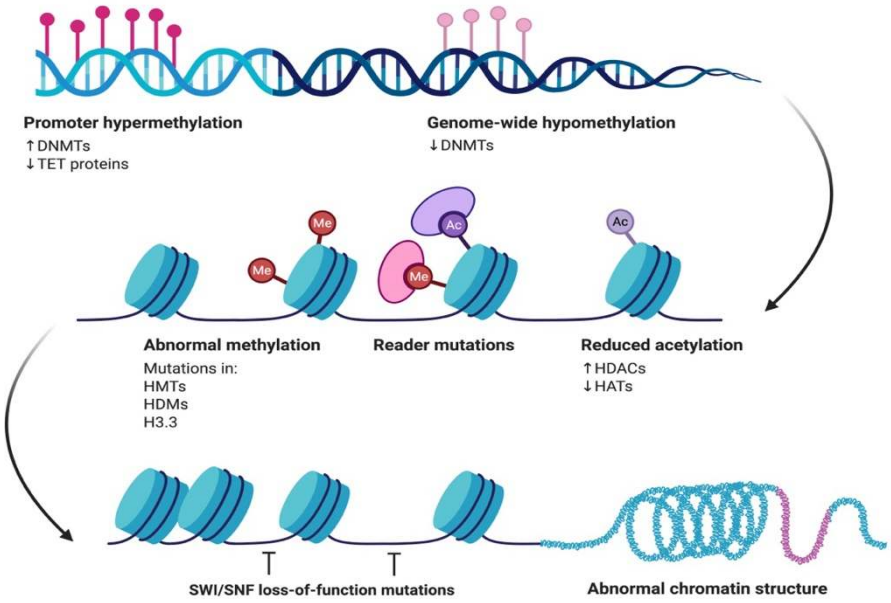

Figure 1.5 Schematic representation of the epigenetic alterations, such as aberrant methylation, reader mutations, and reduced acetylation, disrupt chromatin structure and contribute to transcriptional dysregulation (Generated in Biorender).

1.7.3. Bromodomain-Containing Proteins (BRDs)

Bromodomains are evolutionarily conserved domains that mediate protein-protein interactions, which comprise 110 amino acids. These amino acids form four antiparallel α helices called αZ, αA, αB, and αC, which are linked with two loops ZA and BC. In humans, there are 61 different BRDs, which are branched into eight subfamilies that have structural homology. Human bromodomains contain conserved amino acids in their recognition domain that facilitate hydrogen bonding and hydrophobic interactions, enabling the binding of acetylated lysine residues(M. M. Ali et al., 2023). BRDs can act as binding domains that ease the interaction of other proteins, or they can function as transcription factors or cotranscription factors. Due to their wide range of actions, BRDs are involved in the biological processes and can interact with a variety of complexes or proteins such as histone

acetyltransferases, chromatin remodeling complexes(Zhu et al., 2020), DNA damage response proteins(Chiu et al., 2017), and non-histone proteins(Del Gaudio et al., 2019).

1.8. Bromodomain Containing Protein 9 (BRD9)

BRD9, a specific component of the non-canonical BAF complex, and is a member of the bromodomain family IV (Filippakopoulos et al., 2012). BRD9 is a small protein of 67 kDa composed of 597 amino acids; and it contains two structural compartments, the bromodomain and DU3512 domain. Although the exact molecular function of BRD9 as a component of the SWI/SNF complex remains elusive, it can recognize acetylated lysine residues, which delegates BRD9 to act as a docking protein with its single bromodomain, thereby participating in the regulation of gene transcription. According to a study on histone recognition of BRD-containing proteins, BRD9 exhibits various strong histone targeting that comprises H3K9ac, H3K14ac, H3K18ac, H3K23ac, H3K27ac, H3K56ac, and H4K12ac(Filippakopoulos et al., 2012). Additionally, to these findings, it is indicated that BRD9 can recognize double acetylated lysine residues and much bulkier histone marks, such as butyryllysines and crotonyllysine(Del Gaudio et al., 2019)(Flynn et al., 2015).

Studies have demonstrated that BRD9 is involved in multiple cellular processes, including DDR, stem cell maintenance and differentiation, immune response, transcriptional regulation, and chromatin remodeling. Wang et al. demonstrated that the disrupted function of BRD9 causes changes in self-renewal and differentiation through TGF-β/Activin/Nodal pathways (X. Wang et al., 2023), while also Kenan Sevinç et al. indicated that BRD9 depletion upon chemical and genetic intervention increases somatic reprogramming efficiency (Sevinç et al., 2022). Moreover, Zong Wei et al. reported that alteration in BRD9 activity causes restoration of β-cell function and partially alleviates inflammation (Wei et al., 2018).

BRD9 functions as a regulator in many cellular activities, and when it undergoes mutations, the transcriptional mechanism is disrupted, inevitably leading to various diseases, especially cancer. While its precise mechanisms in cancer are still under investigation, emerging evidence suggests that BRD9 plays both oncogenic and tumor-suppressive roles, depending on the cancer context. This duality highlights the complex nature of its contribution to tumorigenesis.

As mentioned above, one of the most important challenges during cancer treatment is radioresistance, which highly depends on the alterations in the DDR pathway. SWI/SNF is an important complex that is not directly involved in the DDR pathway; however, this complex plays a significant role in the management of DDR. Zhou et al. demonstrated the significance of BRD9 among BRD-containing proteins, highlighting its crucial role in cancer progression. Their study showed that the downregulation of BRD9 halts the progression of various cancers, including ovarian, osteosarcoma, and colon cancer by identifying the orchestrating role of BRD9 in facilitating the interaction and co-localization of RAD51 and RAD54, which are essential for DNA repair processes (Zhou et al., 2020).

In rhabdoid tumors (RT), BRD9 has an important role through the biallelic depletion of SWI/SNF-related matrix-associated actin-dependent regulator of chromatin subfamily B (SMARCB1). Wang et al. reported that disturbance of SMARCB1 expression causes preferential dependency on BRD9, which results in the enhanced formation of BRD9-containing complexes, thus making it a potential therapeutic target (X. Wang et al., 2019a). Recently, Weisberg et al. studied a new enhanced antileukemic chemotherapeutic by using the sensitizer effect of BRD9 on multiple myeloma (MM) and acute myeloid leukemia (AML) (Weisberg et al., 2022). Findings indicate the link between the alterations in essential pathways upon BRD9 degradation. Depletion of BRD9 downregulates important genes associated with DDR, differentiation, inflammation, and cell cycle, including TLR5, ITGAM, and MYC, which upregulate pathways related to cell adhesion and immune response. These studies provide significant evidence that shows there is a strong relationship with the gene MYC, a master regulator of cell growth and proliferation, and BRD9. A prior study demonstrates the negative regulatory relationship between BRD9 and MYC in sensitive and resistant AML cells. Hohmann et al. in 2016, showed the supportive role of BRD9 by localizing 1.7 megabases downstream of MYC enhancer which is covered with active transcription mark H3K27ac. Accordingly, the downregulation of the MYC gene leads to cell cycle arrest at the G1 phase. Moreover, suppression of BRD9 and subsequent MYC downregulation leads to the elimination of the blockage of myeloid differentiation by differentially expressing genes like MPO and ITGAM, which in turn prevents the abnormal hematopoietic cells(Hohmann et al., 2016).

In the Koç University Brain Cancer Research Laboratory, our team was studying an alternative therapy option for GBM treatment. Since the concurrent treatment of a drug and radiation is mostly the gold standard of GBM therapy, the idea was to find a radiosensitizer that would not have a cytotoxic effect by itself while enhancing outcome upon combined treatment with radiation. To be able to obtain an enhanced outcome, epigenetic modifiers were selected as targets.

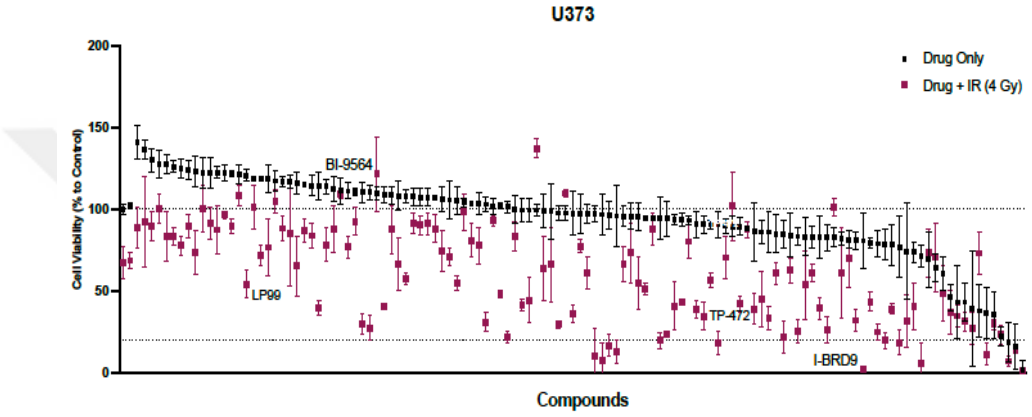

Figure 1.6 A chemical screening in U373 glioblastoma cells reveals synergistic effects of specific compounds, including I-BRD9, TP472, and LP99, **in combination with ionizing radiation (4 Gy),** showing enhanced reduction in cell viability compared to drug-only treat. (Degirmenci et al, unpublished)

Starting from this aim, an epigenetic drug screen was conducted on a GBM cell line with 125 chemicals at low doses and 4 Gy radiation treatment. These drugs target 25 epigenetic modifiers, including histone methyltransferases, histone demethylases, histone acetyltransferases, histone deacetylases, BRD-containing proteins, and arginine methyltransferases. Based on the results of the screening, we identified BRD9 as a potential GBM radiosensitizer that meets the criteria we established (**Figure 1.6**; data not published). Following this, we began investigating the mechanisms of action of BRD9 through literature reviews.

1.9. MYC

The MYC is a part of a proto-oncogene superfamily comprised of three members, C-MYC, MYCN, and MYCL, encoding into c-Myc, N-Myc, and L-Myc. These paralogue proteins, specifically c-Myc, are upregulated in almost all cancer types. While N-Myc is associated with neuroblastomas, L-Myc is linked to small-cell lung cancer. MYC is considered one of

the “super-transcription factors” which indicates the involvement of a gene in 10-15% of all transcription processes. It contributes to almost all important cellular processes, including cell cycle, adhesion, differentiation, self-renewal, apoptosis, immune response, angiogenesis, DDR, protein and ribosomal biogenesis, and many more (Dhanasekaran et al., 2022)(H. Chen et al., 2018). Cancer is a multi-parametric disease; thus, a vast number of genes are differentially expressed and consequently, their related pathways are altered. All these alterations result in hallmarks of the cancer, and since MYC can be influential upon many pathways, MYC itself can be considered a hallmark (Gabay et al., 2014).

MYC is highly regulated due to its versatile functionality in healthy cells. The most common inhibitor of MYC is p53, which is called as the “Guardian of the genome”. Upon stress stimulus, p53 localizes directly to promoter or enhancer regions of Myc, reducing its expression. Additionally, p53 promotes the transcription of ubiquitin ligase called F-box/WD repeat-containing protein 7 (FBW7), which recognizes phosphorylation and accordingly lead to the proteasomal degradation of MYC (Jha et al., 2023a).

Although MYC expression is limited in quiescent cells, abnormal mitogenic stimulation culminates in contrary activity of signal transduction pathways, including RAS, WNT, p53, mTOR, and many more. These signaling pathways that target MYC can exhibit either increased or decreased activity. For instance, increased activity of the WNT receptor induces a complex formation composed of the histone methyltransferases Enhancer of zeste homolog 2 (EZH2) and β-catenin. This complex is initiated with the overexpression of MYC (Dang, 2012).

Another important signaling pathway, mTORC1, is involved in various cellular mechanisms, including cell growth, metabolism, autophagy, and ribosomal biogenesis(Saxton & Sabatini, 2017) while also being altered in angiogenesis (Guertin & Sabatini, 2007) and uncontrolled proliferation (Laplante & Sabatini, 2012). Additionally, there is a strong biochemical crosstalk between c-MYC and the mTOR pathway, which plays a pivotal role in enhancing ribosomal biogenesis. MYC protein can increase the expression of genes involved in mTORC1 pathway such as S6K, 4EBP1, Rheb and eIF4E, which results in cap-dependent translation, a translation process necessary for proteins that has complex 5′UTR such as MYC, VEGF and cyclin-D1 (Chan et al., 2014). Thus, the components of translation process

like ribosomal RNA (rRNA) genes, ribosomal protein genes, and tRNA synthetases are overexpressed. Likewise, the mTORC1 pathway increases the conversion of MYC mRNA to MYC protein; therefore, this crosstalk eventually ends up with elevated ribosomal biogenesis.Additionally, MYC plays a regulatory role not only at the gene expression level, but also through epigenetic mechanisms. MYC involvement primarily affects histone acetylation and methylation states that regulate chromatin accessibility and gene expression, which are regulated by proteins such as HATs, HDACs, HMTs, and DMTs, as explained above MYC recruits HAT proteins, namely GCN5, Tip60, and HBO1, causing hyperacetylation of H3K9, H3K14, H3K18, H4K5, and H4K8 at the enhancer and promoter regions of its downstream targets, resulting in transcriptional activation(Martinato et al., 2008)(Amente et al., 2011). Moreover, promoter regions of MYC targets genes carry activating histone mark H3K4me3 even before their transcription, which suggests chromatin is primed for the binding of MYC. Thus, MYC may act as a reader and a modifier (Amente et al., 2011).

1.10. Ribosome Biogenesis

Ribosome biogenesis is a complex and highly multistep process that involves various cellular pathways and molecular events (**Figure 1.7)**. The entire process involves the maturation of 6 ribosomal RNAs (rRNAs) and the assembly of approximately 70 small nuclear RNAs (snRNAs) and 80 ribosomal proteins (RPs). In eukaryotes, ribosomes consist of two subunits, 40S and 60S, which then combine to form the functional 80S ribosome for translational activity. The 40S subunit binds to mRNA and ensures correct reading, while the 60S subunit links amino acids together through peptide bonds. However, these subunits also consist of distinct rRNAs produced by different RNA polymerases and at different locations. Initially, RNA polymerase I transcribes 47S pre-RNA from rDNA located in the nucleolus. The 47S precursor is transcribed and then processed into 28S, 18S, and 5.8S rRNA components (Dai & Lu, 2008). Meanwhile, RPs that were produced in the cytoplasm and small nucleolar RNAs are imported and assembled with these rRNAs to form ribosomal subunits. After additional cleavage and modifications with small nucleolar RNAs (snoRNAs), while the modified 18S serves as a backbone for the 40S ribosomal subunit, subsequent to the transcription of 5S rRNA with RNA polymerase III, 28S and 5.8S are assembled to form the 60S ribosomal subunit. Lastly, both subunits are transported to the cytoplasm for maturation and

assembly(Jiao et al., 2023; Ni & Buszczak, 2023) to start a functional translation process. **(Figure 1.7)**

Production of ribosomal subunits can be carried out with the recruitment of several cellular components, which initiate a feedback mechanism with related signaling transduction pathways. As mentioned before, one of the most central transcription factors is the MYC proto-oncogene, which is responsible for controlling transcription at various levels. Myc protein directly interacts and enhances the transcriptional activity of RNA polymerase I, II, and III, which results in excessive expression of tRNAs, rRNAs, structural ribosomal protein genes, exporting subunits, translation initiation factors (eIFs), and many proteins involved in transcription and translation(Van Riggelen et al., 2010a). Due to the mediator effect of c-MYC on Polymerase III by recruitment of transcription factor TFIIB, MYC causes enhanced

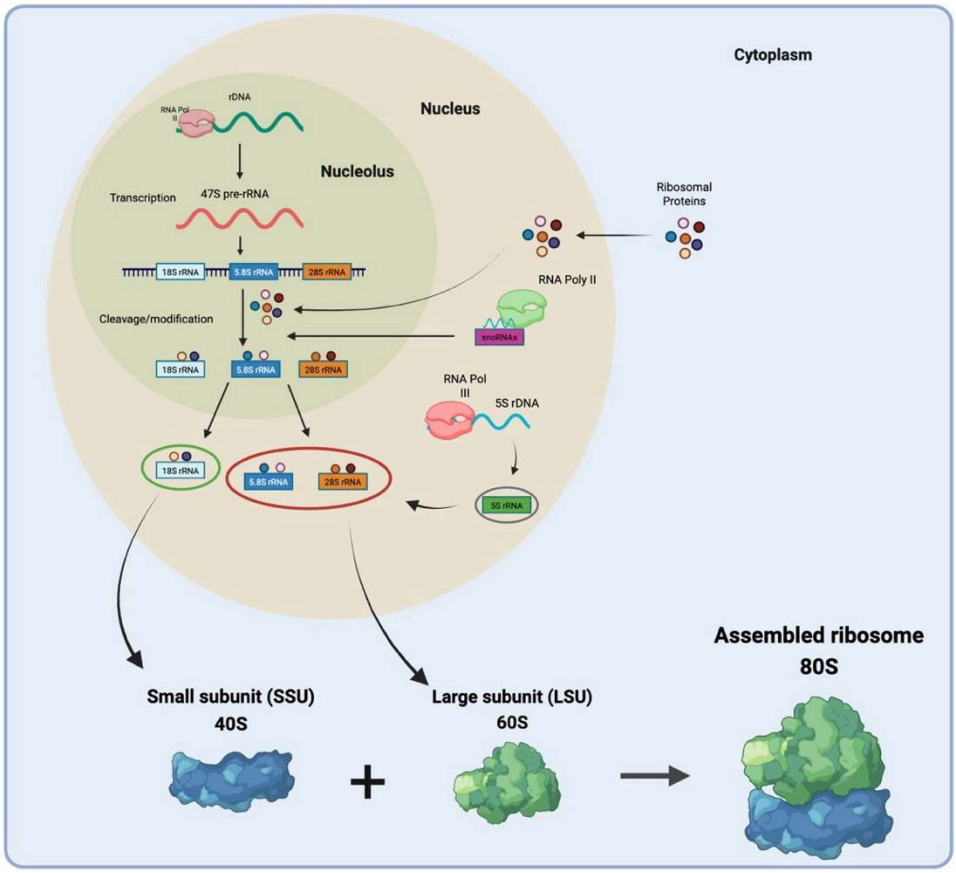

Figure 1.7 Schematic representation of ribosome biogenesis, highlighting rRNA transcription, processing, and assembly with ribosomal proteins in the nucleolus (Generated in Biorender).

transcription of 5S rRNA and tRNAs, thus intervening in the basis of ribosomal biogenesis (Gomez-Roman et al., 2003).

Moreover, a study in Burkitt lymphoma showed that the relation of MYC with its co-factor host cell factor (HCF)-1 is interrelated with ribosomal biogenesis and translation. After the MYC-HCF-1 complex is formed, independent of their existence, they interact with the chromatin of the target gene and make the local environment favorable to the recruitment of additional transcriptional regulators and units. This complex coordinates genes that are required for rRNA synthesis, also facilitating the rRNA processing and ribosomal assembly. While involved in ribosomal generation, they have a significant role in tRNA synthesis. This complex directly functions in the expression of aminoacyl-tRNA synthesis, supplement of amino acids, as mentioned before, indirectly enhances polymerase III activity, which leads to decreased aminoacylation and tRNA production, while also being one of the key regulators of global protein synthesis(Popay et al., 2021).

Importantly, linking BRD9 and MYC function, a study demonstrated that ribosomal biogenesis is also altered by the genetic or chemical depletion of BRD9 in multiple myeloma. According to the study of García et al. (2023), while MYC itself is known to be involved in ribosomal biogenesis, it is stated that there is a convergence between BRD9 and MYC. Moreover, BRD9 facilitates chromatin accessibility, impacts promoters and enhancers of ribosomal biogenesis-related genes such as rDNAs, RPs, proteases, while also, through its ability to recognize acetylated histones, eases the recruitment of factors and cofactors of transcription(Kurata et al., 2023).

1.11. tRNA Synthesis and Aminoacylation

Transfer RNAs (tRNAs) are the building blocks and adaptor molecules that carry the anticodon code that accounts for the mRNA code. In eukaryotes, tRNAs are transcribed by RNA polymerase III, and they can localize either in the nucleolus or nucleoplasm, depending on the species **(Figure 1.8)**. After transcription, to be able to increase efficiency, tRNAs must undergo some modifications. Initially, 5’ leader and 3’ trailer sequences are trimmed by endonucleases and exonucleases(Schultz & Kothe, 2024). After the remaining introns are spliced, the CCA sequence is added to the place of 3’ end through the maturation process by the tRNA nucleotidyltransferase (TRNT1). This sequence is a necessary component where

aminoacyl-tRNA synthetases attach the amino acid to this site(Schultz & Kothe, 2024; Xiong & Steitz, 2004). Subsequently, folding and modification steps follow where tRNA undergo various base and ribose modifications, whose number reaches up to 150. These modifications happen in different parts of the tRNA, such as the Acceptor stem, D-arm, Anticodon Arm, Anticodon, Variable loop, and T-arm, which provide structural stability, translational accuracy, and better codon interaction(Y. Wang et al., 2023).

The last step of tRNA maturation is tRNA aminoacylation, which takes place in the cytoplasm or mitochondria. Aminoacylation relies on enzymes called aminoacyl-tRNA synthetases (aaRSs), which connect the amino acid with its corresponding tRNA. The family of these enzymes consists of at least 20 members for each amino acid. Activating and charging the tRNA is a two-step process that starts with the entry of an amino acid and hydrolysis of an ATP molecule to the active site of aminoacyl-tRNA synthetase (**Figure 1.9)**. This step ends up with the covalent binding of AMP to the amino acid while releasing pyrophosphate. Once the AMP-aminoacyl complex is formed, the enzyme undergoes a conformational change, which leads to opening the second site where the tRNA acceptor stem docks. In the second step, the aminoacyl group is transferred to the -OH of the adenosine group at the CCA region of tRNA after nucleophilic attack. There are two classes of aaRS: type I and type II. Type I aaRS has a monomeric structure and binds amino acid to the 2'-OH, while type II aaRS has a dimeric or oligomeric structure that binds amino acid to the 3'-OH of tRNA. After properly binding, tRNA and AMP are released for further use. Additionally, aaRSs do not always work individually; instead, nine of these proteins merge with an auxiliary group of proteins named p43, p38, and p18, which are also called aminoacyl-tRNA synthetase-interacting multifunctional proteins 1, 2, and 3 (AIMP1-2-3)(Rajendran et al., 2018). This complex is called the Multi-aminoacyl-tRNA synthetase complex (MCS), which directly drives the charged tRNA to the ribosome which decreasing the translation-dependent mistakes by 10 to 100-fold (Brennan & Barford, 2009). tRNAs are dynamic and multifunctional molecules whose cellular roles extend far beyond the delivery of amino acids to the ribosome. In addition to their canonical function in translation, tRNAs have emerged as regulators of gene expression, stress sensors, and signaling molecules in various physiological contexts. Their direct interaction with amino acids during the decoding process positions them as critical

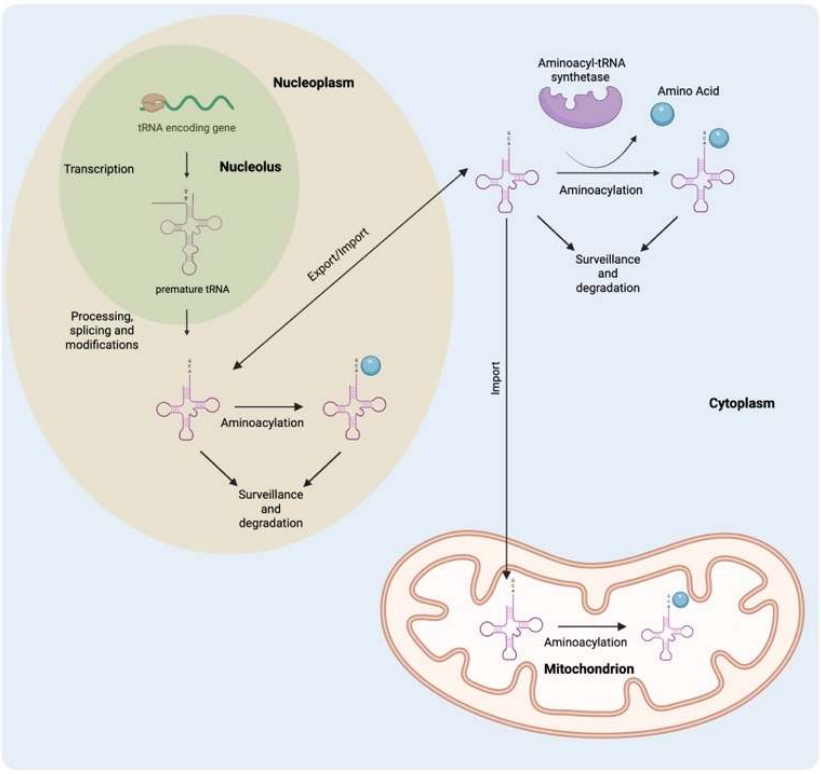

Figure 1.8 Diagram showing nuclear transcription, processing, and export of tRNAs (Generated in Biorender).

nodes for coordinating gene expression with amino acid metabolism, enabling fine-tuned responses to environmental or developmental signals(Schimmel, 2018). Likewise, tRNAs, as their producers, aaRSs, and MCS are involved in other cellular processes beyond their canonical function. Recently, researchers found that the function of aaRSs extends to cell signaling, immune response, angiogenesis, apoptosis, and cell cycle regulation. Malfunctions in these cellular processes lead to various diseases, especially cancer. aaRS expression varies depending on the cancer type(Sung et al., 2022), which indicates each aaRS has significant roles other than canonical ones. Aminoacyl-tRNA synthetases (aaRSs) contribute to tumor progression through various mechanisms, including functioning as secreted proteins, engaging in protein–protein interactions with signaling molecules, and regulating amino acid–dependent signaling pathways. For instance, the level of leucine, which is a crucial indicator of the mTORC1 pathway, is checked by Leucyl–tRNA Synthetase (LARS1) protein(J. M. Han et al., 2012). The inhibition of leucine sensor LARS1 leads to tumor regression in colon and lung cancers(Kim et al., 2017). Another example can be glutamine metabolism, which is regulated by Glutaminyl–tRNA Synthetase (QARS1) protein.

Glutamine, known as a tumorigenic amino acid, in which cell starves glutamine displays apoptotic action, while also in superabundant amounts of glutamine causes blockage to apoptosis. QARS1 can bind to apoptosis signal-regulating kinase 1 (ASK1) in a glutamine-dependent manner, which drives the cell to apoptosis(Ko et al., 2001). Additionally, Methionyl–tRNA Synthetase (MARS1) overexpression was also associated with poor prognosis of breast cancer. While the expression is correlated with HER2 positivity and advanced tumor grade, depletion of MARS1 decreased proliferation, migration, and EMT rates(Q. Jin et al., 2020; Hyeon et al., 2019).

1.12. Aim of the Study

This study builds on a previous finding that inhibition of BRD9 cooperates with radiotherapy in GBM. While the combinatorial efficacy of BRD9 inhibitors and RT have been well documented in the Brain Cancer Research and Therapy Lab, the mechanism behind BRD9 function in regulating RT response remained elusive. While chromatin remodelers like BRD9 are increasingly recognized for their roles in regulating gene expression, their specific contribution to treatment resistance in GBM remains unclear. This thesis aimed to interrogate the mechanisms by which BRD9 operates in GBM, using RNA sequencing and cell-based assays. Here, we explored how BRD9 affects key oncogenic pathways, particularly those driven by MYC, and how its inhibition can make glioblastoma cells more sensitive to radiation. From our work, we uncovered that BRD9 influences MYC expression, translation and ribosome biogenesis. By combining genetic and chemical perturbation strategies with transcriptomic and translational profiling, this work seek to provide new insights into the epigenetic mechanisms behind therapy resistance, with the broader goal of identifying novel ways to enhance the response to radiotherapy in this aggressive tumor type.

Chapter 2:
MATERIALS AND METHODS

2.1. Cell Culture

Glioblastoma cell lines U373 and U87MG, and Human Embryonic Kidney cells HEK293T cell line were acquired/obtained from American Tissue Type Culture Collection (USA). All cell lines were incubated at 5% CO2 at 37°C in Dulbecco's Modified Eagle Medium (DMEM) containing 10% FBS (Gibco, USA) and 1% Penicillin-Streptomycin (Gibco, USA). Primary glioblastoma cell lines GBM4 and GBM8 were provided by Dr. Hiroaki Wakimoto at Massachusetts General Hospital (MGH) (Wakimoto et al., 2014). Both cell lines were cultured in EF containing Neurobasal medium containing 7.5 mL L-glutamine, 1X B-27 supplement (Gibco, USA), 0.5% Pen/Strep, FGF (20 ng/ml), EGF (20 ng/ml), 0.5X N-2 supplement (Gibco, USA), and 0.5 ml heparin solution (0.2%, Stemcell Technologies, Canada). The cells were cultured at 96-well, 12-well, 6-well, 10cm, 6cm plates or T75 flasks and tested in terms of mycoplasma contamination regularly by Lonza Mycoplasma Detection Kit.

2.2. Chemical Reagents

I-BRD9 was purchased from SelleckChem, which was dissolved as 10mM and 1mM aliquots with DMSO. Translation inhibitor Thapsigargin was purchased from Cayman Chemical which was dissolved in DMSO as 10mM and 30mM. Additionally, another translation inhibitor, Cycloheximide, was purchased from Prestwick Chemicals, which was dissolved in DMSO as 10 mM. Puromycin dihydrochloride and Protamine sulfate were purchased from Sigma-Aldrich (USA).

2.3. Cell Viability Assays

2.3.1. Colony Formation

Three replicates of U373 and U87MG cells were seeded at a density of 750 cells/well in 12-well plates. The following day, cells were treated with 2 μM I-BRD9 for 72 hours, which is predetermined according to the prior studies (Değirmenci, 2024 unpublished). After the drug treatment, cells were exposed to 4 Gy of single pulse ionizing radiation. Plates were incubated for approximately 14 days. After reaching desired confluency, the medium is

aspirated, followed by double wash with 1X DBPS, and colonies were fixed with ice-cold methanol, incubating at -20°C for 15 minutes. Subsequently, each well was washed with 1X DBPS and stained with crystal violet by incubating at room temperature for 20 minutes with gentle shaking. Finally, crystal violet was discarded, and the plates were washed, left to dry. Scanned plates were analyzed by using ImageJ **(Figure 2.1)**.

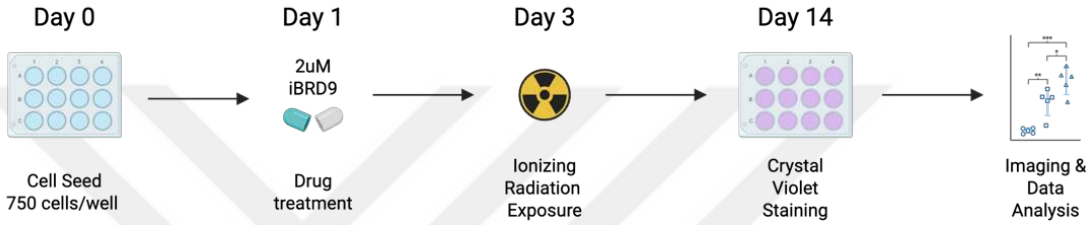

Figure 2.1 Experimental schema representation of colony formation for the period of drug and IR treatment (Generated in Biorender).

2.3.1. MTT

The viability of the cells was assessed through the MTT assay. MTT assay is a colorimetric assay that measures the metabolic activity depending on the active mitochondria. While living cells contain NADPH-dependent cellular oxidoreductase (or mitochondrial reductase) which converts the MTT substance (3-(4,5-dimethylthazolk-2-yl)-2,5-diphenyl tetrazolium bromide) into insoluble formazan (Karakaş et al., 2017). Cells were seeded with the density of 500 cells per well and treated according to the established protocol, which consisted of 3 days of I-BRD9 treatment and followed by exposure to ionizing radiation. The required quantity was calculated for the following days, and an MTT stock solution was prepared with a 3mg/ml concentration by dissolving in PBS. MTT was directly added to the culturing medium with a 1:4 ratio. After cells were incubated for 2 hours, 100 µl DMSO was added and again incubated for 15 minutes. Subsequent to crystal formation, the plate was placed into the Synergy H1 Reader (Biotek, USA) and after 2 minutes shaking, the absorbance was measured with the optical density of 570 nm.

2.4. ***Quantitative Real-Time PCR***

Firstly, RNA was isolated from related cells by using the NucleoSpin® RNA Isolation Kit according to the manufacturer's instructions (Macherey-Nagel), whose concentration was measured with Nanodrop. 1000ng of RNA was mixed with 2.5 µl of 2mM dNTPs and 1 µl of 100 µM random hexamers that resulting in a final volume of 16.5 µl. This mix was incubated at 65ºC for 5 minutes and immediately transferred to ice. In the following step, 5 µl of 5X First Strand Buffer was mixed with 2 µl of 0.1 M DTT and 0.5 µl of RNAsin. After 10 minutes of incubation at room temperature, 1 µl of M-MLV Reverse Transcriptase was added, and samples were incubated at 37 ºC for 1 hour and 70 ºC for 15 minutes for heat inactivation of RT enzyme. After that, samples were completed to 100 µl by adding 75 µl DNAse/RNAse-free H_2O. Lastly, qPCR mix, which consists of 10 µl of SYBR Green I Master (Roche), 7 µl of DNAse/RNAse-free H_2O, and 1 µl of 100 µM relevant primer, was distributed to the qPCR plate. After the addition of 2 µl cDNA to each well, the plate was centrifuged at 1300 rpm for 1 minute at room temperature. Subsequently, the plate was placed into Lightcycler 480 Instrument II (Roche), and an established protocol consisting of 30 seconds at 95 ºC, 30 seconds at 60ºC and 30 seconds at 72 ºC was carried out for 40 cycles. Gene expression levels were normalized to GAPDH, and relative quantification was performed using the 2^–ΔCT method. The primers that were used during the qPCR experiments are listed in **Table 3.1**

Table 3.1 qPCR Sequences

Gene	Forward Primer Sequence (5'-3')	Reverse Primer Sequence (5'-3')
GAPDH	AGCCACATCGCTCAGACAC	GCCCAATACGACCAAATCC
BRD9	GGTGCCAGCTGTTCCCAG	GCTTGTCGGCATAATCCTCG
MYC	TTCCCCTACCCTCTCAACGA	CAGAGAATCCGAGGACGGAG
AARS1	CCAGTGGCAGAAGGATGAAT	GCTTCAAGGCTTCATTCAGG
CARS1	TGAAGACCACGAAGGACTGC	GTGGGCAGACCATTTTCATCA
GARS1	TGCTGCTGAATGAGAAAGGGGAA	TACATGATCCTACCCAGGCCGA
WARS1	GTTTCCACGGACGCCCA	GACGCATTTCCCGCTTTGAG
YARS1	CAACCACGGGCAAACCACAT	CAGGTATGCGTGGAGGTCCG
EIF2S2	GATACCCAAACAGAGGAAACCC	CATCAGCTTCCAAATCCTTGTC
47S	GCTGACACGCTGTCCTCTG	ACGCGCGAGAGAACAGGAG
28S	AGAGGTAAACGGGGGGGTC	GGGGTOGGGGAGGAACGG
18S	GGGGCCCGAAGCGTTTACTTTG	CAAGAATTTCACCTCTAGCGGCGC
5.8S	GOGACGCTCAGACAGG	ACTCGGGCTCGTGCGTC
5S	GGCCATACCACCCTGAACGC	CAGCACCOGGTATTOCCAGG

2.5. Lentiviral Packaging and Transduction

A viral packaging system was utilized for the transduction of BRD9 guide RNA, nontargeting guide RNA (NT1), and MYC expression plasmids. The BRD9 guide RNA plasmids were derived from research conducted by a colleague in our laboratory (Değirmenci, 2024, unpublished) and the sequences used in this thesis are shown in **Table 3.2**. Initially, 2.5×10^6 293T cells were seeded into a 10 cm plate with 8 mL of DMEM +/+ and incubated until 80% confluency was reached for the lentiviral packaging process. Once the desired confluency was obtained, 375 ng of the envelope plasmid VSV-G (Addgene 8454), 3375 ng of the packaging plasmid psPAX2 (Addgene 12260), and 3500 ng of the desired transfer plasmid were mixed together. This DNA mix was completed to a final volume of 300 µL with DMEM that did not contain FBS and PS. Next, a separate mix containing 30 µL of PEI and 270 µL of serum/PS-free DMEM was prepared. The DNA mix was added to the PEI mix and incubated for 20 minutes. After the incubation, the 600 µL mixture was added dropwise to the 10 cm plates based on the virus of interest. During each viral packaging process, a control lentivirus (NT1) was generated using the plentiGuide_NT1 plasmid (nontargeting control gRNA). The medium was changed 16-18 hours post-transfection, and samples were collected at 48 and 72 hours thereafter. The collected 16 mL of medium was filtered into a Falcon tube containing 4 mL of 5X PEG8000 (Sigma P2139, dissolved in PBS at 50% (w/v)) solution using a 45-µm filter. The PEG-virus mixture was kept at +4°C for 2-3 days. After precipitation, the solution was centrifuged at 2500 rpm for 20 minutes at +4°C. The supernatant was discarded until only 1.5 mL remained, and the centrifugation process was repeated. Finally, the remaining supernatant was discarded, and the 100X concentrated virus was aliquoted into 30 µL PBS and stored at -80°C until needed. To assess viral titers, 2×10^5 cells were seeded in each well of a 6-well plate and transduced with various virus volumes (10, 1, 10^{-1}, 10^{-2} µl) in the presence of 8 µg/ml protamine sulfate. After an incubation period of 16 hours, the medium was replaced. The following day, the cells were transferred to 10 cm plates containing puromycin to select for successfully transduced cells. After completing the puromycin selection, the transduced cells were counted and compared to the uninfected, unselected parental controls. The volume of the virus corresponding to a transduction efficiency of 30-50% was used to calculate the Multiplicity of Infection (MOI), which was estimated to be approximately 0.3-0.4.

2.6. Establishing Cell Lines with MYC Overexpression or BRD9 KO

MYC overexpressing (Addgene # 98363) or BRD9 knock-out cell lines were generated by lentiviral transduction. In order to knock-out (KO) BRD9, first, cell lines that were stable in terms of Cas9 (Addgene # 52962) were necessary, and these U373 and U87MG Cas9 stable BRD9 KO cell lines were a product of collaborative research within our laboratory(Değirmenci, 2024, unpublished). After conducting a titration experiment, 1 µL of concentrated virus was determined to be sufficient for the overexpression profile with an MOI of 1. During the transduction, a mix of DMEM +/+ and 8 µg/ml protamine sulfate was added to a 6-well plate with a confluency of 10% which approximately accounts for 2×10^5 cells. Medium was changed 16-18 hours later, and the next day, cells were passaged into 10 cm dishes with fresh 2 mg/mL puromycin-containing medium. 72 hours later, selection was finalized by the addition of fresh DMEM, and cells were ready for further experimentation.

Table 3.2 Sequences for guide cloning

	Forward Sequence	**Reverse Sequence**
BRD9 gRNAs	CACCGAGGATCAACCGGTTCCTCCC	AAACGGGAGGAACCGGTTGATCCTC
NT1	CACCGCGAGGTATTCGGCTCCGCG	AAACCGCGGAGCCGAATACCTCGC

2.7. Western Blotting

2.7.1. Protein Extraction

2.7.1.1. Whole Cell Protein Extraction

Cell pellets were collected for the related experiment and washed with PBS. Later, the whole cell was lysed with RIPA lysis buffer, which was later enriched with 1mM PMSF and 1X Protease inhibitor cocktail (cOmplete Protease Inhibitor Cocktail Tablets, Roche). The solution was vortexed briefly every 30 minutes. Afterwards, the lysate was centrifuged at 13,000xg for 10 minutes at 4 °C. The supernatant was transferred into a fresh tube and stored at -80 °C.

2.7.1.2. Protein Extraction for Surface Sensing of Translation (SUnSET) Assay

Prior to pellet collection, cells were treated with 1 µg/ml of puromycin for 30 minutes and kept in the incubator. Since puromycin is a strong tRNA analog, translation is hampered due to the blockage of polypeptide elongation in the ribosome. This truncation generates puromycin-labeled polypeptides. After incubation, a routine Western procedure was conducted. The membrane was blotted with puromycin antibody, which was followed by a stripping process. All related procedures have been obtained from Schmidt et al. and briefly shown in **Figure 2.2** (Schmidt et al., 2009).

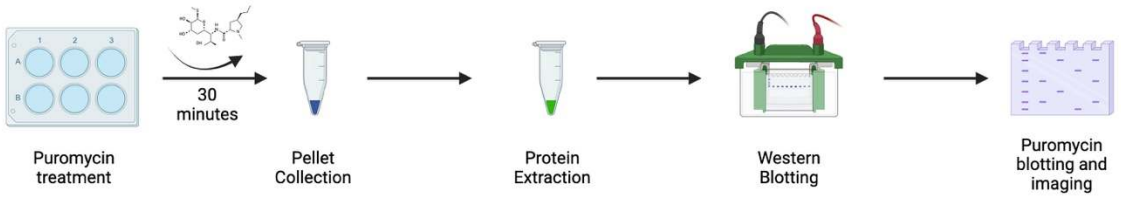

Figure 2.2 Schematic representation of the SUnSET assay workflow used to assess translational activity (Generated in Biorender) **.**

2.7.1.3. Histone Extraction

For histone extraction, cells were harvested and washed with ice-cold PBS. This process is followed by resuspension of the pellet with Triton extraction buffer (TEB), which is PBS containing 0.5% Triton X-100 (v/v), 2 mM phenylmethylsulfonyl fluoride (PMSF), and 0.02% (w/v) NaN3. Resuspension was performed at 1 mL per 10^7 cells. Following this, cells were gently stirred on ice for 10 minutes and centrifuged at 6,500 x g for 10 minutes at 4°C.

Supernatant was discarded, and the pellet was washed with TEB with half of the first resuspension volume. Lysate was centrifuged under the same conditions and resuspended in 0.2N hydrochloric acid (HCl) at 1 mL per $4x10^7$ cells. Lysate was centrifuged in a rotator overnight at 4 °C. The Next day, the solution was neutralized with 1M sodium hydroxide (NaOH) with 1/5 of the HCl solution added at prior day. Samples were centrifuged as before, and the supernatant, which contains histones, was transferred into a fresh tube and stored at -80 °C.

2.7.2. Protein Quantification and Western Blot Protocol

Protein concentration in the samples was determined by using Pierce BCA Protein Assay Kit (Thermo Scientific, 23225, USA), and the process was conducted according to the manufacturer's guidelines. The absorbance of the resulting plate was measured at 562 nm in the Synergy H1 Reader (Biotek, USA). After assessment of the protein concentration in each sample, 20 µg of protein was mixed with the 5 µL 4X Laemlli buffer (Bio-Rad, 1610747, USA) containing 10% beta-mercaptoethanol and diluted into 20 µl with Nuclease Free Ultra-Pure Water (ECOTECH, DW010L, Turkey). After the protein mix was prepared, the sample was heated at 95 °C for 10 minutes and transferred directly to ice. Subsequently, the samples were loaded onto 4-12% Mini Protean TGX Precast Polyacrylamide Gels (Bio-Rad, 456-1044) with a volume of 30 µl or 50 µl for each well. The gels were placed into a tank filled with 1X TGS (Ecotech), and the samples were run with gel electrophoresis for 60 minutes at 100 V. Afterwards, the proteins were transferred to PVDF membrane by using Trans-Blot Transfer System (Bio-Rad, USA) for 30 minutes at 30V and 1mA. 1X TGS(Ecotech) containing 20% (v/v) of absolute methanol was used as the transferring buffer. In the next step, the membrane was placed in a blocking solution prepared with % 5% non-fat dry milk dissolved in 1X TBST, which was prepared prior to the experiment and incubated for 1 hour at room temperature on a shaker. Blocking solution was discarded, and the membrane was washed three times for 10 minutes at room temperature in 1X TBS-T solution. The blot was incubated with the primary antibody overnight at 4 °C on a shaker. The antibodies that are used for these experiments are listed in the **Table 3.3.** The next day, the primary antibody was collected and returned to its original tube. After three washes each for 10 minutes with 1X TBS-T, the membrane was incubated on a shaker with the secondary antibody for 1 hour at room temperature. Lastly, the membrane was subjected to the washing step again and

incubated with ClarityTM Western ECL Substrate (Biorad, Philadelphia, PA, USA) for 2 minutes. The visualization was achieved by Odyssey Fc Imager and analyzed with LiCor software (LiCor Biosciences, Lincoln, NE, USA). If necessary, the membrane blot was stripped with 1M NaOH for 20 minutes at room temperature for removal of all bindings, including blocking and primary-secondary antibody, which necessitates the need to repeat the blotting process. Mostly, stripping was used for histone extract and SUnSET samples to validate the housekeeping protein translation.

Table 3.3 Primary antibody list used in western blotting.

Antibody	**Catalog number**
GAPDH	Abcam/ab9485
BRD9	Invitrogen/PA5-110872
MYC (D3N8F)	Cell Signaling/13987
Anti- Histone H3 Total (D1H2)	Cell Signaling/ 4499
Anti- Histone H3K9ac (C5B11)	Cell Signaling/9649T
Anti- Histone H3K14ac (E3Q6W)	Cell Signaling/7627T
Anti- Histone H3K18ac (E2A8S)	Cell Signaling/13998T
Anti- Histone H3K27ac (D5E4)	Cell Signaling/13969S
Anti- Histone H3K27me3 (C36B11)	Cell Signaling/ 9733S
Anti- Histone H3K4me3 (C42D8	Cell Signaling/ 9751
Anti- Histone H4K5ac (D5G4S)	Cell Signaling/8647S
Anti- Histone H4K8ac (D20F3)	Cell Signaling/2594S
Anti-Puromycin (4G11)	Sigma-Aldrich/MABE343

2.8. RNA Sequencing and Analysis

RNA samples required for sequencing were isolated from the cell pellets of U373 DMSO, U373 I-BRD9, U87 DMSO, U87 I-BRD9, U373 NT1, U373 BRD9 KO, U87 NT1, and U87 BRD9 KO groups, with three biological replicates for each condition, using the Macherey-Nagel NucleoSpin® RNA Isolation Kit. The purity and concentration of the isolated RNAs were subsequently measured using a NanoDrop 2000. U373 DMSO- I-BRD9, U373 NT1-

BRD9 KO, and U87 DMSO- I-BRD9 samples were prepared and sequenced according to the protocols of the BGISEQ-500, while the U87 NT1-BRD9 KO sample was sent to Oxford University NDORMS for preparation and sequencing by Adam Cribbs. The raw FASTQ files were uploaded to the Genialis Expressions Platform (Texas, USA) for analysis. First, paired-end reads underwent quality filtering and adapter trimming using BBDuk. Then the reads were aligned by the STAR alignment method, and transcripts were quantified through the Salmon RNA sequencing pipeline. MultiQC was used to summarize quality control metrics across all samples. Differential expression analysis was performed by applying a false discovery rate (FDR) threshold of 0.1 and a $\log_2FC = 0$ cutoff.

Heatmaps were generated for visualization of differentially expressed genes and were generated by using Genialis. Volcano plots were generated using the list of differentially expressed genes, with $\log_2$ fold-change and $-\log_{10}$ p-value as plotting parameters in GraphPad software, while heatmaps were generated in Genialis software. Pathway analysis was performed using Enrichr, which is a gene set enrichment analysis tool that employs MSigDB and Reactome gene sets and can be accessed from the Genialis platform. Graphs were generated using Python 3.9.

2.9. Statistical Analysis

All calculations were normalized to the control group, which was defined as 100%. Statistical analyses were performed using GraphPad Prism (USA) version 10.0 and Microsoft Excel Office 2024. Significance was determined by Student's t-test or one-way and two-way ANOVA, with a p-value of <0.05, * $p< 0.05$, **** $p<0.0001$.

Chapter 3:
RESULTS

3.1.1. Impact Of BRD9 Perturbation with/without Radiation Exposure on Cell Viability And Proliferation of Human Glioblastoma Cell Lines U373 and U87MG

3.1.2. BRD9 Inhibition and/or Radiation in U373 and U87MG

According to previous work in our lab, I-BRD9 was selected our main drug to accomplish radiosensitizer effect on GBM when cells combined with radiation treatment. Initially, cells were treated with 2 μM of I-BRD9 for 72 hours followed by a predetermined 4 Gy of ionizing radiation. To investigate the change in the cell viability, colonies were incubated for 14 days, as shown in **Figure 3.1.A,** the colonies were stained with crystal violet, and the colony numbers were quantified. Accordingly, the combinational treatment decreased the colony formation capabilities of both GBM cells, U373 and U87 MG GBM cells. The quantifications were shown in **Figure 3.1.B and C**. Simultaneously, an MTT assay was also conducted to investigate the impact of IR and/or I-BRD9 in a time-dependent manner. In **Figure 3.1.C and D**, which shows the quantification of MTT results, the viability increases in U373 and U87 MG DMSO-treated samples were clearly observed over time. However, on day 4, the combination effect was more evident in both cell lines.

A

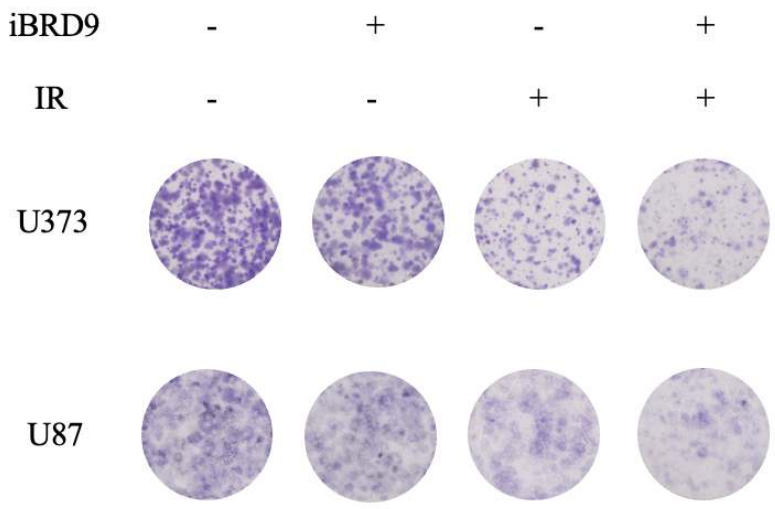

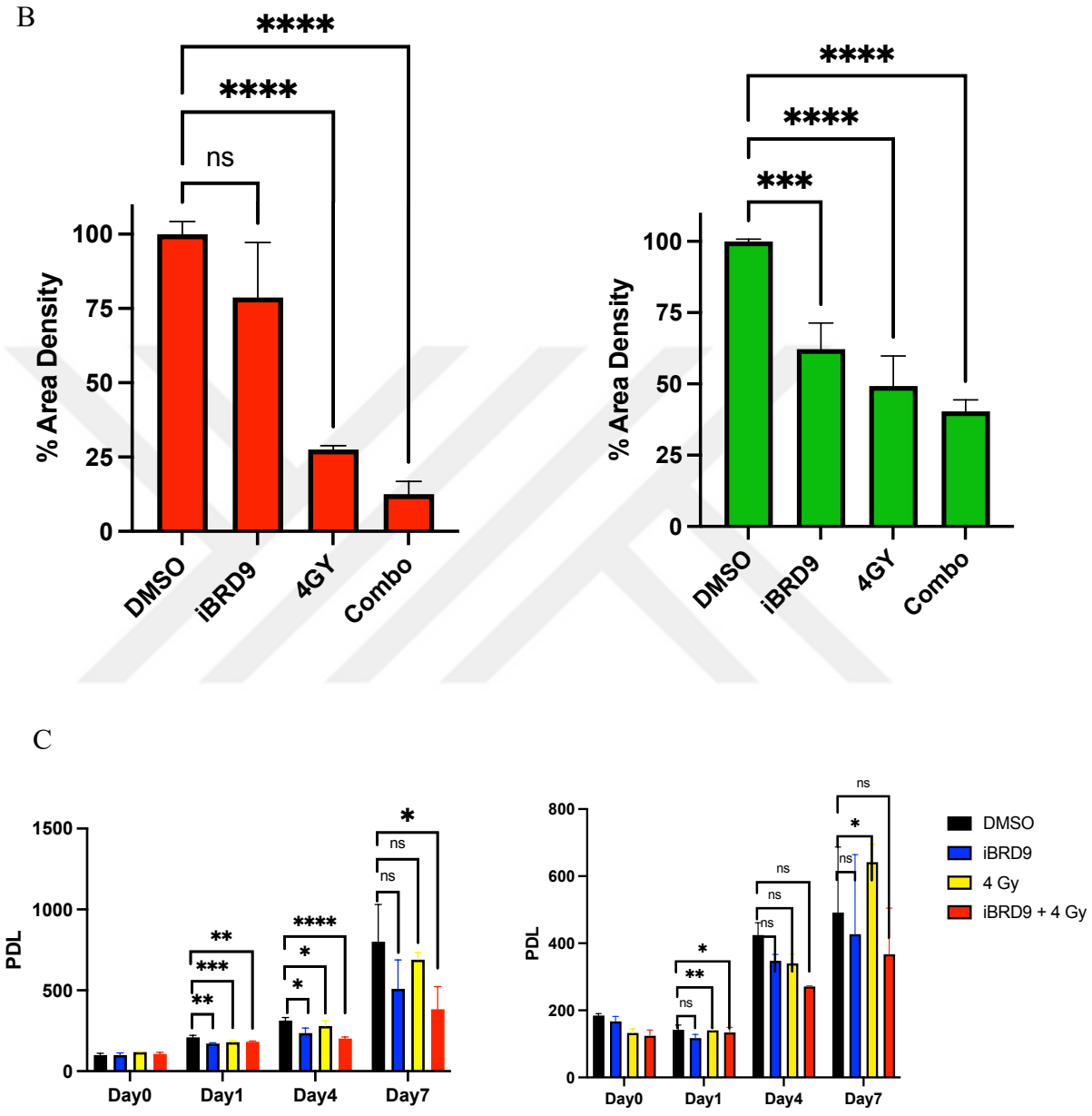

Figure 3.1 Effect of BRD9 inhibitor and/or radiation on U373 and U87 cell viability A) Representative image of colony formation assay B) Quantification of colony numbers * p< 0.05, **** p<0.0001 C) MTT assay first for U373 second for U87 MG quantification * p< 0.05, **** p<0.0001.

3.1.3. BRD9 Knock Out and/or Radiation in U373 and U87

After BRD9 inhibitor was identified as a potential radiosensitizer, CRISPR/Cas9-based gene knockout was performed. Initially, U373 and U87 MG BRD9 knockout cell lines were generated, and their BRD9 protein expression levels were assessed by Dr. Nareg Degirmenci, a former PhD student who identified BRD9 inhibitors as radiosensitizers in glioblastoma as part of her doctoral thesis. Western blotting was conducted to assess BRD9 depletion in both cell lines, which are shown in **Figure 3.2.A**. The results show BRD9 downregulation, rather than complete loss of expression. Six days after guide RNA transduction, cells were seeded into 12-well plates, and they were exposed to ionizing radiation (IR) the following day. As illustrated in **Figure 3.2.B**, U373 cells tolerated BRD9 depletion alone but were significantly impaired when BRD9 knockout was combined with IR treatment. In contrast, U87 cells showed a substantial reduction in colony formation with BRD9 knockout alone, and radiation had no additional effect. Quantitative results of the clonogenic assay are shown in **Figure 3.2.C.**

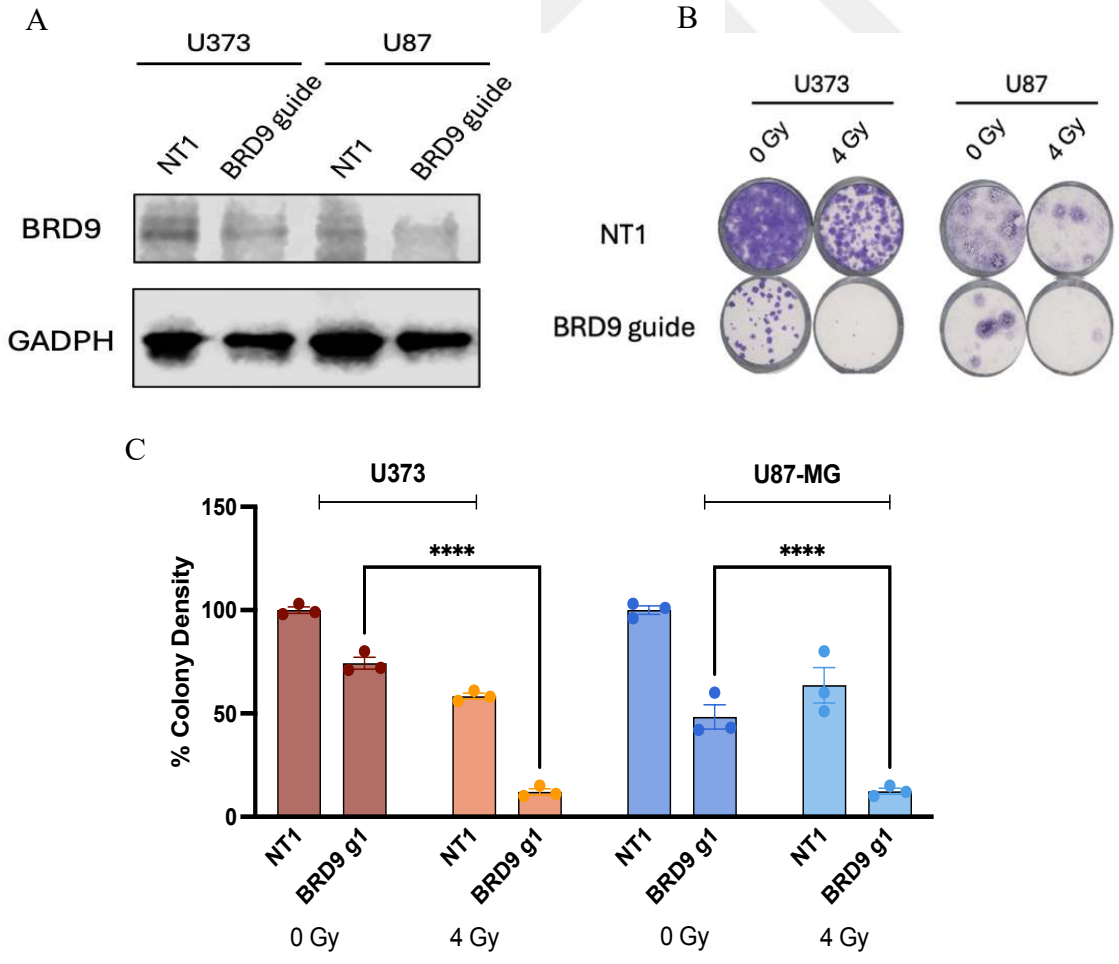

Figure 3.2 Effect of BRD9 knockout and/or radiation on U373 and U87 cell viability. A) Western blot validation of BRD9 knockout in U373 and U87 cells using BRD9-specific guide RNAs. GAPDH served as a loading control. B) Representative images of colony formation assay following BRD9 knockout and 4 Gy ionizing radiation. C) Quantification of colony density in U373 and U87 cells. ****p<0.0001.

3.2. Epigenetic Alterations in U373 upon I-BRD9 and/or IR Treatment

Since BRD9 is an acetyl reader protein, we investigated the global epigenetic alterations in U373 upon I-BRD9 and/or IR treatment. Known histone marks of BRD9 are H3K27ac, H3K4me1, H3K4me3, H3K9ac and H3K18Ac, however we also investigated additional marks, such as H3K27me3, H4K5ac and H4K8ac, as epigenetic modifications can indirectly lead to alterations in other histone marks. Each of the protein-transferred membranes were blotted with respective antibody and stripped subsequently for H3 total blotting. Most of the histone marks in the **Figure 3.3.A** are related with transcription activation. While H4K5ac and H4K8ac is about euchromatin, H3K4me3 and H3K9acindicates promoter activation (Kouzarides, 2007). H3K27ac and H3K18ac is related with enhancer activation (Creyghton et al., 2010). Unlike the others, H3K27me3 is correlated with transcriptional repression (Schuettengruber et al., 2007). All analysis were done with LiCor software and done by normalizing the absorbance of the mark to its H3 total. Then the values were again normalized to the DM SO-H3 normalization.

Accordingly, the H3K27me3 mark wasn't altered with any kind of treatment, which shows there is no I-BRD9 dependent repressive marks (**Figure 3.3.A, B**). Radiation alone increased the levels of H3K4me3, H3K18ac, H3K9ac and especially in H3K27ac, which are related with enhancers and promoter accessibility (**Figure 3.3.A, B**). When I-BRD9 treatment was combined with radiation, these increases were reversed. These indicates there is an interference of BRD9 inhibition to the effect of radiation. The other marks such as H4K5ac and H4K8ac, although showed some change in the acetylation profile individually, the radiation and/or I-BRD9 treatment did not display any strong change (**Figure 3.3.A, B**).

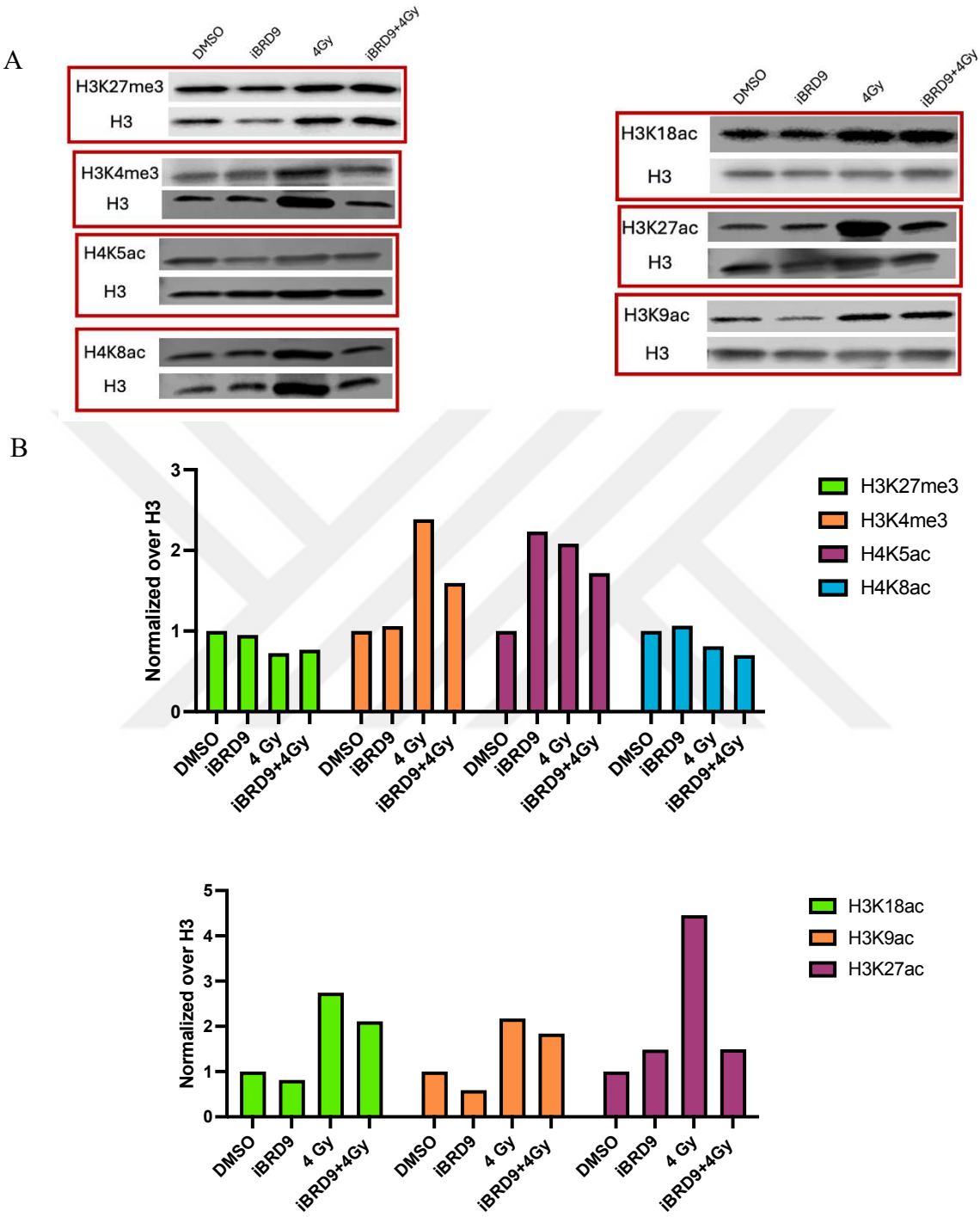

Figure 3.3 Western blot and quantification of histone modifications upon BRD9 inhibition and/or radiation. A) Levels of various histone acetylation and methylation marks were assessed in U373 cells treated with DMSO, iBRD9 (2 μM), 4 Gy IR, or their combination. B) Quantification of each modification was performed by normalizing band intensities to total H3 levels.

3.3. Transcriptomic Analysis of Genetic and Chemical Inhibition of BRD9 in U373 and U87MG Cells Showed Differentially Expressed Genes

Our previous results suggest that U373 and U87MG cell viability and proliferation capability decrease upon I-BRD9 treatment for 72h, followed by exposure to 4 Gy of ionizing radiation treatment. Moreover, the same impact has been obtained upon genetic manipulation of BRD9. To be able to knock out BRD9 in U373 and U87MG cells, a CRISPR/Cas9-based system was used. After cells were transduced with Cas9 and selected with Blasticidin, cells were transduced with BRD9 gRNA lentivirus and selected with puromycin. Selections continued for 3 days and 9 days after initial transduction; cells were exposed to ionizing radiation according to the experiment setup. Rather than focusing on the combined effect of BRD9 loss and ionizing radiation, our primary aim was to investigate how BRD9 inhibition—either through chemical compounds or CRISPR-mediated knockout—affects cellular mechanisms on its own. To assess transcriptomic alterations resulting from the absence of BRD9 activity, samples were collected according to the treatment conditions described above. Once RNA quality was confirmed for each triplicate sample, the samples were submitted for RNA sequencing.

3.3.1. Distinct Transcriptomic Profiles upon Genetic vs Chemical Targeting of BRD9 in U373 and U87MG

3.3.1.1. U373 DMSO vs I-BRD9

PCA plots generated based on the analysis of sequencing data reveal that the variance between replicates was low, especially in the control group. The PCA plot showed a 39% of distinct PC1 separation between BRD9-inhibited samples, which suggests that BRD9 inhibition leads to a distinct transcriptomic shift. Additionally, the clustering of control replicates indicated low intra-group variability. In total, there were 6125 genes that were differentially expressed. While 3340 genes were downregulated, 2785 genes were upregulated shown in (**Figure 3.4.B**). The distribution of differentially expressed genes in the volcano plot show chemical inhibition of BRD9 tends to transcriptional repression, as the blue dots indicate. Additionally, when the downregulated genes were subject to gene set analysis, the significantly downregulated pathways were revealed as MYC target V1, mTORC1 signaling, and EMT, while also hypoxia-related pathways, TNF-, and E2F targets

were altered upon I-BRD9(**Figure 3.4.C**). Together, these findings suggest that chemical inhibition of BRD9 disrupts key regulatory programs related to cell growth, proliferation, metabolic activity and induces a transcriptional response associated with cellular stress adaptation (**Figure 3.4**).

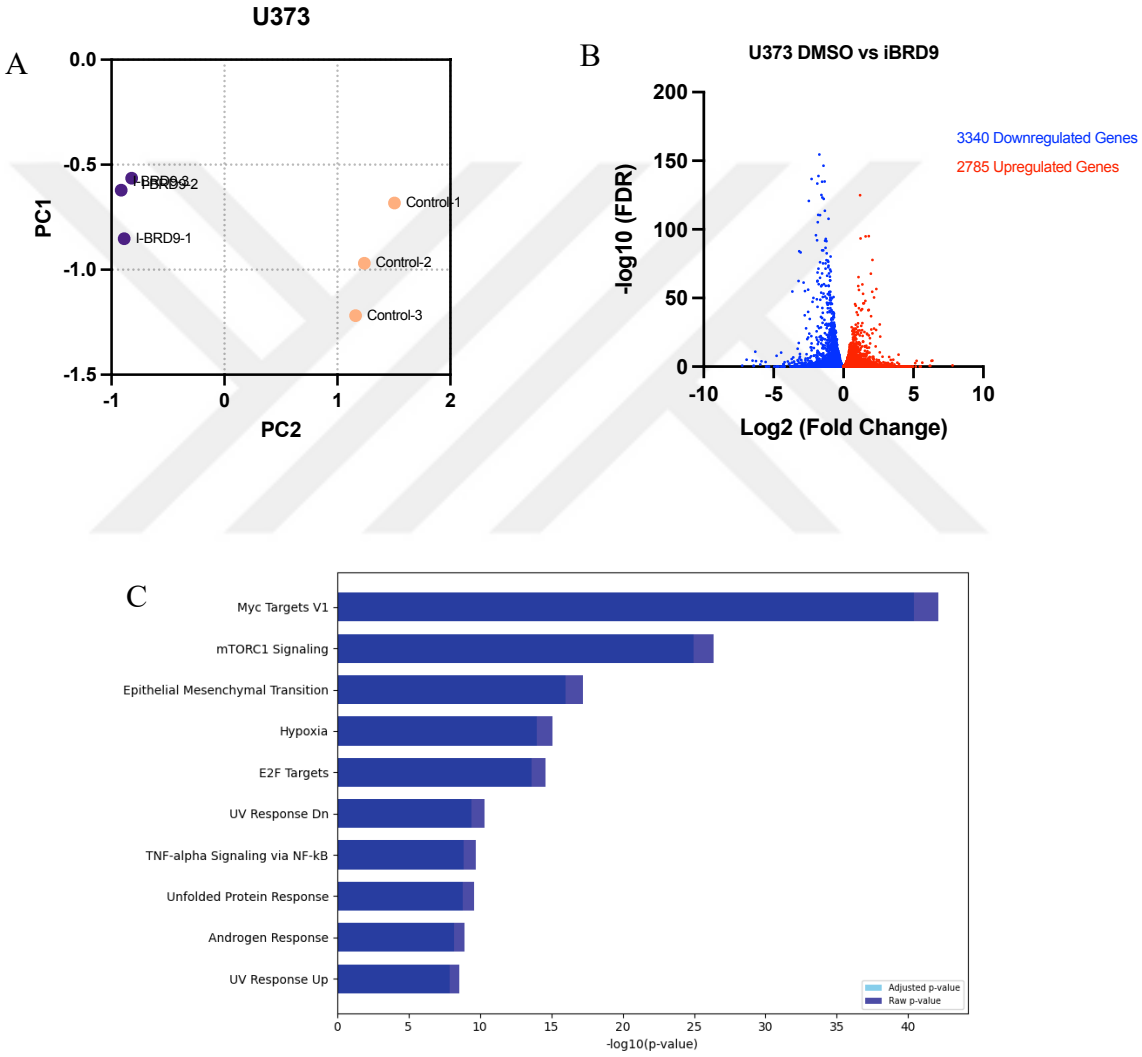

Figure 3.4 Transcriptomic analysis of U373 cells upon BRD9 inhibition. A) Principal component analysis (PCA) shows clear separation between 1BRD9-treated and control samples. B) Volcano plot depicts differentially expressed genes with 3340 downregulated (blue) and 2785 upregulated (red) genes (FDR < 0.1). C) Pathway analysis reveals significant variance of MYC targets V1, mTORC1 signaling, and other key oncogenic pathways.

3.3.1.2. U373 NT1 vs BRD9 KO

In the knock-out samples, the divergence between replicates was also minimal and the clusters were tight, especially in non-targeting samples. The variance in PC1 was 37% which indicates a significant shift in transcriptomic level between the two clusters. In knock-out samples, 6056 genes were differentially expressed. 3044 genes were upregulated, and 3012 genes were downregulated, which is shown in the volcano plot **Figure 3.5.B**. These results suggest that depletion of BRD9 causes a clear transcriptional response. Pathway analysis revealed that the differentially expressed genes were most significantly shifted hallmark pathways, involving TORC1 signaling, MYC targets V1, and hypoxia-related response, while also the G2-M checkpoint, oxidative phosphorylation, and glycolysis pathways were downregulated (**Figure 3.5.C.)** These findings indicate that the transcriptional program was largely altered in terms of MYC-driven signaling, cell cycle progression and proliferation, metabolic regulation, and cellular stress response mechanisms.

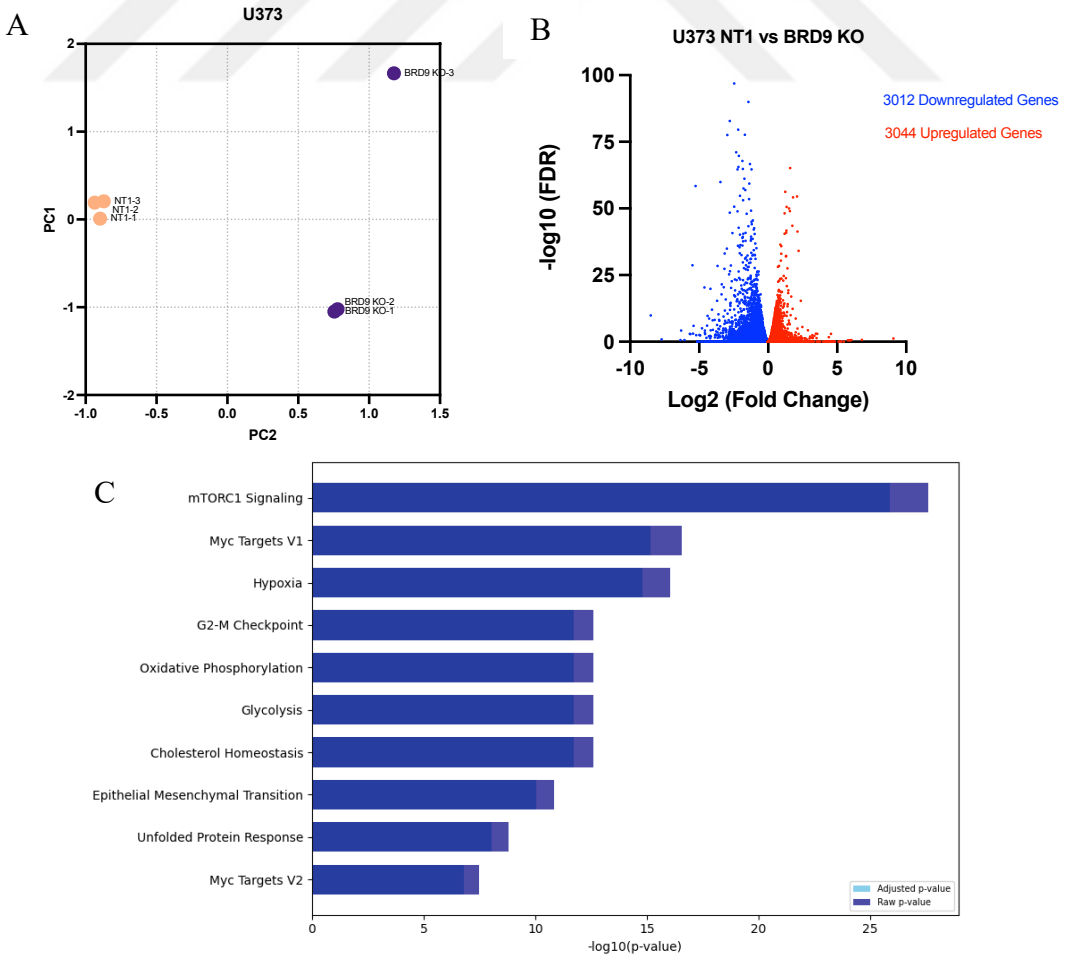

Figure 3.5 Transcriptomic analysis of U373 cells following BRD9 knockout. A) A) PCA plot demonstrates distinct clustering of BRD9 KO and NT1 control samples. B) Volcano plot shows differential expression with 3012 downregulated and 3044 upregulated genes (FDR < 0.1). C) Pathway analysis of downregulated genes reveals significant enrichment of mTORC1 signaling, MYC targets V1, and other key

3.3.1.3. U87MG DMSO vs I-BRD9

The replicate variance in control samples was low, while minimal in drug-treated U87MG samples. Total deviation was 55% (**Figure 3.6.A**).; the sum of the principal component percentages indicated a significant shift in the transcriptomic profile between treatment conditions. Expression analysis identified 3,102 differentially expressed genes (DEGs), consisting of 1,567 downregulated and 1,535 upregulated (**Figure 3.6.B**). As shown in the volcano plot, a substantial portion of genes that have higher statistical significance were downregulated genes. This trend was consistent with previous plots, which indicates a dominant downregulatory effect under BRD9 inhibition. Moreover, the downregulated gene set was enriched in pathways including MYC targets V1, mTORC1 signaling, E2F targets, DNA repair, and oxidative phosphorylation (**Figure 3.6.C**). Many of these pathways were altered in previous comparisons, suggesting a conserved transcriptional signature associated with genetic and chemical manipulation of BRD9 in U373.

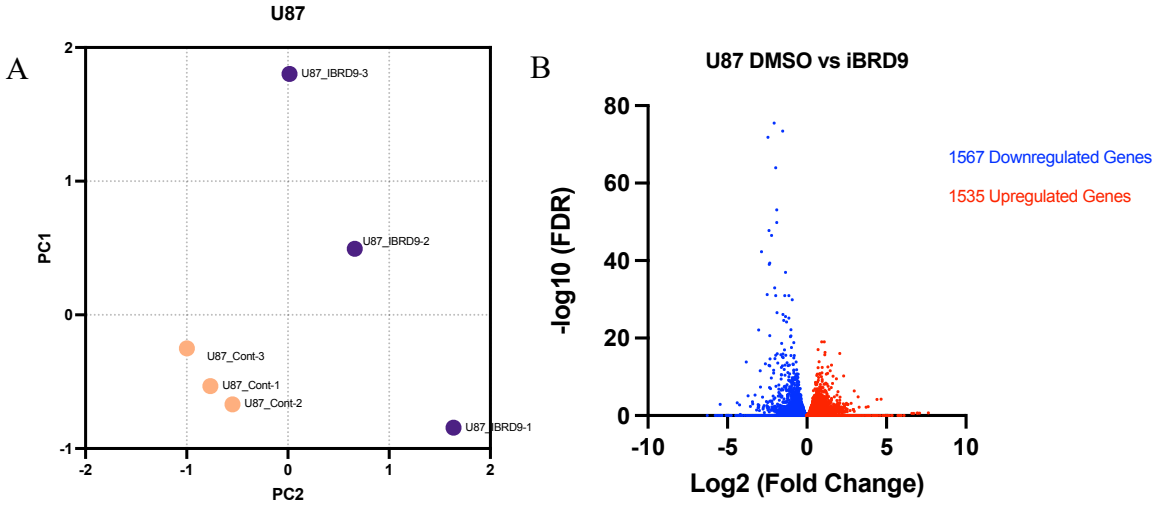

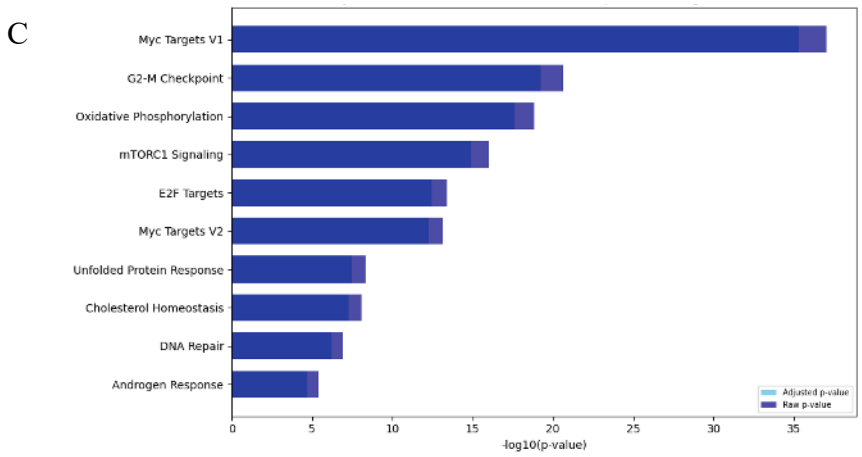

Figure 3.6 Transcriptomic analysis of U87MG cells following BRD9 inhibition. A) PCA plot demonstrates clear separation between I-BR D9 -treated and DMSO control groups. B) Volcano plot reveals 1567 downregulated and 1535 upregulated genes (FDR <0.1). C) Pathway analysis with downregulated genes indicates significant alterations in MYC targets V1, G2-M checkpoint, oxidative phosphorylation, and mTORC1 signaling.

3.3.1.4. U87MG NT1 vs BRD9 KO

The PCA plot showed a distinct separation between BRD9 knockout and non-targeting control samples along PC1, which explains 35% of the total variance(**Figure 3.7.A**). Replicates within each group were closely clustered, indicating minimal variation within conditions. In this comparison, 3,290 transcripts were found to be differentially expressed. Among them, 3,032 genes were downregulated, while 258 were upregulated. Similar to previous findings, most of the significantly affected genes were reduced in expression (**Figure 3.7.B**). This demonstrates that BRD9 knockout leads to a strong downregulatory effect on the transcriptome, consistent with the trend observed in the I-BRD9-treated group. Assessment of altered pathways showed that similar results to I-BRD9-treated U87MG, which includes MYC target V1, oxidative phosphorylation, G2/M checkpoint, and E2F targets (**Figure 3.7.C**). These pathways show the critical role of BRD9 in regulating gene networks involved in proliferation, mitochondrial activity, cell cycle progression, and transcriptional amplification.

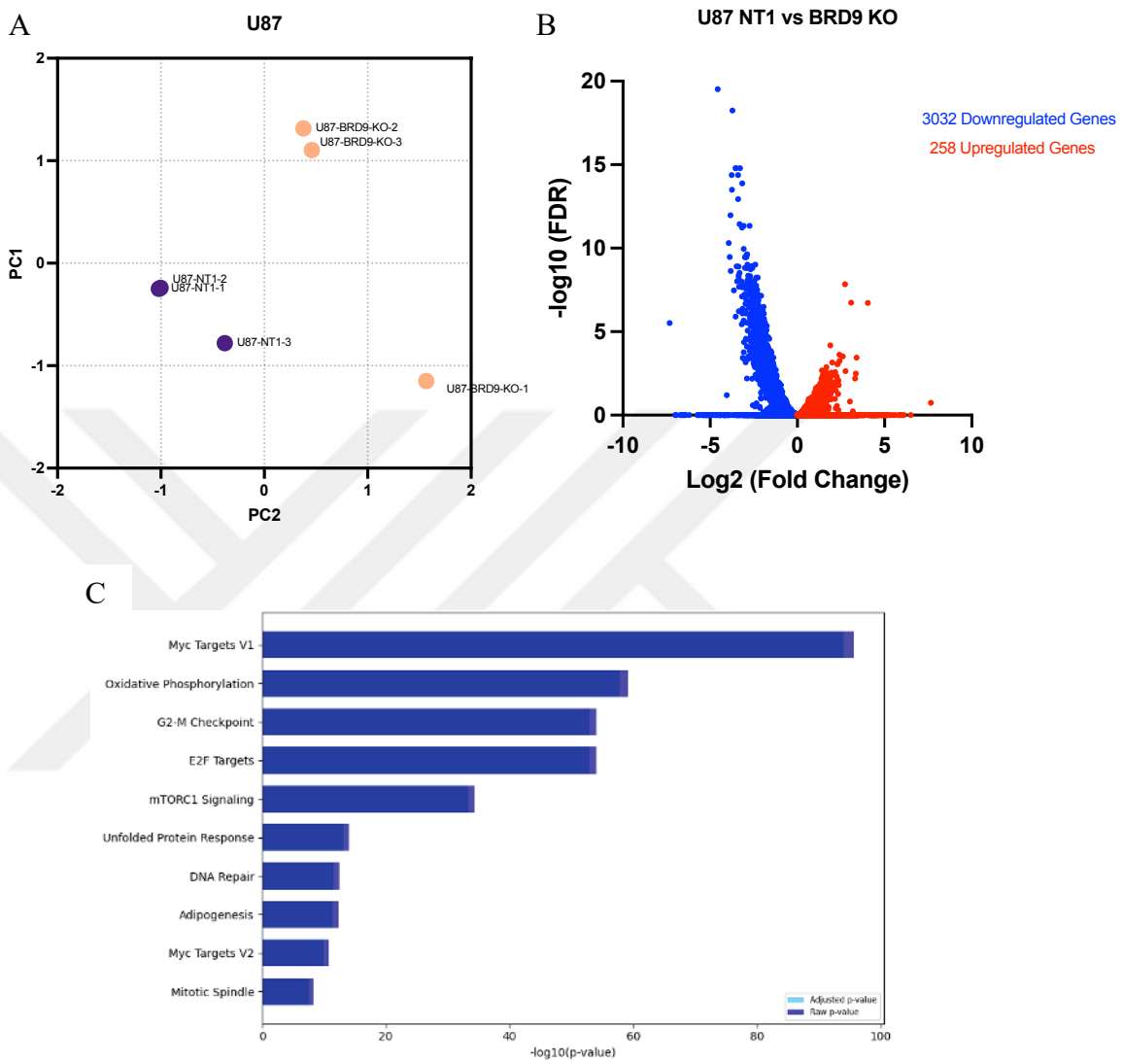

Figure 3.7 Transcriptomic analysis of U87MG cells following BRD9 knockout. A) PCA plot shows distinct separation between BRD9 KO and NT1 control samples. B) Volcano: plot indicates 3032 downregulated and 258 upregulated genes (FDR < 0.1). C) Pathway analysis reveals with downregulated genes indicates significant alterations in MYC targets V1, oxidative phosphorylation, G2-M checkpoint, and mTORC1 signaling.

3.3.2. Identification of Common Genes Across BRD9-Targeted Datasets in U373 and U87MG Cells and Their Functional Enrichment Through MSigDB and Reactome

The commonality was searched between downregulated genes among all RNA sequencing data, and the gene sets were compared with each other. After comparison, 31 shared genes were identified (**Figure 3.8.A**). These genes were assigned to several cellular processes such as tRNA synthesis, RNA processing, protein degradation, membrane transportation, and cell adhesion proteins. Subsequently, these 31 genes were subjected to the pathway analysis to understand which pathways were downregulated in common between two different GBM cell lines and two different models of inhibition.

To gain insights into the biological relevance of these commonly downregulated genes, pathway analysis was conducted using MSigDB and Reactome databases (**Figure 3.8.C, Figure 3.8.D**). As a result, consistent with the pathway analysis of individual RNA sequencing, MSigDB analysis revealed significant involvement of gene sets related to regulatory programs, specifically highlighting the MYC target pathway v1, epithelial-mesenchymal transition, and G2/M checkpoint. Reactome analysis identified tRNA aminoacylation, cytosolic tRNA acetylation, and translational pathways as particularly striking molecular pathways in our dataset.

A

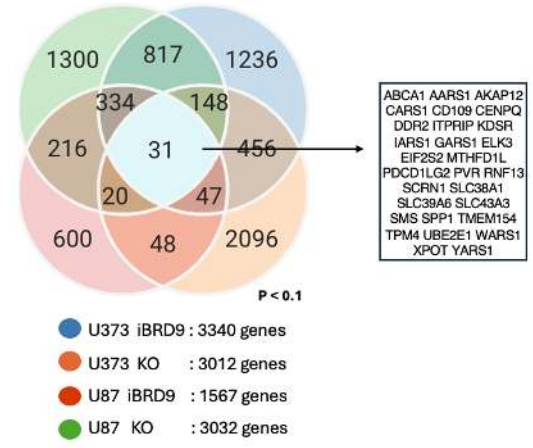

B

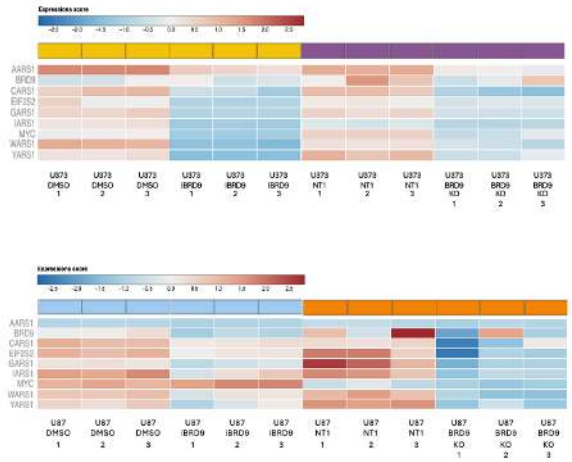

C

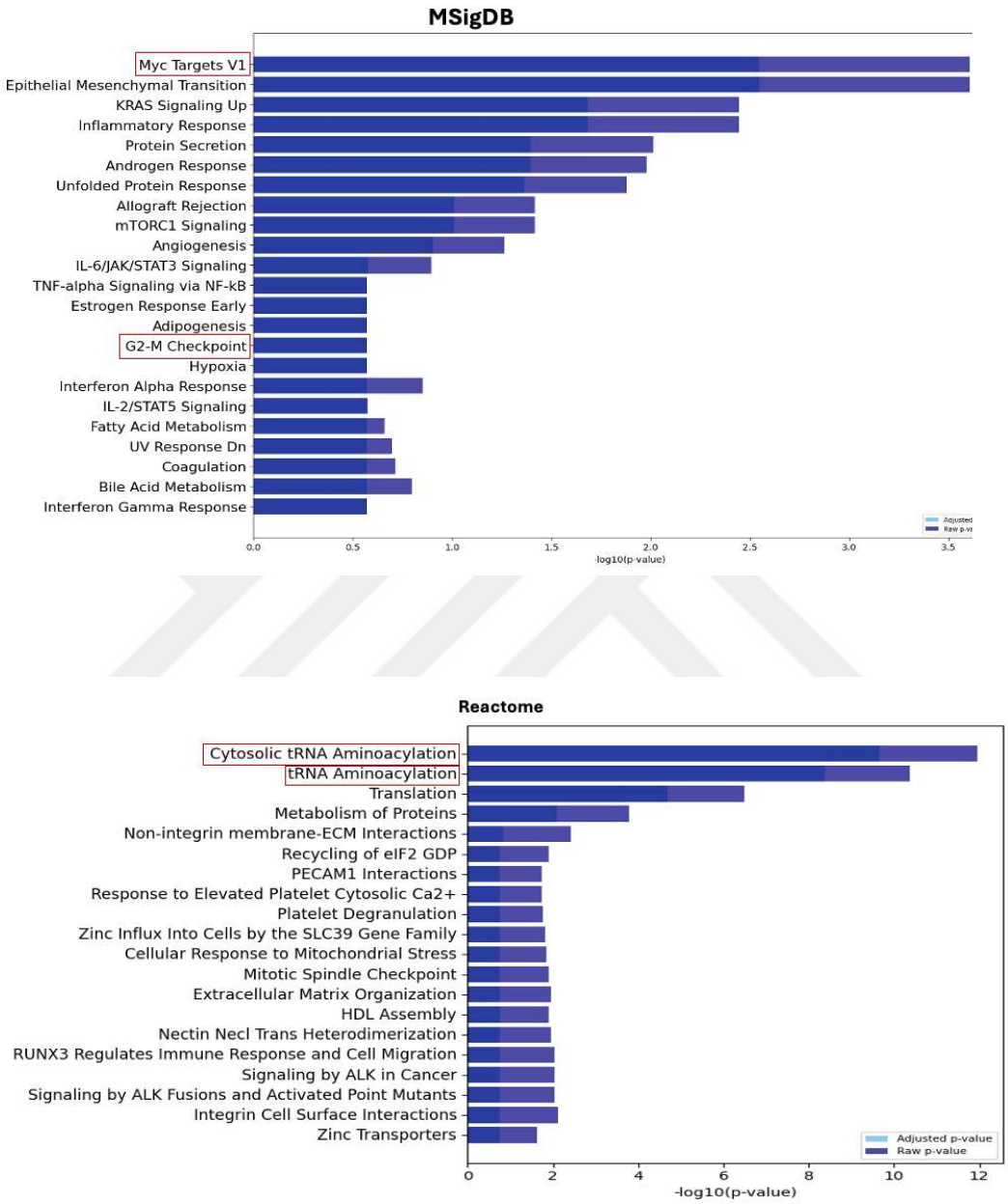

Figure 3.8 Combined transcriptomic analysis of four RNA-seq datasets. A) Venn diagram illustrates 31 genes commonly downregulated across U373 and U87 cells treated with either BRD9 inhibitor or BRD9 knockout. B) Heatmaps show consistent downregulation of these - genes across all treatment conditions. C) Pathway analyses (first MSigDB and Reactome) reveal variance in MYC targets, tRNA aminoacylation, translation, and cell stress - response pathways.

3.3.3. Validation of Commonly Downregulated Genes After BRD9 Perturbation

The downregulated genes that are common to all 4 RNA sequencing analysis revealed the alterations in tRNA synthesis and translation, aminoacyl tRNA synthetases and translation-related EIF2S2 genes. Therefore these genes, namely, AARS1, CARS1, GARS1, WARS1, YARS1 and EIF2S2 were selected as targets. In order to confirm the changes observed with RNA sequencing, qPCR was conducted for each treatment condition and cell line. Apart from checking the expression of the genes selected, BRD9 was also investigated. All qPCR calculations were normalized to GAPDH as the housekeeping gene. Accordingly, the expression of translation-related genes was downregulated upon I-BRD9 treatment or BRD9 KO in U373 cells; but the effect was not as striking with I-BRD9 treatment as it was with BRD9 KO (**Figure 3.9.A**). The genetic targeting of BRD9 was evident in both U373 and U87MG cells, as BRD9 expression was lowered in both cell lines and BRD9 KO decreased the expression of all selected genes by more than 50% (**Figure 3.9.A and 3.9.B)**.

A

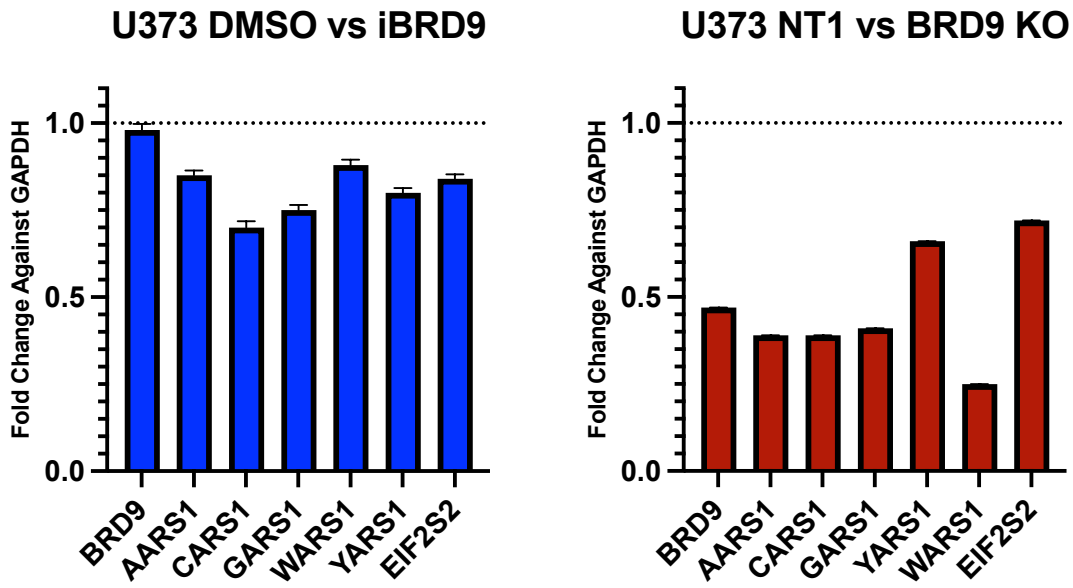

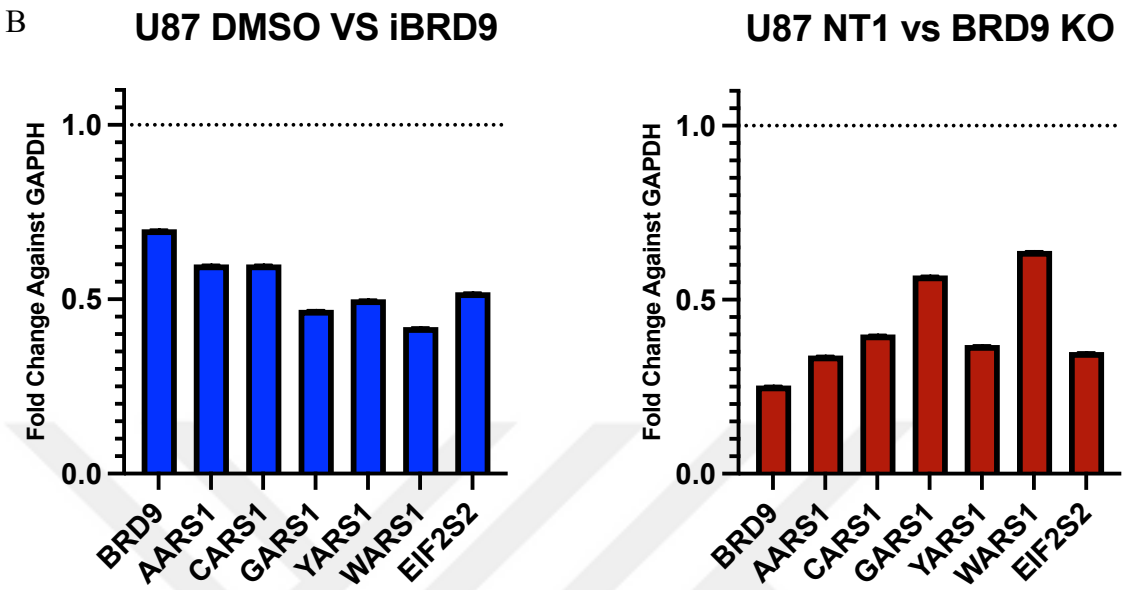

Figure 3.9 BRD9 perturbation leads to transcriptional downregulation of translation-related genes. A) qPCR analysis of BRD9, aminoacyl-tRNA synthetases (AARS1, CARS1, GARS1, YARS1, WARS1), and EIF2S2 in U373 cells upon chemical inhibition (I-BRD9) and genetic knockout of BRD9 B) Same targets analyzed in U87MG cells under identical treatment conditions. All values were normalized to GAPDH. While I-BRD9 treatment modestly reduced the expression of translation-associated genes, BRD9 knockout caused a pronounced effect.

3.4. Expression Levels of RNA-seq & Ribosomal Genes in MYC Overexpressing U373 cells

3.4.1. Generation of MYC Overexpressing Cells

According to the RNA sequencing results, the MYC and translational pathways were disturbed, and these findings strengthened the hypothesis that BRD9 is involved in the regulation of the MYC transcriptional program in glioblastoma. To test the involvement of BRD9 on Myc pathways and further study their relation, ectopic expression of MYC was established. Accordingly, MYC was initially overexpressed in U373 cells to investigate its potential role in regulating the affected gene set. U373 cells were infected with the MYC overexpression encoding virus at a predetermined 1 MOI, based on prior viral titration. 1µL concentrated virus was chosen as the infection amount (**Figure 3.10.A**). To validate the

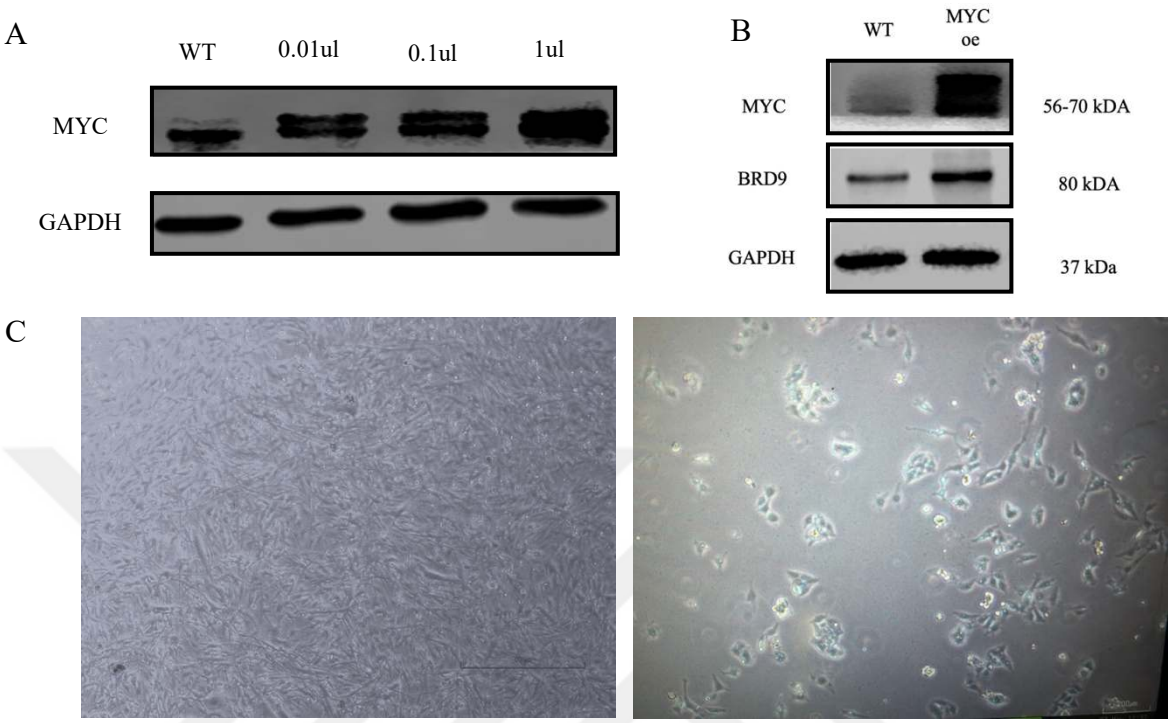

Figure 3.10 Validation of MYC overexpression in U373 cells. A) Western blot showing MYC expression in U373 cells transduced with increasing concentrations of MYC lentivirus (0.01–1 µL). B) Western blot comparing MYC and BRD9 expression levels in wild-type (WT) and MYC-overexpressing (MYC oe) U373 cells; GAPDH was used as a loading control C) Representative brightfield microscopy images of wild-type and overexpressing MYC-U373 cells, displaying altered cellular morphology upon transduction.

overexpression, MYC expression was examined with a western blot, shown in **Figure 3.10.B**, and the image of the infected cells that could be selected from Myc infection was shown in **Figure 3.10.C**. There was a clear overexpression at the protein level, which was corroborated with a slight increase in BRD9 levels. These results showed a connection between MYC and BRD9 expression in U373 cells.

3.4.2. Investigation of Alterations of Gene Expressions of BRD9, MYC, Ribosomal, and Translation-related Genes

After U373 cells were verified as MYC overexpressing cells, ribosomal genes and translational genes selected from RNA sequencing were examined. As expected, MYC gene was expressed 6-fold more, while BRD9 was also expressed almost 3-fold of controls (**Figure 3.11)**. This result also supports the data obtained from western blotting in **Figure**

3.10.B. Moreover, the expression changes of ribosomal genes were variable. While 47S, 28S, and 18S rRNAs were overexpressed nearly 2-fold, the 28S rRNAs were overexpressed almost 3-fold; however, 5S was downregulated. Similar to ribosomal genes, translation-related genes, AARS1, CARS1, GARS1, and WARS1 expressions were approximately 2-fold while YARS1 and EIF2S2 were not differentially expressed **(Figure 3.11.)**

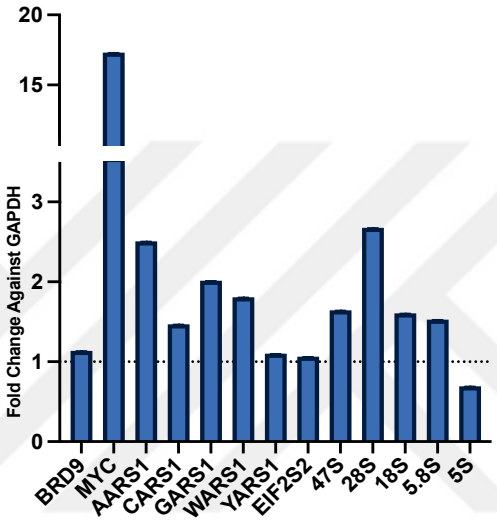

Figure 3.11 Expression levels of translational and ribosomal genes upon MYC overexpression in U373 cells. qPCR analysis showing fold change of BRD9, MYC, translation related, and ribosomal RNA genes relative to GAPDH. MYC and several translational and ribosomal genes show moderate to strong upregulation, while 5S rRNA is downregulated.

3.4.3. Effect of MYC Overexpression on Radiation Response of I-BRD9-treated Cells

Given the impact of I-BRD9 on MYC-related pathways, the combined treatment with I-BRD9 and irradiation was applied to MYC-overexpressing cells to determine whether the cytotoxic effect observed in WT cells could be rescued. As shown in the colony formation assay, MYC-overexpressing cells exhibited a significant survival advantage, suggesting a rescue effect. Contrary to what was observed in wild-type U373 cells, MYC-overexpressing cells did not exhibit the same defree of inhibition of growth upon I-BRD9 and IR treatment (**Figure 3.12)**.

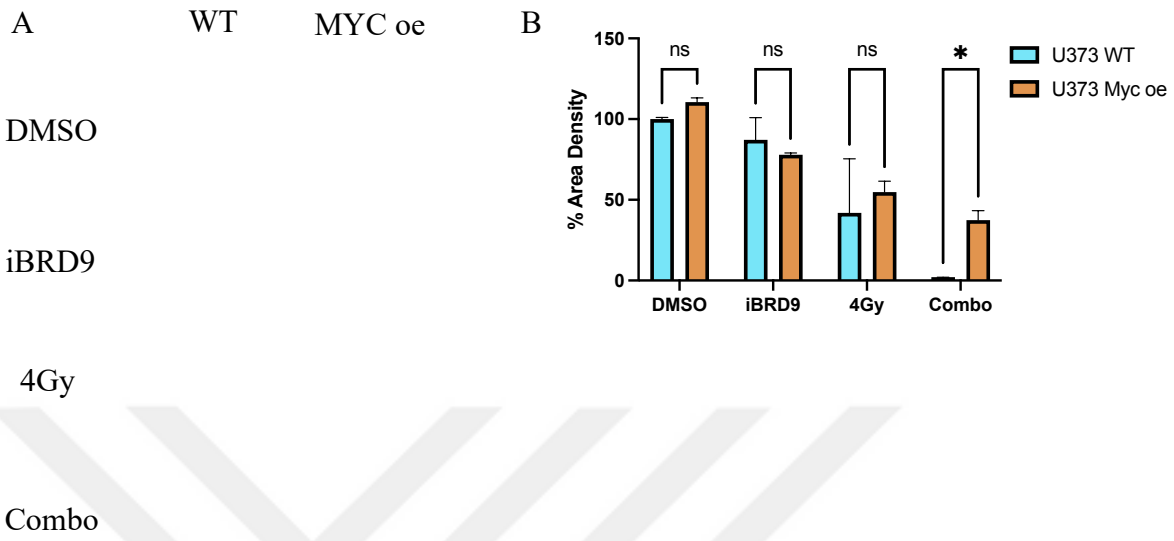

Figure 3.12 MYC overexpression rescues BRD9 inhibition and radiation-induced cytotoxicity in U373 cells. A) Colony formation assay shows the survival of U373 wild-type (WT) and MYC-overexpressing (MYC oe) cells treated with DMSO, 2 µM I-BRD9, 4 Gy ionizing radiation (IR), and the combination treatment. B) Quantification of colony area density indicates that MYC overexpression provides a protective effect under combination treatment (I-BRD9 + 4 Gy), significantly increasing survival relative to WT cells (*$p < 0.05$). No significant differences were observed under single-agent treatments.

3.5. Chemical Inhibition of BRD9 Alters Translational Machinery

Translation relies on several distinct processes, such as ribosome biogenesis, tRNA synthesis, availability of transcription factors, and so much more. To assess the impact of BRD9 on the translation capacity, we conducted the SUnSET assay, which provides the quantification of the newly made proteins based on their puromycin labeling.

3.5.1. Optimization of SUnSET Assay

Initially, to optimize the procedure, U373 cells were treated with 2.5 µM, 5 µM, and 10 µM of Thapsigargin and Cycloheximide, which inhibit translation by modulating eIF2 activity. As shown in **Figure 3.13** translation was slightly decreased in Thapsigargin treatment but not significantly. In contrast, Cycloheximide effectively inhibited global translation in a dose-dependent fashion, with a prominent reduction observed at 10 µM. GAPDH levels remained served as loading control.

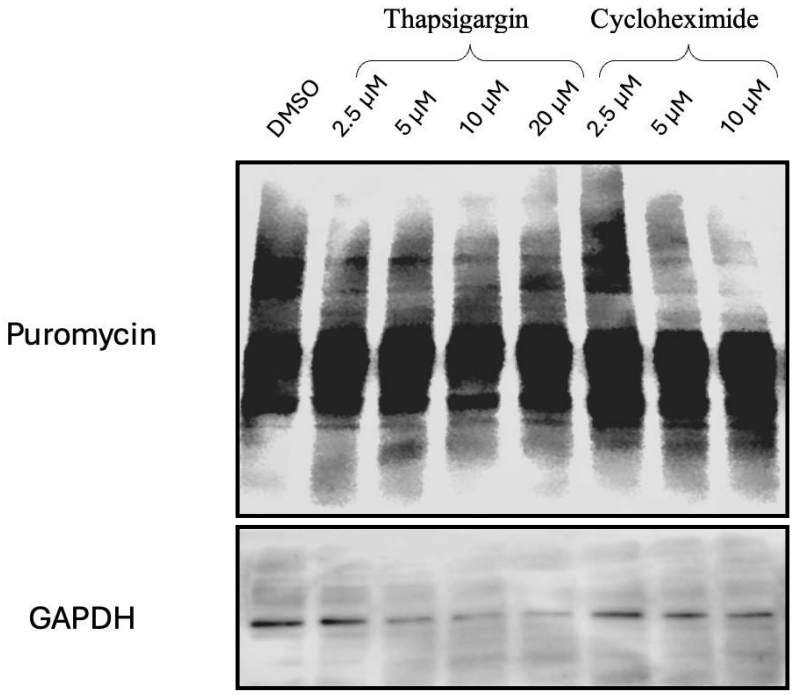

Figure 3.13 Optimization of SUnSET assay using translation inhibitors in U373 cells. Western blot showing puromycin incorporation following treatment with Thapsigargin (2.5 µM, 5 µM, 10 µM) and Cycloheximide (2.5 µM, 5 µM, 10 µM). While Thapsigargin moderately reduced translation, Cycloheximide strongly suppressed protein synthesis in a dose-dependent manner. GAPDH was used as a loading control.

3.5.2. Changes in Overall Translation upon BRD9 Inhibition

Based on the translational shift that was observed in RNA sequencing, we wished test the effect of BRD9 inhibition on global translational capacity. Translational activity of a primary cell line, GBM4, U87MG, U373, and U373 MYC overexpression was evaluated by the Sunset assay in different I-BRD9 treatment conditions. In GBM4 cells, a patient-derived glioblastoma model, BRD9 treatment with 2 µM I-BRD9 showed no decline in translational capacity of the cells over the control condition (**Figure 3.14)** .Similar to the GBM4, U87MG wasn't affected significantly upon any treatment condition, where 2 µM and 5 µM slightly decreased the global translation.

In U373 wild-type cells, 2 μM I-BRD9 treatment didn't change the overall translation. However, a decrease was observed with 5 μM I-BRD9 treatment over DMSO-treated samples, which indicated a dose-dependent inhibition of translation induced by BRD9 targeting (**Figure 3.14**). Lastly, the MYC overexpressing U373 cells rescued the translational capacity regardless of the drug dose.

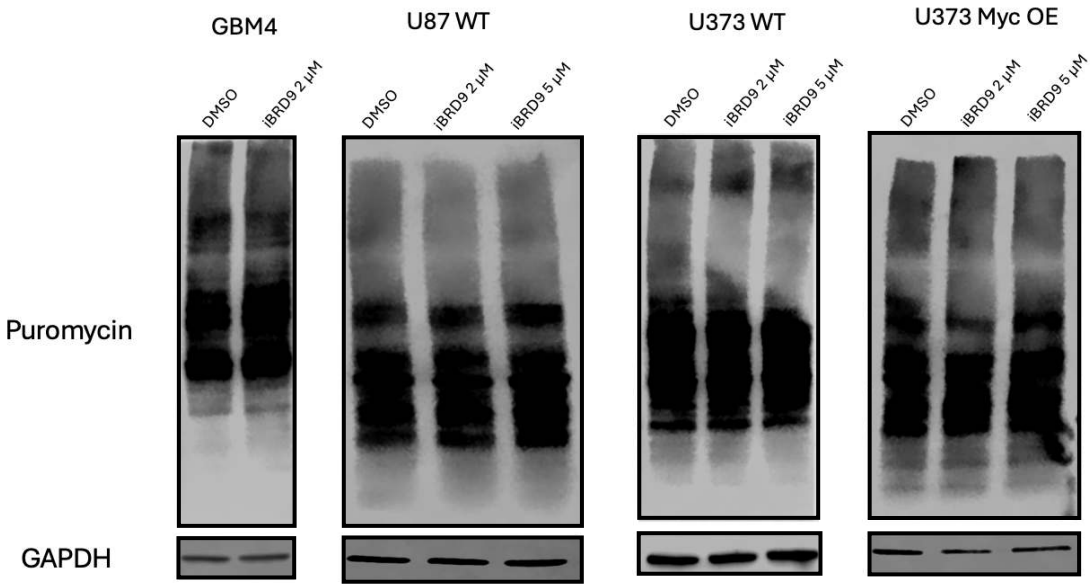

Figure 3.14 Assessment of global translation upon BRD9 inhibition in glioblastoma cells using the SUnSET assay. Western blot showing puromycin incorporation in GBM4, U87MG, U373 wild-type, and MYC-overexpressing U373 cells treated with DMSO, 2 μM I-BRD9, or 5 μM I-BRD9. GAPDH was used as a loading control.

Altogether, these findings indicate that BRD9 plays a role in maintaining global translation in glioblastoma cells. Interestingly, the difference in response between U87MG and U373 cells may be linked to their p53 status, suggesting that BRD9's impact on translation could be influenced by tumor-specific genetic context. Notably, MYC overexpression was able to restore translation even under BRD9 inhibition, pointing to a functional connection between BRD9 and MYC in supporting the translational machinery.

3.5.3. The Effect of BRD9 Perturbation on Gene Expression of Ribosomal RNA-related Genes

Since the translation was related to ribosomal biogenesis, the effect of BRD9 perturbation on rRNA expression was investigated in glioblastoma cell lines. For this purpose, the RNA extracts that were sent to RNA sequencing were used, and rRNA levels were examined. Apart from ribosomal subunit transcripts, as the MYC gene was also involved in ribosome biogenesis, this gene was also involved in the experiment. Upon BRD9 inhibition, in U373 cells, we observed a downregulation in all ribosomal and MYC transcripts of almost 25 percent, however this effect was not observed in the transcription of rRNAs in U87MG cells (**Figure 3.15.A**., **Figure 3.15.B**.), which also supports the Sunset data (**Figure 3.14**.)

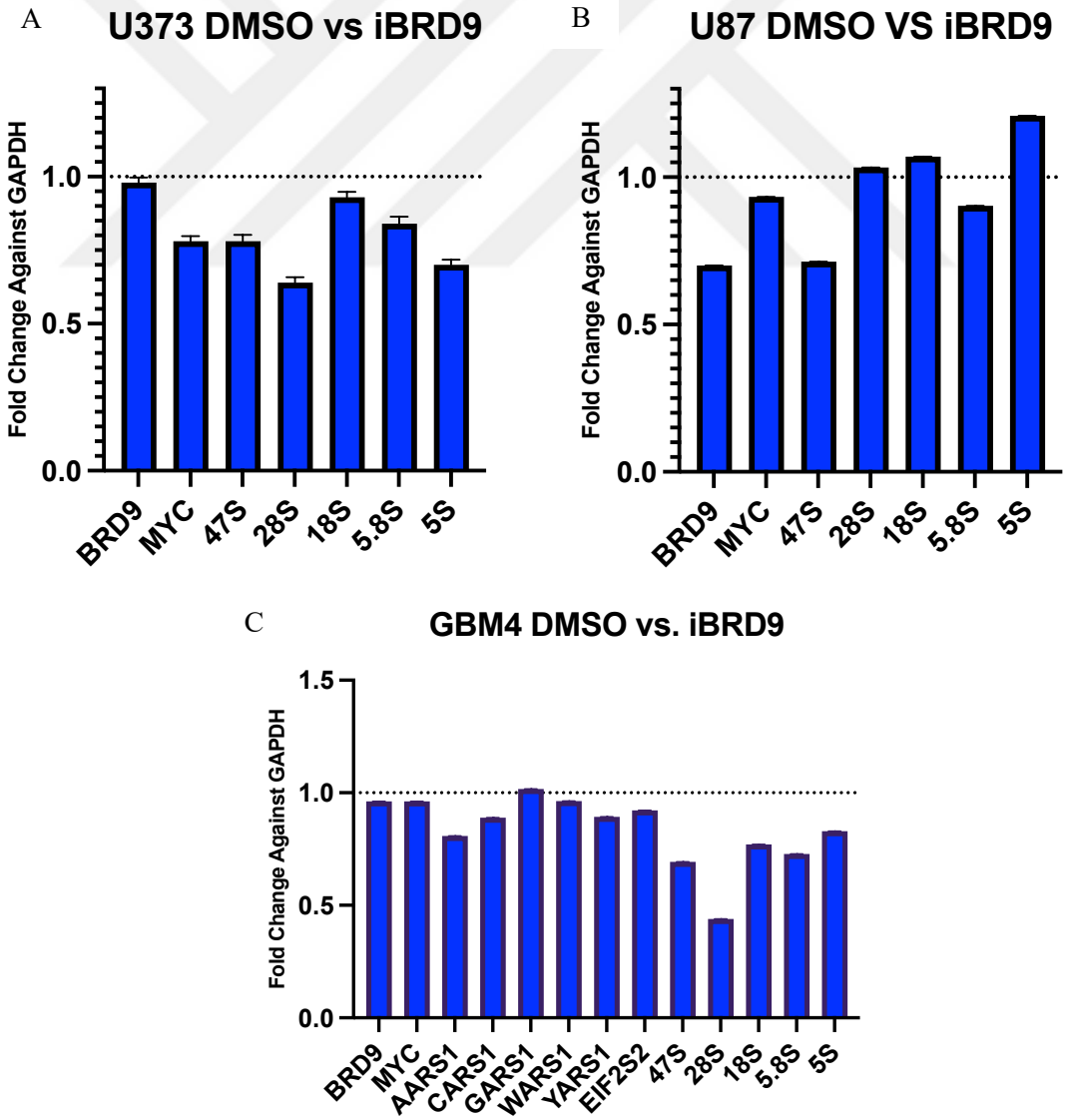

Figure 3.15 Expression analysis of ribosomal RNA and MYC genes upon BRD9 inhibition in GBM4, U373, and U87-MG and GBM4 cells A) Quantification of mRNA levels in U373 cells treated with 2 μM I-BRD9 shows a downregulation in rRNA subunit genes (47S, 28S, 18S, 5.8S, 5S) and MYC. B) U87MG cells do not show significant transcriptional alterations in rRNAs or MYC. C) Quantification of mRNA levels in GBM4 cells treated with 2 μM I-BRD9 shows a downregulation in rRNA subunit genes (47S, 28S, 18S, 5.8S, 5S) and modest effect on translation related genes.

Lastly, rRNA and translation-related gene levels of the primary cell line GBM4 were also investigated. While almost all rRNA transcription was downregulated, in the case of translation-related genes, besides AARS1 and CARS1, expression levels didn't change significantly **(Figure 3.15.C)**. These results suggest that, while chemical inhibition of BRD9 leads to a mild suppression of ribosome-related gene expression, genetic ablation of BRD9 has a more profound impact, indicating a stronger dependency of ribosomal gene transcription on the sustained presence of BRD9.

Chapter 4:
DISCUSSION

Glioblastoma is the most common and aggressive type of brain cancer, which is classified as a Grade IV IDH-wildtype tumor. The current gold standard for the therapy of GBM includes surgical resection, radiotherapy, and chemotherapy. The most established treatment methodology is the Stupp Protocol, which is applied by combining Temozolomide with IR, significantly prolonging the patient's survival. However, despite initial effectiveness in some patients, GBM often recurs in a more aggressive and radioresistant form. The gain of resistance has several mechanisms originating from the tumor environment, structure, and molecular alterations, which include tumor heterogeneity, hypoxia, epigenetic modifications, signaling pathway alterations, and glioma-initiating cells. Moreover, some limitations to treatment arise from the nature of the brain due to structures like the BBB and BBTB worsen drug delivery, which confines therapeutic efficiency.

To overcome radioresistance, the underlying mechanisms must be elucidated. While some drugs induce changes in signaling pathway dynamics, targeting epigenetic factors has gained increasing attention in recent years in cancer treatments due to their broader and more systemic effects on gene expression and chromatin structure.

Radiotherapy is employed for inducing DNA damage by causing strand breaks and generating reactive oxygen species. However, even with the improvements in the radiation beam technologies that provide more targeted and concentrated RT and implementation of TMZ, the effectiveness of the treatment remains unsatisfactory and does not fully prevent tumor recurrence.

In this thesis, we investigated the individual effects of bromodomain-containing protein 9 inhibition using both chemical and genetic approaches on GBM cells and examined the underlying mechanisms of the radiosensitizing effect observed in combinatorial treatments, which significantly reduce cell viability, based on previous studies conducted in our laboratory. In this context, first, we replicated our hypothesis by conducting cell viability assays with disturbing activity of BRD9 using CRISPR-based gene silencing and chemical inhibition in U373 and U87MG cells, and combined the treatment with IR. Later on, since

BRD9 is an acetyl reader protein, we examined the global histone acetylation changes. Next, we studied the impact of these treatments on the transcriptomic level; therefore, we performed RNA sequencing for 2 different cell lines and 2 different BRD9 perturbations. After each analysis, we focused on the commonly altered genes to exclude the cell-based differences. After obtaining and validating the derived pathways, which led us to MYC regulation, we overexpressed the MYC gene to test whether it rescues the I-BRD9 induced phenotypes or not. In the last part, overall translational changes were investigated, and translation-related genes were quantified.

BRD9 perturbation upon chemical and genetic approaches decreases cell viability

Initially, our aim was to reproduce the experimental conditions required to test our hypothesis that combinational treatment of BRD9 manipulation and ionizing radiation impairs the cells' ability to survive. To this end, U373 and U87MG cells were treated with I-BRD9 for 72 hours and subsequently exposed to IR. After 14 days of incubation, while the cell viability of U373 decreased by around 25% with the drug alone, the combined treatment led to an almost 90% reduction **(Figure 3.1.A, B)**. In the case of U87MG, BRD9 inhibition alone caused about a 30% decrease, whereas the combination of I-BRD9 and IR reduced viability by roughly 60% compared to the control **(Figure 3.1.A, C)**. Correspondingly, knocked-out U373 and U87MG cells also showed a similar pattern with a stronger phenotype. While IR alone decreased cell viability 50% for NT1-infected cell lines, the CRISPR-based knocked-out cells were almost completely depleted. The guide RNA itself did not affect the viability of U373 KO; however, U87MG KO went down to nearly 40% **(Figure 3.2.B, C)**. Gaudio et. al conducted a study on acute myeloid leukemia cell lines MOLM-13 and MV4-1, although in different cancers, showed sensitivity upon BRD9 inhibition and knock-out, parallel to our results (Del Gaudio et al., 2019). The treatment with IR alone also caused a significant decrease in both cell lines and both conditions. However, the combinatorial effect was not the same, which is most likely due to the p53 status of the cells, as U373 is p53 mutant and U87MG retains wild type p53. Even though U87MG exhibits a more resilient profile during IR exposure, its cell viability was still reduced to a notable extent. This long-term reduction is not easily visible in short-term assays **(Figure 3. 1.D)**, suggesting that the effects of radiation persist and that cells eventually lose the capacity to repair radiation-induced damage. BRD9 manipulation,

whether through inhibition or gene silencing, mainly causes epigenetic changes that are tightly linked to the DNA damage repair system. Zhou et al. investigated the variability in homologous recombination efficiency across different cancer types, including bone, colorectal, and ovarian. Their results showed that BRD9 knockout disrupts the formation of the RAD51–RAD54 complex, leading to impaired DNA repair(Zhou et al., 2020). Another aspect to consider is the epigenetic function of BRD9, which can cause a signaling cascade that will end up with changes in chromatin accessibility. Acetylation signature around DDR-related genes is recognized by acetyl reader proteins like BRD9, which is a part of a larger complex, SWI/SNF. Sadek et al. indicate that transcriptional inactivation of genes at sites of DNA damage, as well as the proper recruitment of DNA damage response proteins, depends on the binding of SWI/SNF complexes(Sadek et al., 2022). According to the work of Wang et. al, BRD9 containing SWI/SNF complex is involved in cell survival and BRD9 regulates the binding efficiency of the complex itself (X. Wang et al., 2019b). Therefore, broader research should be conducted to elucidate the function of BRD9 in cell survival and DDR.

Epigenetic changes upon BRD9 inhibition and/or IR treatment

We aimed to understand how BRD9 inhibition and/or IR treatment alter the global histone modifications. Given that BRD9 is a bromodomain-containing protein known to recognize acetylated histones and regulate transcriptional activity (Du et al., 2023), its inhibition may disrupt chromatin structure and weaken the transcriptional response to external stress such as radiation(Du et al., 2023). Therefore, we profiled seven histone marks that are closely related to promoter and enhancer activity, thus, transcription and chromatin accessibility (Ito et al., 2022).

Our data revealed that H3K27me3, a repression mark that is localized by Enhancer of Zeste Homolog 2 (EZH), which is the catalytic subunit of Polycomb Repressive Complex 2 (PRC2), was not changed upon any treatment condition. This suggests that BRD9 inhibition and/or ionizing radiation (IR) do not directly interfere with PRC2 activity. On the other hand, several activation marks that we scanned showed that IR treatment solely increased H3K9ac, H3K18ac, H3K27ac, and H3K4me3 **(Figure 3.3.B, Figure 3.3.C, Figure 3.3.D)**. While in literature, the acetylation marks were decreased upon IR, our data showed an increase in

acetylation. This may be caused by the global reacetylation where the heterochromatin structure was promoted during early phases of IR, which has been reported as a transient chromatin condensation response to DNA double-strand breaks (Ziv et al., 2006). However, the closed chromatin structure at the early phases, where it converts into an open chromatin structure, remains during combination application after combined treatment at a late time, especially in H3K27ac. This effect is most clearly seen in H3K27ac and H3K9ac, and less clearly in H3K18ac levels. This data suggests that the BRD9 inhibition keeps the genes supressed during IR and maintains their heterochromatin structure, which may result in deficient repair machinery and thus, survival. Remaining histone marks, H4K5ac and H4K8ac, which are also related to enhancer and promoter activation, didn't show a significant change upon I-BRD9 and/or IR were treatment.

Altogether, while this data does not directly show the function of BRD9 and consequent pathway alterations upon inhibition, it provides a large-scale observation of histone marks with BRD9 and IR or both. Additionally, all these marks should also be investigated in the U87 MG cell line for better assessment of p53 involvement.

Transcriptomic analysis reveals altered pathways upon BRD9 perturbation

Transcriptomic data provide significant insights into alterations in global gene expression patterns and key regulatory pathways. By analyzing the interaction between differentially expressed genes and the affected pathways, we gained a clearer understanding of the specific effects of BRD9 perturbation alone. In this context, we performed four independent RNA sequencing analyses, involving two different cell lines and two treatment conditions (inhibition and knockout). Although transcriptomic analyses following BRD9 perturbation have been conducted in various cancer types (Weisberg et al., 2022; Alpsoy et al., 2021), to our knowledge, no such investigation has been carried out in glioblastoma using this approach. Pathway analysis revealed that, across all four datasets, MYC target V1 and translational regulation pathways were commonly affected in both U87MG and U373 cells treated with I-BRD9 or subjected to BRD9 knockout. As a result, the general translational machinery changed. To further strengthen these findings, we merged all downregulated genes and identified 31 commonly downregulated genes across all experimental groups. Functional

annotation of these shared genes using MSigDB and Reactome databases once again highlighted pathways such as tRNA aminoacylation, translation initiation, and MYC signaling.

According to our findings, the downregulated aaRS genes upon BRD9 perturbation were all cytosolic tRNA synthetases, which are essential for charging tRNAs with their respective amino acids, a process fundamental to accurate and efficient protein synthesis. Their coordinated suppression suggests that BRD9 loss affects core translational capacity more broadly, not only ribosome-related genes.

Previous studies have shown that MYC directly upregulates components of the translation machinery, including tRNA synthetases, to support the high protein synthesis demand in glioblastoma (Kuzuoglu-Ozturk et al., 2023; Cencioni et al., 2023). Our data align with these findings, suggesting that BRD9 may help maintain MYC-dependent transcription of these targets, further linking BRD9 to MYC-driven translation control (Kurata et al., 2023; Klein et al., 2024). Interestingly, these transcriptomic effects were consistent in both U87MG and U373 cell lines, which differ in p53 status, pointing to a p53-independent role for BRD9 in regulating translation in glioblastoma. Interestingly, these transcriptomic effects were consistent in both U87MG and U373 cell lines, which differ in p53 status, pointing to a p53-independent role for BRD9 in regulating translation in glioblastoma. For future studies, testing BRD9 inhibition in in vivo GBM models could reveal whether the radiosensitization observed in vitro holds therapeutic potential. Additionally, chromatin accessibility assays like ATAC-seq (Buenrostro et al., 2013) could help determine if the observed gene suppression stems from direct effects on enhancer or promoter regions.

The effects obtained upon BRD9 ablation support the prior results related to maintaining acetylation architecture. Additionally, G2/M phase, hypoxia, epithelial-mesenchymal transition (EMT), and angiogenesis pathways were derived upon BRD9 inhibition and depletion. While translation is reduced, since cancer is dependent on high translation activity, the expression of key cell cycle and angiogenesis proteins could be downregulated. Moreover, alteration in hypoxia, one of the main barriers to radiotherapy, could indicate the inclination to a radiosensitivity which supports our preliminary data. Also, since our false threshold of 0.1 and $\log_2 FC = 0$, the genes obtained from this analysis were not significantly

differentially expressed significantly but our data shows these genes are collectively involved in key pathways and exhibit survival characteristics. Together, these findings emphasize the regulatory role of BRD9 in maintaining transcriptional programs that support translation and oncogenic signaling. Given BRD9's druggable bromodomain and its convergent influence on cancer-critical pathways, our data support its candidacy as a therapeutic target in glioblastoma, independent of p53 status.

MYC expression rescue cell survival upon combination treatment of I-BRD9 and IR

As MYC target genes and translation-related genes were downregulated in I-BRD9 treatment, we aimed to assess whether the opposite condition—MYC overexpression—could rescue the cells. Thus, after successfully overexpressing the MYC gene in U373 cells, we treated them using the same setup described previously. MYC is a well-established master regulator of cellular growth and metabolism, and it is estimated to influence nearly 15% of global translation by acting as a transcription factor and enhancing RNA polymerase recruitment to target gene promoters (Van Riggelen et al., 2010b). Accordingly, due to its ability to enhance ribosome biogenesis, MYC not only drives global protein synthesis but also increases the expression of genes involved in multiple signaling pathways. Initially, we investigated the ribosomal and translation-related gene expressions in our MYC overexpressing cell lines. After qPCR analysis confirmed successful overexpression of MYC in U373 cells, we observed upregulation in ribosomal genes but not a striking increase in translation-related genes obtained from RNA-seq. This could be the result of the global amplification of MYC rather than uniform, thus transcriptionally accessible genes may respond more strongly to MYC overexpression, whereas other genes remain less affected, despite MYC's known role in regulating tRNA synthesis(J. Wang et al., 2024).

Next, we conducted a colony formation assay to obtain functional evidence for the protective role of MYC overexpression under combinatorial treatment with I-BRD9 and ionizing radiation. Unlike wild-type U373 cells, which showed a dramatic decrease in colony formation following combination therapy, MYC-overexpressing cells retained significant survival, indicating a MYC-mediated rescue effect (**Figure 3.12**). This may cause the restored capacity to repair DNA in less time and prevent cytotoxic effects caused by DNA damage, thus promoting cell survival under stress. In order to discuss the interaction of MYC

and BRD9, overexpression of BRD9 can be subjected to further experiments. While also the cell cycle profiles can also be compared with U373 WT and U373 BRD9 overexpressing cells.

All together, these data validate that MYC plays a crucial role in supporting cell survival under stress conditions and the observed rescue of cell viability upon MYC overexpression under combined BRD9 inhibition and IR treatment further reinforces the notion that MYC can counteract the cytotoxic effects induced by dual targeting, potentially by sustaining transcriptional programs essential for DNA repair and protein synthesis.

Translational rewiring following BRD9 perturbation

To investigate the global translation alterations in different glioblastoma cell lines, we employed the Sunset assay, a non-reactive experiment that measures ongoing protein synthesis through puromycin incorporation into nascent peptide chains(Schmidt et al., 2009). BRD9 is a member of the SWI/SNF complex, which is strongly involved in the regulation of translation by changing chromatin accessibility, such as histone ejection and sliding, particularly at MYC loci (Jones et al., 2022). While Kurata et al. demonstrated MYC and BRD9 are involved in ribosomal rRNA transcription in multiple myeloma, we hypothesized that BRD9 inhibition might disrupt MYC-dependent transcriptional programs and impair translation. Therefore, at first, we treated the patient-derived glioblastoma cell line, GBM4, with 2 μM I-BRD9. BRD9 inhibition did not show a significant decline in global translation while the MYC, ribosomal rRNA, and translation-related genes were downregulated upon treatment **(Figure 3.11)**, suggesting that the machinery responsible for translation is transcriptionally affected, even if total protein synthesis remains stable **(Figure 3.14).** These results may arise due to primary cell lines activating a strong compensatory mechanism or buffering the decreased translation capacity. Although this transcription–translation contradiction can occur from characteristics of the primary cell line, it should be further investigated by assessing ribosome occupancy and translation efficiency through polysome profiling.

Our investigations reveal that U87MG demonstrated resilience in translational capacity **(Figure 3.14)** upon even higher concentrations of I-BRD9, which is also consistent with transcriptomic analysis of MYC and ribosomal RNA gene expressions **(Figure 3.15.B)** while

U373 WT displays decreased translation with also significant decrease in MYC and ribosomal RNA transcription. Unlike U87MG, U373 WT also exhibited dose-dependent global translational decline, which indicates 5 μM I-BRD9 significantly reduces protein synthesis.

This discrepancy draws attention to the importance of genetic heterogeneity and different intrinsic cellular mechanisms in treatment strategies. The main distinction between U373 and U87MG is the p53 status (Gomez-Manzano et al., 1997), which is the guardian of the genome that downregulates protein synthesis under DNA damage or stress conditions (Kasteri et al., 2018). Additionally, it could be possible that alternative chromatin remodeling pathways employed after BRD9 inhibition compensate for the absence of BRD9 and maintain MYC and rRNA transcription, which may provide a proper environment for the translational machinery of U87MG rather than U373. In the future, alteration of p53 status in U87MG or transduction of p53 to U373 could provide a better comparison opportunity, while also the basal MYC transcript level can be evaluated to understand the reason behind compensation of 5 μM I-BRD9 treatment. Polysome profiling could be an additional option to understand the efficiency of translation.

Lastly, we investigated whether the overexpression of MYC could compensate for the effects of I-BRD9, as in U373 WT. Even under 5 μM I-BRD9 treatment, protein synthesis was restored in U373 cells upon MYC overexpression. This outcome suggests that high MYC levels can effectively bypass the loss of BRD9 function in sustaining translation. MYC likely reactivates the expression of key components of the translational machinery, such as rRNA and translation-associated genes, thereby neutralizing the inhibitory effects of BRD9 suppression. This is consistent with the literature that indicates MYC enhancing the activity of polymerases I, II, and III. Increasing the binding efficiency of polymerases to the relevant gene facilitates the transcription of tRNAs and rDNA, which directly affects translation rate and efficiency (Jha et al., 2023). It could be inferred that increased MYC overexpression could be a blockade to BRD9 inhibition; MYC expression level could serve as a biomarker for BRD9 inhibition treatment. For future investigations, overexpressing BRD9 will be a way to understand the involvement of BRD9 in general translation activity, while also validating this rescue effect in in vivo models will be critical for its translational relevance.

Altogether, our results suggest that BRD9 contributes to the regulation of protein synthesis in glioblastoma, but this role appears to depend heavily on the genetic context of the cells. In particular, U373 cells showed reduced translation when BRD9 was inhibited, whereas U87MG and GBM4 cells were more resistant due to differences in their genetic background or adaptive responses. Ultimately, elevated MYC levels in U373 cells was enough to restore protein production, even under high-dose BRD9 inhibition. This points to MYC's powerful ability to sustain the transcription of genes involved in ribosome function and protein synthesis (**Figure 4.1**)

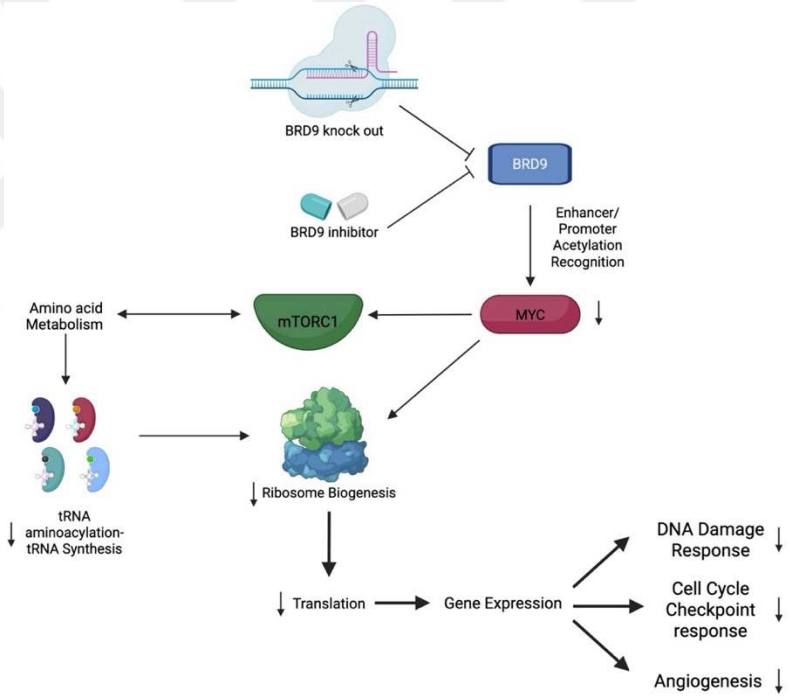

Figure 4.1 Schematic overview summarizing the regulatory role of BRD9 in glioblastoma. BRD9 perturbation, via genetic knockout or chemical inhibition, affects MYC activity and downstream pathways, including mTORC1 signaling, tRNA aminoacylation, ribosome biogenesis, and global translation. These alterations ultimately impact gene expression programs related to DNA damage response, cell cycle regulation, and angiogenesis. (Created by Biorender)

This study highlights the critical role of BRD9 in regulating translation and ribosome biogenesis in glioblastoma through a MYC-dependent axis. Using both chemical inhibition and genetic knockout strategies, we identified a BRD9–MYC–aaRS/EIF2S2 pathway linking chromatin remodeling to translational output. BRD9 was shown to sustain the expression of key translational genes, and MYC overexpression was sufficient to rescue BRD9 loss effects, suggesting functional interplay. The context-dependent nature of BRD9 function, particularly influenced by p53 status, emphasizes its therapeutic relevance. Overall, our findings indicates that BRD9 show a potential of epigenetic target to impair protein synthesis and enhance radiosensitivity in GBM.

Building upon the findings of this study, several future directions may help further define the therapeutic potential of BRD9 in glioblastoma. First, in vivo validation using orthotopic glioblastoma models will be essential to assess whether BRD9 inhibition can enhance the efficacy of radiotherapy in a more physiologically relevant context. Coupling such studies with survival analysis and tumor progression tracking could provide critical translational value. Additionally, chromatin accessibility assays such as ATAC-seq or ChIP-seq for BRD9 and MYC could help confirm whether the downregulated translation-related genes are direct targets affected by BRD9-mediated chromatin remodeling. Given the differential responses observed between U87MG and U373 cells, further exploration of p53 dependent and independent mechanisms will clarify how BRD9's function is modulated by genetic context. Moreover, overexpression studies of BRD9 in MYC-deficient settings, and vice versa, may illuminate the interplay between these two regulators in sustaining translational homeostasis. Finally, ribosome profiling and polysome analysis will offer deeper insights into how BRD9 inhibition alters translation efficiency and fidelity, beyond transcript abundance. Together, these future studies will not only validate the mechanistic findings presented here but also lay the groundwork for potential clinical translation of BRD9-targeted therapies in glioblastoma.

Chapter 5:

APPENDIX

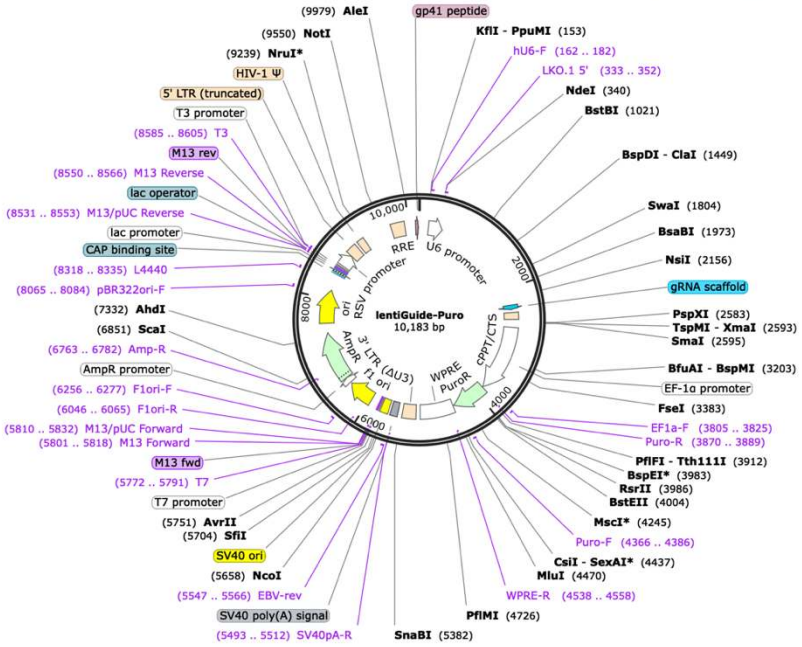

Figure 5.1 Plasmid map of the lentiGuide-Puro vector used for CRISPR/Cas9-mediated BRD9 knockout experiments.

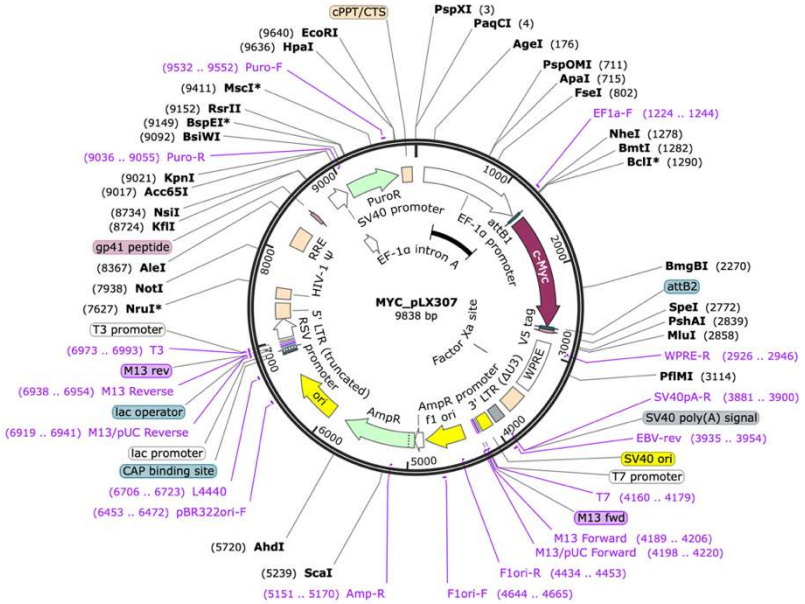

Figure 5.2 Plasmid map of the MYC_pLX307 vector used for MYC overexpression.

Appendix

Bibliography

Ali, M. M., Naz, S., Ashraf, S., Knapp, S., & Ul-Haq, Z. (2023). Epigenetic modulation by targeting bromodomain containing protein 9 (BRD9): Its therapeutic potential and selective inhibition. In *International Journal of Biological Macromolecules* (Vol. 230). Elsevier B.V. https://doi.org/10.1016/j.ijbiomac.2023.123428

Ali, M. Y., Oliva, C. R., Noman, A. S. M., Allen, B. G., Goswami, P. C., Zakharia, Y., Monga, V., Spitz, D. R., Buatti, J. M., & Griguer, C. E. (2020). Radioresistance in glioblastoma and the development of radiosensitizers. In *Cancers* (Vol. 12, Issue 9). https://doi.org/10.3390/cancers12092511

Alpsoy, A., Utturkar, S. M., Carter, B. C., Dhiman, A., Torregrosa-Allen, S. E., Currie, M. P., Elzey, B. D., & Dykhuizen, E. C. (2021). BRD9 is a critical regulator of androgen receptor signaling and prostate cancer progression. *Cancer Research*, *81*(4), 820–833. https://doi.org/10.1158/0008-5472.CAN-20-1417

Alver, B. H., Kim, K. H., Lu, P., Wang, X., Manchester, H. E., Wang, W., Haswell, J. R., Park, P. J., & Roberts, C. W. M. (2017). The SWI/SNF chromatin remodelling complex is required for maintenance of lineage specific enhancers. *Nature Communications*, *8*. https://doi.org/10.1038/ncomms14648

Amente, S., Luigi, L., & Majello, B. (2011). *Epigenetic reprogramming of Myc target genes*. www.ajcr.us

Arabzadeh, A. A., Mortezazadeh, T., Aryafar, T., Gharepapagh, E., Majdaeen, M., & Farhood, B. (2021). Therapeutic potentials of resveratrol in combination with radiotherapy and chemotherapy during glioblastoma treatment: a mechanistic review. In *Cancer Cell International* (Vol. 21, Issue 1). https://doi.org/10.1186/s12935-021-02099-0

Bannister, A. J., & Kouzarides, T. (2011). Regulation of chromatin by histone modifications. In *Cell Research* (Vol. 21, Issue 3, pp. 381–395). https://doi.org/10.1038/cr.2011.22

Behrooz, A. B., Talaie, Z., Jusheghani, F., Łos, M. J., Klonisch, T., & Ghavami, S. (2022). Wnt and PI3K/Akt/mTOR Survival Pathways as Therapeutic Targets in Glioblastoma. In *International Journal of Molecular Sciences* (Vol. 23, Issue 3). https://doi.org/10.3390/ijms23031353

Bhat, K., Saki, M., Cheng, F., He, L., Zhang, L., Ioannidis, A., Nathanson, D., Tsang, J., Bensinger, S. J., Nghiemphu, P. L., Cloughesy, T. F., Liau, L. M., Kornblum, H. I., & Pajonk, F. (2021). Dopamine Receptor Antagonists, Radiation, and Cholesterol Biosynthesis in Mouse Models of Glioblastoma. *Journal of the National Cancer Institute*, *113*(8). https://doi.org/10.1093/jnci/djab018

Brennan, D. F., & Barford, D. (2009). Eliminylation: a post-translational modification catalyzed by phosphothreonine lyases. *Trends in Biochemical Sciences*, *34*(3). https://doi.org/10.1016/j.tibs.2008.11.005

Buenrostro, J. D., Giresi, P. G., Zaba, L. C., Chang, H. Y., & Greenleaf, W. J. (2013). Transposition of native chromatin for fast and sensitive epigenomic profiling of open chromatin, DNA-binding proteins and nucleosome position. *Nature Methods*, *10*(12), 1213–1218. https://doi.org/10.1038/nmeth.2688

CBTRUS Fact Sheet. (n.d.). Retrieved 16 July 2025, from https://cbtrus.org/cbtrus-fact-sheet/

Cencioni, C., Scagnoli, F., Spallotta, F., Nasi, S., & Illi, B. (2023). The "Superoncogene" Myc at the Crossroad between Metabolism and Gene Expression in Glioblastoma Multiforme. In *International Journal of Molecular Sciences* (Vol. 24, Issue 4). Multidisciplinary Digital Publishing Institute (MDPI). https://doi.org/10.3390/ijms24044217

Chan, C. H., Jo, U., Kohrman, A., Rezaeian, A. H., Chou, P. C., Logothetis, C., & Lin, H. K. (2014). Posttranslational regulation of Akt in human cancer. In *Cell and Bioscience* (Vol. 4, Issue 1). https://doi.org/10.1186/2045-3701-4-59

Chen, H., Liu, H., & Qing, G. (2018). Targeting oncogenic Myc as a strategy for cancer treatment. In *Signal Transduction and Targeted Therapy* (Vol. 3, Issue 1). https://doi.org/10.1038/s41392-018-0008-7

Chen, Q. W., Zhu, X. Y., Li, Y. Y., & Meng, Z. Q. (2014). Epigenetic regulation and cancer (review). In *Oncology Reports* (Vol. 31, Issue 2). https://doi.org/10.3892/or.2013.2913

Chiu, L. Y., Gong, F., & Miller, K. M. (2017). Bromodomain proteins: Repairing DNA damage within chromatin. In *Philosophical Transactions of the Royal Society B: Biological Sciences* (Vol. 372, Issue 1731). https://doi.org/10.1098/rstb.2016.0286

Clapier, C. R., Iwasa, J., Cairns, B. R., & Peterson, C. L. (2017a). Mechanisms of action and regulation of ATP-dependent chromatin-remodelling complexes. In *Nature Reviews Molecular Cell Biology* (Vol. 18, Issue 7, pp. 407–422). Nature Publishing Group. https://doi.org/10.1038/nrm.2017.26

Clapier, C. R., Iwasa, J., Cairns, B. R., & Peterson, C. L. (2017b). Mechanisms of action and regulation of ATP-dependent chromatin-remodelling complexes. In *Nature Reviews Molecular Cell Biology* (Vol. 18, Issue 7). https://doi.org/10.1038/nrm.2017.26

Creyghton, M. P., Cheng, A. W., Welstead, G. G., Kooistra, T., Carey, B. W., Steine, E. J., Hanna, J., Lodato, M. A., Frampton, G. M., Sharp, P. A., Boyer, L. A., Young, R. A., & Jaenisch, R. (2010). Histone H3K27ac separates active from poised enhancers and predicts developmental state. *Proceedings of the National Academy of Sciences of the*

United States of America, *107*(50), 21931–21936. https://doi.org/10.1073/pnas.1016071107

Cruz, J. A., & Wishart, D. S. (2019). *Brain and Other Nervous System Cancer — Cancer Stat Facts*. National Cancer Instıtute.

Dai, M. S., & Lu, H. (2008). Crosstalk between c-Myc and ribosome in ribosomal biogenesis and cancer. In *Journal of Cellular Biochemistry* (Vol. 105, Issue 3). https://doi.org/10.1002/jcb.21895

Dang, C. V. (2012). MYC on the path to cancer. In *Cell* (Vol. 149, Issue 1). https://doi.org/10.1016/j.cell.2012.03.003

Değirmenci, N. (2024). *Epigenetic Therapies to Augment Radiation Response in Glioblastoma*.

Del Gaudio, N., Di Costanzo, A., Liu, N. Q., Conte, L., Migliaccio, A., Vermeulen, M., Martens, J. H. A., Stunnenberg, H. G., Nebbioso, A., & Altucci, L. (2019). BRD9 binds cell type-specific chromatin regions regulating leukemic cell survival via STAT5 inhibition. *Cell Death and Disease*, *10*(5). https://doi.org/10.1038/s41419-019-1570-9

Dhanasekaran, R., Deutzmann, A., Mahauad-Fernandez, W. D., Hansen, A. S., Gouw, A. M., & Felsher, D. W. (2022). The MYC oncogene — the grand orchestrator of cancer growth and immune evasion. In *Nature Reviews Clinical Oncology* (Vol. 19, Issue 1). https://doi.org/10.1038/s41571-021-00549-2

Du, J., Liu, Y., Wu, X., Sun, J., Shi, J., Zhang, H., Zheng, A., Zhou, M., & Jiang, X. (2023). BRD9-mediated chromatin remodeling suppresses osteoclastogenesis through negative feedback mechanism. *Nature Communications*, *14*(1). https://doi.org/10.1038/s41467-023-37116-5

Filippakopoulos, P., Picaud, S., Mangos, M., Keates, T., Lambert, J. P., Barsyte-Lovejoy, D., Felletar, I., Volkmer, R., Müller, S., Pawson, T., Gingras, A. C., Arrowsmith, C. H., & Knapp, S. (2012). Histone recognition and large-scale structural analysis of the human bromodomain family. *Cell*, *149*(1). https://doi.org/10.1016/j.cell.2012.02.013

Flynn, E. M., Huang, O. W., Poy, F., Oppikofer, M., Bellon, S. F., Tang, Y., & Cochran, A. G. (2015). A subset of human bromodomains recognizes butyryllysine and crotonyllysine histone peptide modifications. *Structure*, *23*(10). https://doi.org/10.1016/j.str.2015.08.004

Gabay, M., Li, Y., & Felsher, D. W. (2014). MYC activation is a hallmark of cancer initiation and maintenance. *Cold Spring Harbor Perspectives in Medicine*, *4*(6). https://doi.org/10.1101/cshperspect.a014241

Gerber, D. E., Grossman, S. A., Zeltzman, M., Parisi, M. A., & Kleinberg, L. (2007). The impact of thrombocytopenia from temozolomide and radiation in newly diagnosed adults with high-grade gliomas. In *Neuro-Oncology* (Vol. 9, Issue 1). https://doi.org/10.1215/15228517-2006-024

Gomez-Manzano, C., Fueyo, J., Kyritsis, A. P., Mcdonnell, T. J., Steck, P. A., Levin, V. A., & Yung, W. K. A. (1997). *Characterization of p53 and p21 Functional Interactions in Glioma Cells en Route to Apoptosis*. https://academic.oup.com/jnci/article/89/14/1036/2526277

Gomez-Roman, N., Grandori, C., Eisenman, R. N., & White, R. J. (2003). Direct activation of RNA polymerase III transcription by c-Myc. *Nature*, *421*(6920). https://doi.org/10.1038/nature01327

Guertin, D. A., & Sabatini, D. M. (2007). Defining the Role of mTOR in Cancer. In *Cancer Cell* (Vol. 12, Issue 1). https://doi.org/10.1016/j.ccr.2007.05.008

Han, J. M., Jeong, S. J., Park, M. C., Kim, G., Kwon, N. H., Kim, H. K., Ha, S. H., Ryu, S. H., & Kim, S. (2012). Leucyl-tRNA synthetase is an intracellular leucine sensor for the mTORC1-signaling pathway. *Cell*, *149*(2). https://doi.org/10.1016/j.cell.2012.02.044

Han, S., Liu, Y., Cai, S. J., Qian, M., Ding, J., Larion, M., Gilbert, M. R., & Yang, C. (2020). IDH mutation in glioma: molecular mechanisms and potential therapeutic targets. In *British Journal of Cancer* (Vol. 122, Issue 11). https://doi.org/10.1038/s41416-020-0814-x

Hockings, H., & Miller, R. E. (2023). The role of PARP inhibitor combination therapy in ovarian cancer. In *Therapeutic Advances in Medical Oncology* (Vol. 15). https://doi.org/10.1177/17588359231173183

Hohmann, A. F., Martin, L. J., Minder, J. L., Roe, J. S., Shi, J., Steurer, S., Bader, G., McConnell, D., Pearson, M., Gerstberger, T., Gottschamel, T., Thompson, D., Suzuki, Y., Koegl, M., & Vakoc, C. R. (2016). Sensitivity and engineered resistance of myeloid leukemia cells to BRD9 inhibition. *Nature Chemical Biology*, *12*(9). https://doi.org/10.1038/nchembio.2115

Hyeon, D. Y., Kim, J. H., Ahn, T. J., Cho, Y., Hwang, D., & Kim, S. (2019). Evolution of the multi-tRNA synthetase complex and its role in cancer. *Journal of Biological Chemistry*, *294*(14). https://doi.org/10.1074/jbc.REV118.002958

Ito, S., Das, N. D., Umehara, T., & Koseki, H. (2022). Factors and Mechanisms That Influence Chromatin-Mediated Enhancer–Promoter Interactions and Transcriptional Regulation. In *Cancers* (Vol. 14, Issue 21). MDPI. https://doi.org/10.3390/cancers14215404

Jawhari, S., Ratinaud, M. H., & Verdier, M. (2016). Glioblastoma, hypoxia and autophagy: A survival-prone 'ménage-à-trois'. In *Cell Death and Disease* (Vol. 7, Issue 10). https://doi.org/10.1038/cddis.2016.318

Jha, R. K., Kouzine, F., & Levens, D. (2023a). MYC function and regulation in physiological perspective. In *Frontiers in Cell and Developmental Biology* (Vol. 11). https://doi.org/10.3389/fcell.2023.1268275

Jha, R. K., Kouzine, F., & Levens, D. (2023b). MYC function and regulation in physiological perspective. In *Frontiers in Cell and Developmental Biology* (Vol. 11). Frontiers Media SA. https://doi.org/10.3389/fcell.2023.1268275

Jiao, L., Liu, Y., Yu, X. Y., Pan, X., Zhang, Y., Tu, J., Song, Y. H., & Li, Y. (2023). Ribosome biogenesis in disease: new players and therapeutic targets. In *Signal Transduction and Targeted Therapy* (Vol. 8, Issue 1). https://doi.org/10.1038/s41392-022-01285-4

Jin, B., Li, Y., & Robertson, K. D. (2011). DNA methylation: Superior or subordinate in the epigenetic hierarchy? In *Genes and Cancer* (Vol. 2, Issue 6). https://doi.org/10.1177/1947601910393957

Jin, Q., Liu, G., Wang, B., Li, S., Ni, K., Wang, C., Ren, J., Zhang, S., & Dai, Y. (2020). High methionyl-tRNA synthetase expression predicts poor prognosis in patients with breast cancer. *Journal of Clinical Pathology*, *73*(12). https://doi.org/10.1136/jclinpath-2019-206175

Jones, C. A., Tansey, W. P., & Weissmiller, A. M. (2022). Emerging Themes in Mechanisms of Tumorigenesis by SWI/SNF Subunit Mutation. In *Epigenetics Insights* (Vol. 15). SAGE Publications Ltd. https://doi.org/10.1177/25168657221115656

Kadoch, C., & Crabtree, G. R. (2015). Mammalian SWI/SNF chromatin remodeling complexes and cancer: Mechanistic insights gained from human genomics. In *Science Advances* (Vol. 1, Issue 5). https://doi.org/10.1126/sciadv.1500447

Kadoch, C., Hargreaves, D. C., Hodges, C., Elias, L., Ho, L., Ranish, J., & Crabtree, G. R. (2013). Proteomic and bioinformatic analysis of mammalian SWI/SNF complexes identifies extensive roles in human malignancy. *Nature Genetics*, *45*(6). https://doi.org/10.1038/ng.2628

Karakaş, D., Ari, F., & Ulukaya, E. (2017). The MTT viability assay yields strikingly false-positive viabilities although the cells are killed by some plant extracts. *Turkish Journal of Biology*, *41*(6), 919–925. https://doi.org/10.3906/biy-1703-104

Kasteri, J., Das, D., Zhong, X., Persaud, L., Francis, A., Muharam, H., & Sauane, M. (2018). Translation control by p53. *Cancers*, *10*(5). https://doi.org/10.3390/cancers10050133

Khoei, S., Shoja, M., Mostaar, A., & Faeghi, F. (2016). Effects of resveratrol and methoxyamine on the radiosensitivity of iododeoxyuridine in U87MG glioblastoma cell line. *Experimental Biology and Medicine*, *241*(11). https://doi.org/10.1177/1535370215622583

Kim, J. H., Lee, C., Lee, M., Wang, H., Kim, K., Park, S. J., Yoon, I., Jang, J., Zhao, H., Kim, H. K., Kwon, N. H., Jeong, S. J., Yoo, H. C., Kim, J. H., Yang, J. S., Lee, M. Y., Lee, C. W., Yun, J., Oh, S. J., … Kim, S. (2017). Control of leucine-dependent mTORC1 pathway through chemical intervention of leucyl-tRNA synthetase and RagD interaction. *Nature Communications*, *8*(1). https://doi.org/10.1038/s41467-017-00785-0

Klein, D. C., Lardo, S. M., & Hainer, S. J. (2024). The ncBAF Complex Regulates Transcription in AML Through H3K27ac Sensing by BRD9. *Cancer Research Communications*, *4*(1), 237–252. https://doi.org/10.1158/2767-9764.CRC-23-0382

Ko, Y. G., Kim, E. K., Kim, T., Park, H., Park, H. S., Choi, E. J., & Kim, S. (2001). Glutamine-dependent Antiapoptotic Interaction of Human Glutaminyl-tRNA Synthetase with Apoptosis Signal-regulating Kinase 1. *Journal of Biological Chemistry*, *276*(8). https://doi.org/10.1074/jbc.M006189200

Kouzarides, T. (2007). Chromatin Modifications and Their Function. In *Cell* (Vol. 128, Issue 4, pp. 693–705). https://doi.org/10.1016/j.cell.2007.02.005

Kurata, K., Samur, M. K., Liow, P., Wen, K., Yamamoto, L., Liu, J., Morelli, E., Gulla, A., Tai, Y. T., Qi, J., Hideshima, T., & Anderson, K. C. (2023). BRD9 Degradation Disrupts Ribosome Biogenesis in Multiple Myeloma. *Clinical Cancer Research*, *29*(9). https://doi.org/10.1158/1078-0432.CCR-22-3668

Kuzuoglu-Ozturk, D., Aksoy, O., Schmidt, C., Lea, R., Larson, J. D., Phelps, R. R. L., Nasholm, N., Holt, M., Contreras, A., Huang, M., Wong-Michalak, S., Shao, H., Wechsler-Reya, R., Phillips, J. J., Gestwicki, J. E., Ruggero, D., & Weiss, W. A. (2023). N-myc-Mediated Translation Control Is a Therapeutic Vulnerability in Medulloblastoma. *Cancer Research*, *83*(1), 130–140. https://doi.org/10.1158/0008-5472.CAN-22-0945

Laplante, M., & Sabatini, D. M. (2012). MTOR signaling in growth control and disease. In *Cell* (Vol. 149, Issue 2). https://doi.org/10.1016/j.cell.2012.03.017

Lathia, J. D., Mack, S. C., Mulkearns-Hubert, E. E., Valentim, C. L. L., & Rich, J. N. (2015). *Cancer stem cells in glioblastoma*. https://doi.org/10.1101/gad.261982

Liu, R., Chen, Y., Liu, G., Li, C., Song, Y., Cao, Z., Li, W., Hu, J., Lu, C., & Liu, Y. (2020). PI3K/AKT pathway as a key link modulates the multidrug resistance of cancers. In *Cell Death and Disease* (Vol. 11, Issue 9). https://doi.org/10.1038/s41419-020-02998-6

Lord, C. J., & Ashworth, A. (2012). The DNA damage response and cancer therapy. In *Nature* (Vol. 481, Issue 7381, pp. 287–294). https://doi.org/10.1038/nature10760

Luger, K., Mä Der, A. W., Richmond, R. K., Sargent, D. F., & Richmond, T. J. (1997). Crystal structure of the nucleosome core particle at 2.8 A ˚ resolution. In *Nature © Macmillan Publishers Ltd* (Vol. 389).

Lurje, G., & Lenz, H. J. (2010). EGFR signaling and drug discovery. In *Oncology* (Vol. 77, Issue 6). https://doi.org/10.1159/000279388

Majd, N. K., Yap, T. A., Koul, D., Balasubramaniyan, V., Li, X., Khan, S., Gandy, K. S., Yung, W. K. A., & De Groot, J. F. (2021). The promise of DNA damage response inhibitors for the treatment of glioblastoma. *Neuro-Oncology Advances*, *3*(1). https://doi.org/10.1093/noajnl/vdab015

Martinato, F., Cesaroni, M., Amati, B., & Guccione, E. (2008). Analysis of myc-induced histone modifications on target chromatin. *PLoS ONE*, *3*(11). https://doi.org/10.1371/journal.pone.0003650

Mohiuddin, I. S., & Kang, M. H. (2019). DNA-PK as an Emerging Therapeutic Target in Cancer. *Frontiers in Oncology*, *9*. https://doi.org/10.3389/fonc.2019.00635

Ni, C., & Buszczak, M. (2023). Ribosome biogenesis and function in development and disease. In *Development (Cambridge)* (Vol. 150, Issue 5). https://doi.org/10.1242/dev.201187

Ong, D. S. T., Hu, B., Ho, Y. W., Sauvé, C. E. G., Bristow, C. A., Wang, Q., Multani, A. S., Chen, P., Nezi, L., Jiang, S., Gorman, C. E., Monasterio, M. M., Koul, D., Marchesini, M., Colla, S., Jin, E. J., Sulman, E. P., Spring, D. J., Yung, W. K. A., … DePinho, R. A. (2017). PAF promotes stemness and radioresistance of glioma stem cells. *Proceedings of the National Academy of Sciences of the United States of America*, *114*(43). https://doi.org/10.1073/pnas.1708122114

Popay, T. M., Wang, J., Adams, C. M., Howard, G. C., Codreanu, S. G., Sherrod, S. D., McLean, J. A., Thomas, L. R., Lorey, S. L., Machida, Y. J., Weissmiller, A. M., Eischen, C. M., Liu, Q., & Tansey, W. P. (2021). Myc regulates ribosome biogenesis and mitochondrial gene expression programs through its interaction with host cell factor–1. *ELife*, *10*. https://doi.org/10.7554/eLife.60191

Rajendran, V., Kalita, P., Shukla, H., Kumar, A., & Tripathi, T. (2018). Aminoacyl-tRNA synthetases: Structure, function, and drug discovery. In *International Journal of Biological Macromolecules* (Vol. 111). https://doi.org/10.1016/j.ijbiomac.2017.12.157

Sabari, B. R., Zhang, D., Allis, C. D., & Zhao, Y. (2017). Metabolic regulation of gene expression through histone acylations. In *Nature Reviews Molecular Cell Biology* (Vol.

18, Issue 2, pp. 90–101). Nature Publishing Group. https://doi.org/10.1038/nrm.2016.140

Sadek, M., Sheth, A., Zimmerman, G., Hays, E., & Vélez-Cruz, R. (2022). The role of SWI/SNF chromatin remodelers in the repair of DNA double strand breaks and cancer therapy. In *Frontiers in Cell and Developmental Biology* (Vol. 10). Frontiers Media S.A. https://doi.org/10.3389/fcell.2022.1071786

Saxton, R. A., & Sabatini, D. M. (2017). mTOR Signaling in Growth, Metabolism, and Disease. In *Cell* (Vol. 168, Issue 6). https://doi.org/10.1016/j.cell.2017.02.004

Schimmel, P. (2018). RNA Processing and Modifications: The emerging complexity of the tRNA world: Mammalian tRNAs beyond protein synthesis. In *Nature Reviews Molecular Cell Biology* (Vol. 19, Issue 1). https://doi.org/10.1038/nrm.2017.77

Schmidt, E. K., Clavarino, G., Ceppi, M., & Pierre, P. (2009). SUnSET, a nonradioactive method to monitor protein synthesis. *Nature Methods*, *6*(4), 275–277. https://doi.org/10.1038/nmeth.1314

Schuettengruber, B., Chourrout, D., Vervoort, M., Leblanc, B., & Cavalli, G. (2007). Genome Regulation by Polycomb and Trithorax Proteins. In *Cell* (Vol. 128, Issue 4, pp. 735–745). Elsevier B.V. https://doi.org/10.1016/j.cell.2007.02.009

Schultz, S. K., & Kothe, U. (2024). RNA modifying enzymes shape tRNA biogenesis and function. In *Journal of Biological Chemistry* (Vol. 300, Issue 8). American Society for Biochemistry and Molecular Biology Inc. https://doi.org/10.1016/j.jbc.2024.107488

Scully, R., Panday, A., Elango, R., & Willis, N. A. (2019). DNA double-strand break repair-pathway choice in somatic mammalian cells. In *Nature Reviews Molecular Cell Biology* (Vol. 20, Issue 11). https://doi.org/10.1038/s41580-019-0152-0

Sevinç, K., Sevinç, G. G., Cavga, A. D., Philpott, M., Kelekçi, S., Can, H., Cribbs, A. P., Yıldız, A. B., Yılmaz, A., Ayar, E. S., Arabacı, D. H., Dunford, J. E., Ata, D., Sigua, L. H., Qi, J., Oppermann, U., & Onder, T. T. (2022). BRD9-containing non-canonical BAF complex maintains somatic cell transcriptome and acts as a barrier to human reprogramming. *Stem Cell Reports*, *17*(12). https://doi.org/10.1016/j.stemcr.2022.10.005

Stupp, R., Mason, W. P., van den Bent, M. J., Weller, M., Fisher, B., Taphoorn, M. J. B., Belanger, K., Brandes, A. A., Marosi, C., Bogdahn, U., Curschmann, J., Janzer, R. C., Ludwin, S. K., Gorlia, T., Allgeier, A., Lacombe, D., Cairncross, J. G., Eisenhauer, E., & Mirimanoff, R. O. (2005). Radiotherapy plus Concomitant and Adjuvant Temozolomide for Glioblastoma. *New England Journal of Medicine*, *352*(10). https://doi.org/10.1056/nejmoa043330

Sung, Y., Yoon, I., Han, J. M., & Kim, S. (2022). Functional and pathologic association of aminoacyl-tRNA synthetases with cancer. In *Experimental and Molecular Medicine* (Vol. 54, Issue 5). https://doi.org/10.1038/s12276-022-00765-5

Tejaswi Kanderi, Sunil Munakomi, & Vikas Gupta. (2024). *Glioblastoma Multiforme*. StatPearls .

Torrisi, F., Alberghina, C., D'aprile, S., Pavone, A. M., Longhitano, L., Giallongo, S., Tibullo, D., Di Rosa, M., Zappalà, A., Cammarata, F. P., Russo, G., Ippolito, M., Cuttone, G., Li Volti, G., Vicario, N., & Parenti, R. (2022). The Hallmarks of Glioblastoma: Heterogeneity, Intercellular Crosstalk and Molecular Signature of Invasiveness and Progression. In *Biomedicines* (Vol. 10, Issue 4). https://doi.org/10.3390/biomedicines10040806

Van Riggelen, J., Yetil, A., & Felsher, D. W. (2010a). MYC as a regulator of ribosome biogenesis and protein synthesis. In *Nature Reviews Cancer* (Vol. 10, Issue 4). https://doi.org/10.1038/nrc2819

Van Riggelen, J., Yetil, A., & Felsher, D. W. (2010b). MYC as a regulator of ribosome biogenesis and protein synthesis. In *Nature Reviews Cancer* (Vol. 10, Issue 4, pp. 301–309). https://doi.org/10.1038/nrc2819

Wang, J., Hong, M., Cheng, Y., Wang, X., Li, D., Chen, G., Bao, B., Song, J., Du, X., Yang, C., Zheng, L., & Tong, Q. (2024). Targeting c-Myc transactivation by LMNA inhibits tRNA processing essential for malate-aspartate shuttle and tumour progression. *Clinical and Translational Medicine*, *14*(5). https://doi.org/10.1002/ctm2.1680

Wang, X., Song, C., Ye, Y., Gu, Y., Li, X., Chen, P., Leng, D., Xiao, J., Wu, H., Xie, S., Liu, W., Zhao, Q., Chen, D., Chen, X., Wu, Q., Chen, G., & Zhang, W. (2023). BRD9-mediated control of the TGF-β/Activin/Nodal pathway regulates self-renewal and differentiation of human embryonic stem cells and progression of cancer cells. *Nucleic Acids Research*, *51*(21). https://doi.org/10.1093/nar/gkad907

Wang, X., Wang, S., Troisi, E. C., Howard, T. P., Haswell, J. R., Wolf, B. K., Hawk, W. H., Ramos, P., Oberlick, E. M., Tzvetkov, E. P., Vazquez, F., Hahn, W. C., Park, P. J., & Roberts, C. W. M. (2019a). BRD9 defines a SWI/SNF sub-complex and constitutes a specific vulnerability in malignant rhabdoid tumors. *Nature Communications*, *10*(1). https://doi.org/10.1038/s41467-019-09891-7

Wang, X., Wang, S., Troisi, E. C., Howard, T. P., Haswell, J. R., Wolf, B. K., Hawk, W. H., Ramos, P., Oberlick, E. M., Tzvetkov, E. P., Vazquez, F., Hahn, W. C., Park, P. J., & Roberts, C. W. M. (2019b). BRD9 defines a SWI/SNF sub-complex and constitutes a specific vulnerability in malignant rhabdoid tumors. *Nature Communications*, *10*(1). https://doi.org/10.1038/s41467-019-09891-7

Wang, Y., Tao, E. W., Tan, J., Gao, Q. Y., Chen, Y. X., & Fang, J. Y. (2023). tRNA modifications: insights into their role in human cancers. In *Trends in Cell Biology* (Vol. 33, Issue 12). https://doi.org/10.1016/j.tcb.2023.04.002

Wanior, M., Krämer, A., Knapp, S., & Joerger, A. C. (2021). Exploiting vulnerabilities of SWI/SNF chromatin remodelling complexes for cancer therapy. In *Oncogene* (Vol. 40, Issue 21). https://doi.org/10.1038/s41388-021-01781-x

Wei, Z., Yoshihara, E., He, N., Hah, N., Fan, W., Pinto, A. F. M., Huddy, T., Wang, Y., Ross, B., Estepa, G., Dai, Y., Ding, N., Sherman, M. H., Fang, S., Zhao, X., Liddle, C., Atkins, A. R., Yu, R. T., Downes, M., & Evans, R. M. (2018). Vitamin D Switches BAF Complexes to Protect β Cells. *Cell*, *173*(5). https://doi.org/10.1016/j.cell.2018.04.013

Weisberg, E., Chowdhury, B., Meng, C., Case, A. E., Ni, W., Garg, S., Sattler, M., Azab, A. K., Sun, J., Muz, B., Sanchez, D., Toure, A., Stone, R. M., Galinsky, I., Winer, E., Gleim, S., Gkountela, S., Kedves, A., Harrington, E., … Griffin, J. D. (2022). BRD9 degraders as chemosensitizers in acute leukemia and multiple myeloma. *Blood Cancer Journal*, *12*(7). https://doi.org/10.1038/s41408-022-00704-7

Weller, M., Wick, W., Aldape, K., Brada, M., Berger, M., Pfister, S. M., Nishikawa, R., Rosenthal, M., Wen, P. Y., Stupp, R., & Reifenberger, G. (2015). Glioma. In *Nature Reviews Disease Primers* (Vol. 1). Nature Publishing Group. https://doi.org/10.1038/nrdp.2015.17

Wu, W., Klockow, J. L., Zhang, M., Lafortune, F., Chang, E., Jin, L., Wu, Y., & Daldrup-Link, H. E. (2021). Glioblastoma multiforme (GBM): An overview of current therapies and mechanisms of resistance. In *Pharmacological Research* (Vol. 171). https://doi.org/10.1016/j.phrs.2021.105780

Xiong, Y., & Steitz, T. A. (2004). Mechanism of transfer RNA maturation by CCA-adding enzyme without using an oligonucleotide template. *Nature*, *430*(7000). https://doi.org/10.1038/nature02711

Yalamarty, S. S. K., Filipczak, N., Li, X., Subhan, M. A., Parveen, F., Ataide, J. A., Rajmalani, B. A., & Torchilin, V. P. (2023). Mechanisms of Resistance and Current Treatment Options for Glioblastoma Multiforme (GBM). In *Cancers* (Vol. 15, Issue 7). https://doi.org/10.3390/cancers15072116

Yang, Y. P., Chang, Y. L., Huang, P. I., Chiou, G. Y., Tseng, L. M., Chiou, S. H., Chen, M. H., Chen, M. T., Shih, Y. H., Chang, C. H., Hsu, C. C., Ma, H. I., Wang, C. T., Tsai, L. L., Yu, C. C., & Chang, C. J. (2012). Resveratrol suppresses tumorigenicity and enhances radiosensitivity in primary glioblastoma tumor initiating cells by inhibiting the STAT3 axis. *Journal of Cellular Physiology*, *227*(3). https://doi.org/10.1002/jcp.22806

Yu, Y., Yu, J., Ge, S., Su, Y., & Fan, X. (2023). Novel insight into metabolic reprogrammming in cancer radioresistance: A promising therapeutic target in radiotherapy. In *International Journal of Biological Sciences* (Vol. 19, Issue 3). https://doi.org/10.7150/ijbs.79928

Zhou, Q., Huang, J., Zhang, C., Zhao, F., Kim, W., Tu, X., Zhang, Y., Nowsheen, S., Zhu, Q., Deng, M., Chen, Y., Qin, B., Luo, K., Liu, B., Lou, Z., Mutter, R. W., & Yuan, J. (2020). The bromodomain containing protein BRD-9 orchestrates RAD51–RAD54 complex formation and regulates homologous recombination-mediated repair. *Nature Communications*, *11*(1). https://doi.org/10.1038/s41467-020-16443-x

Zhu, X., Liao, Y., & Tang, L. (2020). Targeting brd9 for cancer treatment: A new strategy. In *OncoTargets and Therapy* (Vol. 13, pp. 13191–13200). Dove Medical Press Ltd. https://doi.org/10.2147/OTT.S286867

Ziv, Y., Bielopolski, D., Galanty, Y., Lukas, C., Taya, Y., Schultz, D. C., Lukas, J., Bekker-Jensen, S., Bartek, J., & Shiloh, Y. (2006). Chromatin relaxation in response to DNA double-strand breaks is modulated by a novel ATM-and KAP-1 dependent pathway. *Nature Cell Biology*, *8*(8), 870–876. https://doi.org/10.1038/ncb1446